People's Democratic Republic of Algeria

Ministry of Higher Education and Scientific Research

Mohamed Boudiaf University of M'sila

Faculty of Technology

الجمهورية الجزائرية الديمقراطية الشعبية

وزارة التعليم العالي والبحث العلمي

جامعة المسيلة

كلية التكنولوجيا

Department of Mechanical Engineering

END OF STUDIES THESIS

In order to obtain the degree of:

MASTER'S DEGREE

In Mechanical Engineering

Specialization :Energetics

Presented by:

- Seghiour Chamesseddine

- Diab Nidhal Chemseddine

Theme

NUMERICAL STUDY OF THE EFFECT OF USING A ROTATING TWISTED TAPE AND A NANOFLUID ON THE THERMAL PERFORMANCE OF CYLINDRICAL-PARABOLIC COLLECTOR

Before the jury composed of:

BOUAOUINA Lalouani	MCB	President
BAKHTI Fatima Zohra	MCA	Supervisor
HEBICHE Noureddine	MAA	Examiner

Academic Year: 2023 / 2024

Acknowledgments

At the end of this modest work, we express our gratitude firstly to ALLAH Almighty for the will, health, and patience that He has bestowed upon us during all these long years of study. And to all the teachers who have contributed to our education throughout the school years. Our thanks go to BAKHTI.F for proposing and directing this work, and for their continuous support during the preparation of this thesis.

TABLE OF CONTENTS

TABLE OF CONTENTS

TABLE OF CONTENTS

CHAPTER II :Nanofluids

Chapter III:MATHEMATICAL FORMULATION

The list of figures

Chapter I

Chapter II

Chapter III

Chapter IV

Chapter V

The list of tables

Naming system

Latin symbols :

A : heat exchange surface [m^2]

a : absorption coefficient

C: solar constant

C : coefficient of linear-anisotropic phase function

Cl: speed of light in (m/s)

Cp: specific heat capacity at constant pressure

Cp: specific heat capacity at constant pressure

D: direct radiation

Dae: outer diameter of the absorber

Dai: inner diameter of the absorber

Dga: outer diameter of the glass

Dgi: inner diameter of the glass

Dh: hydraulic diameter [m]

D* : the radiation diffuse on a horizontal plan

E: energy, expressed in Joules

G: global radiation

G: incident radiation

h: solar altitude

hc: Planck's constant (h= $6.626.10^{-37}$ J/s).

hm: average convection coefficient [W/m^2 k]

($\boldsymbol{h_{r,int}}$) : The heat transfer coefficient by radiation between the absorber tube and the glass envelope

($h_{r,ext}$) : The heat transfer coefficient by radiation between the glass envelope and the sky

kf: thermal conductivity of the fluid [W/m K]

kn: thermal conductivity of the nanofluid

Ks: thermal conductivity of the solid particles

TABLE OF CONTENTS

L: longitude

L: length of the receive

$\dot{m}$: mass flow rate [kg/s]

N: is the day number in the year

n: the day number in the year counting from January 1st

n: ordinal day of the year $1 \leq n \leq 365$

n: refractive index

Nu: the Nusselt number of the heat transfer fluid

Re: the Reynolds number of the heat transfer fluid

qc: the amount of heat

ρ_{nf} : The density of the nanofluid

ρ_{bf} : The density of the base fluid

ρ_{sp}: The density of nanopartucles

ν : Kinematic viscosity (m^2/s)

k_b : Boltzmann constant (-)

A: Empirical constant (-)

Pr: Pranddtl number of base fluids (-)

T0 : Reference temperature (k)

Rb : Thermal boundary resistance ((m^2.K)/W)

R : Radius (m)

n : Emprical shape factor (-)

Bi: Biot number

D : Diameter (m)

Ibf : Mean free path (nm)

I : The radiation intensity (it depends on the direction and position of the vector)

I_d : solar radiation at normal incidence

I^* : the direct radiation on a plane perpendicular

$\vec{r}$: The position vector

$\vec{s}$: The direction vector

$\vec{s}'$: The direction of the diffusion vector

a : The absorption coefficient

s : The path length

Grec symbols :

ϕ :Volume fraction of nanoparticle in base fluid (-)

δ_{nl} : Nanolayer thickness (-)

β_{nl} : Dimensionless nanolayer parameters (-)

β : Empirical correlation

γ : Ration of nanolayer thickness to nanoparticle radius

P : Density (kg/m^3)

Σ : Emprical constant (-)

β : The coefficient of isobaric expansion of the fluid

μ : Dynamic viscosity of the fluid

σs : The diffusion coefficient

σ : The Stefan-Boltzmann constant (5.672x10-8 W/m2K 4)

Φ : The phase function

T :The local temperature

Ω : The solid angle

General Introduction

General Introduction

Renewable energies are energies derived from natural sources that renew themselves at a rate higher than their consumption. They are powered by the sun, wind, heat from the earth, waterfalls, tides, biomass, etc. They allow for the production of electricity, heat, cold, gas, fuel, and combustibles. They are considered inexhaustible energies and are available in unlimited quantities.

Solar energy originates from the nuclear fusion reactions that power the Sun and is diffused by its radiation, where solar energy concentration systems such as polar solar collectors and parabolic cylindrical solar collectors have greatly contributed to the development of the use of solar thermal energy. The majority of solar thermal electricity production systems (or thermodynamic systems) use cylindrical-parabolic concentrators with a linear concentration of solar thermal flux.

To reduce energy consumption in solar collectors, compact and efficient thermal systems are also designed and developed. Researchers have always strived to increase their efficiency and effectiveness. Additionally, increasing thermal efficiency leads to a decrease in the absorber tube temperature, there by reducing the temperature gradients on it, which minimizes potential thermomechanical issues.

Improving convective heat transfer in industrial heating or cooling devices involves enhancing heat exchange between a heat transfer fluid and a hot surface.

All heat transfer enhancement techniques will affect these two factors: the traditional heat transfer coefficient and the heat transfer surface between the fluid and the wall. Adding the twisted tape will primarily affect the heat transfer surface, while the thermal conductivity of the heat transfer medium will affect the heat transfer coefficient.

Using metal particle-based nanofluids with the twisted tape show better values than using nanofluids alone, while employing metal particle-based nanofluids presents superior values compared to the base fluid for thermal conductivity and convective heat transfer coefficient. Certainly, using metal particle-based nanofluids with the twisted tape is the most promising solution in the field of heat transfer enhancement.

It is in this context that we conducted our study entitled :

Numerical study of the effect of using a rotating twisted tape and a nanofluid on the thermal performance of a cylindrical-parabolic collector.

The work we are developing in this memoir focuses on the simulation of a three-dimensional laminar flow of the absorber of a cylindrical-parabolic solar concentrator equipped with a collector fitted with a twisted tape. This work has been conducted with a focus on improving the thermal performance of the solar collector by using a nanofluid as the heat transfer fluid.

To achieve our objectives, we first used Syltherm 800 as the heat transfer fluid. In the second case, we replaced Syltherm 800 with the nanofluid (Syltherm 800+Cu) at different concentrations φ=1%, 2%, 3%, and 4%. In the third case, we added a twisted tape.

The numerical simulations were conducted for Reynolds numbers ranging from 100 to 1000.

This study is organized into five chapters preceded by a general introduction and followed by a general conclusion.

The first chapter provides a literature review allowing an understanding of solar potential, solar collectors. A more detailed presentation has been dedicated to cylindrical-parabolic concentrators.

In the second chapter, we presented a better understanding of nanofluids and their classification, different types, preparation methods, etc. Without forgetting an understanding of our fluid Syltherm 800.

In the third chapter, we presented the studied configurations, simplifying assumptions, as well as the continuity and momentum equations coupled with the energy equation for the fluid.

In the fourth chapter, we presented general information about the two software programs used. We explained the various main steps of creating the geometry under study and meshing using Gambit software, as well as the steps of the numerical simulation using Fluent software.

The fifth and final chapter is the most important part of our study. It includes the numerical results obtained and their interpretations for the three cases studied. A comparative study between the three cases was also conducted.

Finally, we conclude with a general conclusion summarizing the main results obtained.

Chapter I

General information about Solar Energy and Solar Collectors

Chapter I *: General information about solar energy and solar collectors*

I.1. Introduction

The sun is an inexhaustible and renewable source of energy. Every day, it emits a huge amount of solar radiation that can be harnessed to meet our energy needs, that's why we're going to talk about solar energy.

Solar energy is a form of renewable energy that comes from the sun's rays. It is considered one of the most abundant and sustainable energy resources on Earth, Solar energy can be captured in two main ways:

Photovoltaic solar panels convert sunlight directly into electricity using photovoltaic cells. Solar thermal systems use collectors to absorb heat from the sun and transfer it to a fluid, usually water or a heat transfer liquid, which can then be used for heating or power generation.

Solar technologies have advanced significantly over the years, with constant improvements in efficiency, cost, and sustainability. These advances are making solar energy increasingly competitive with conventional energy sources in many parts of the world.

I.2. General information about the sun and the earth

I.2.1. The sun

From our vantage point on Earth, the Sun may appear like an unchanging source of light and heat in the sky. But the Sun is a dynamic star, constantly changing and sending energy out into space. The science of studying the Sun and its influence throughout the solar system is called heliophysics.

The Sun is the largest object in our solar system. Its diameter is about 865,000 miles (1.4 million kilometers). Its gravity holds the solar system together, keeping everything from the biggest planets to the smallest bits of debris in orbit around it.[2]

I .2.2. Characteristics of the sun

In terms of statistics, the sun's diameter is about 1.4 million km (864,000 miles), and its circumference is about 4.4 million km (2.7 million miles). It has a volume of 1.4×10^{27} cubic meters and a mass of 2×10^{30} kilograms, which is about 330,000 times the mass of the earth.[3]

I.2.3. Temperature of the sun

The hottest part of the Sun is its core, where temperatures top 27 million °F (15 million °C). The part of the Sun we call its surface – the photosphere – is a relatively cool 10,000 °F (5,500 °C). In one of the Sun’s biggest mysteries, the Sun’s outer atmosphere, the corona, gets hotter the farther it stretches from the surface. The corona reaches up to 3.5 million °F (2 million °C) – much, much hotter than the photosphere.[4]

I.2.4. Structure

The core is the hottest part of the Sun. Nuclear reactions here – where hydrogen is fused to form helium – power the Sun's heat and light. Temperatures top 27 million °F (15 million °C) and it's about 86,000 miles (138,000 kilometers) thick. The density of the Sun's core is about 150 grams per cubic centimeter (g/cm³). That is approximately 8 times the density of gold (19.3 g/cm³) or 13 times the density of lead (11.3 g/cm³).

Energy from the core is carried outward by radiation. This radiation bounces around the radiative zone, taking about 170,000 years to get from the core to the top of the convection zone. Moving outward, in the convection zone, the temperature drops below 3.5 million °F (2 million °C). Here, large bubbles of hot plasma (a soup of ionized atoms) move upward toward the photosphere, which is the layer we think of as the Sun's surface.[5]

I.2.5.The solar constant C

The solar constant expresses the amount of solar energy (actually lighting power) that would be received by a surface of 1m² located at a distance of 1 astronomical unit (average distance from the earth to the sun) exposed perpendicular to the sun's rays if the Earth's atmosphere did not exist.

It is equal to 1.367 kW/m² (i.e. 1367 W/m²).

I.2.6. The Earth

Earth is the planet we live on, one of eight planets in our solar system and the only known place in the universe to support life, earth is the largest and most massive of the rocky inner planets, although it is dwarfed by the gas giants beyond the Asteroid Belt. Its diameter is about 12,700 kilometers (7,900 miles), and its mass is about 5.97×10^{24} kilograms (6.58×10^{21} tons).

Earth's core is mostly made of iron and nickel. It consists of a solid center surrounded by an outer layer of liquid. The core is found about 2,900 kilometers (1,802 miles) below Earth's surface, and has a radius of about 3,485 kilometers (2,165 miles).

Each journey around the sun, a trip of about 940 million kilometers (584 million miles), is called a revolution. A year on Earth is the time it takes to complete one revolution, about 365.25 days. Earth orbits the sun at a speedy rate of about 30 kilometers per second (18.5 miles per second), earth's rotation causes the periods of light and darkness we call day and night. The part of Earth facing the sun is in daylight; the part facing away from the sun is in darkness. If Earth did not rotate, one-half of Earth would always be too hot to support life, and the other half would be frozen. Earth rotates from west to east, so the sun appears to rise in the east and set in the west.

FAST FACT :

Earth by the Numbers

Surface Gravity: 1 (one kilogram on Earth)

Orbital Period: 365.256 days

Satellites: 1 (the Moon)

Atmosphere: nitrogen (78%), oxygen (21%), argon, carbon dioxide, neon

Average Temperature: 15° Celsius (77 Kelvin, 59° Fahrenheit)[6]

I.2.7. How long the Earth rotates on its axis

The Earth rotates from west to east (in the opposite direction of the clocks, seen from the north side), as well as the stars, including the Sun and the Moon, seem to be animated by an opposite movement, going from east to west.The duration of this rotation with respect to the stars (sidereal rotation) is approximately 23 h 56 min 4 sec. This is called the sidereal day, However, over the course of the year, the Earth moves forward in its orbit. Thus, for an observer. In order for the Sun to pass south again from one day to the next, it will be necessary to add about 4 minutes in the sidereal day (Figure I.1). So it's only after 24 hours that the Sun is in the same position as the day before. This is called the solar day. [7]

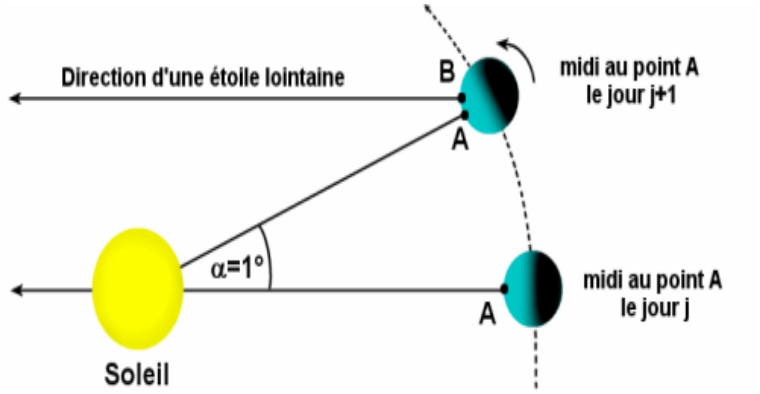

Figure I.1. Differences between sidereal and solar days, due to the advance of the Earth in its orbit (scales not respected)[8]

I.3. Solar radiation

Solar radiation, often called the solar resource or just sunlight, is a general term for the electromagnetic radiation emitted by the sun. Solar radiation can be captured and turned into useful forms of energy, such as heat and electricity, using a variety of technologies. However, the technical feasibility and economical operation of these technologies at a specific location depends on the available solar resource.The solar radiation moves in a vacuum with a speed of

3,108 m/s. has an energy linked to the frequency ν or δ to the wavelength by the following relationship:

$$\boldsymbol{E = hv = \frac{h_c}{\lambda}} \quad \text{(I.1)}$$

E: energy, expressed in Joules.

Cl : the speed of light in (m/s).

hc: Planck's constant (h= $6.626.10^{-37}$ J/s).

I.4. The component of solar radiation

I.4.1. Diffuse (S) and Direct (D) Solar Radiation

As sunlight passes through the atmosphere, some of it is absorbed, scattered, and reflected by:

• Air molecules

• Water vapor

• Clouds

• Dust

• Pollutants

• Forest fires .

• Volcanoes.

This is called diffuse solar radiation. The solar radiation that reaches the Earth's surface without being diffused is called direct beam solar radiation. The sum of the diffuse and direct solar radiation is called global solar radiation. Atmospheric conditions can reduce direct beam radiation by 10% on clear, dry days and by 100% during thick, cloudy days The direct radiation received by a surface permanently oriented towards the sun and which therefore receives solar radiation at normal incidence is designated by I, We have the following relationship:

$$\boldsymbol{I_d = I^* sin(h)} \quad \text{(I.2)}$$

h : height of the sun.

In the case where we do not have any measurements, we can evaluate the direct radiation on a plane perpendicular to the solar radiation by the relation :

$$I^* = 1370\exp\left[\frac{T_i}{0{,}9+9{,}4\sin(h)}\right] \quad \text{(I.3)}$$

Where $\boldsymbol{T_i}$ is the linke disorder factor calculable by:

$$T_i = 2{,}4 + 14{,}6\beta + 0{,}4(1+2\beta)\mathrm{Ln}(P_9) \quad \text{(I.4)}$$

β :is the atmospheric haze coefficient.

PV :is the partial pressure of water vapor expressed in mmHg.

With: h: Height of the sun.

• For an observer at home, the radiation diffuse on a horizontal plan:[9]

$$D^* = 54{,}8\sqrt{\sin(h)}\left[T_i - 0{,}5 - \sqrt{\sin(h)}\right] \quad (I.5)$$

I.4.2. Albedo

Albedo is the amount of sunlight a surface reflects compared to the amount of incoming solar radiation. The albedo of white snow and ice is very different from the brown tundra. Having accurate data on how albedo changes through time is important for providing inputs into computer simulations of the climate.[10]

ALB= $\frac{\textbf{reflectedenergy}}{\textbf{ecycledenergy}}$

I.4.3. Global radiation

Global radiation (G) is the sum of diffuse and direct radiation.

G =S+D

With:

G: Global radiation.

S: Diffuse radiation.

D: direct radiation.

I.5. Position of the sun relative to the earth

I.5.1. Celestial coordinates

I.5.1.a. Celestial sphere

The apparent surface of the heavens, on which the stars seem to be fixed. For the purpose of establishing coordinate systems to mark the positions of heavenly bodies, it can be considered a real sphere at an infinite distance from the Earth. The Earth's axis, extended to infinity, touches this sphere at the north and south celestial poles, around which the heavens seem to turn. The plane of the Earth's Equator, extended to infinity, marks the celestial equator.[11]

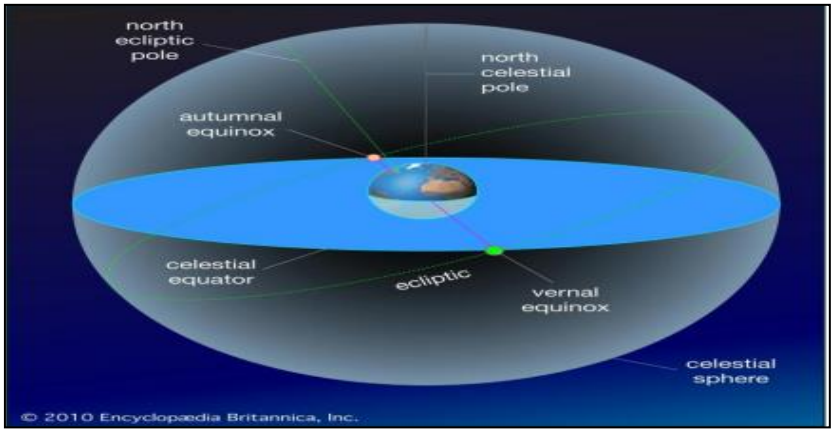

Figure I.2. Celestial sphere[10]

I.5.1.b. Declination angle

The declination angle, denoted by δ, varies seasonally due to the tilt of the Earth on its axis of rotation and the rotation of the Earth around the sun. If the Earth were not tilted on its axis of rotation, the declination would always be 0°. However, the Earth is tilted by 23.45° and the declination angle varies plus or minus this amount. Only at the spring and fall equinoxes is the declination angle equal to 0°. The rotation of the Earth around the sun and the change in the declination angle is shown in the animation below.

The declination angle can be calculated by the equation :

$$\boldsymbol{\delta = -23.45^{*} \times cos\left(\frac{360}{365} \times (d + 10)\right)} \quad \text{(I.6)}$$

where d is the day of the year with Jan 1 as d = 1

The declination angle can also be defined in other ways. The derivation of the declination angle assumes a circular orbit and gives the following result:

$$\boldsymbol{sin\delta = sin(-23.45^{0})cos\left[\frac{360}{365}(d + 10)\right]} \quad \text{(I.7)}$$

In radians, δ ≈ sin δ, for small values of δ so the derivation reduces to the equation given in the previous section:

$$\boldsymbol{\delta = -23.45 \times cos\left(\frac{360}{365} \times (d + 10)\right)} \quad \text{(I.8)}$$

The difference between the two equations is very small (< 0.3°), whereas the error to the true declination (e.g. the PSA algorithm below) is up to 1°. Thus the simpler equation is preferred since it is equally accurate.[12]

The equations:

$$\boldsymbol{\delta = 23.45^{*} \times sin\left(\frac{360}{365} \times (d + 284)\right)} \quad \text{(I.9)}$$

$$\delta = 23.45^{*} \times sin\left(\frac{360}{365} \times (d - 81)\right) \quad \text{(I.10)}$$

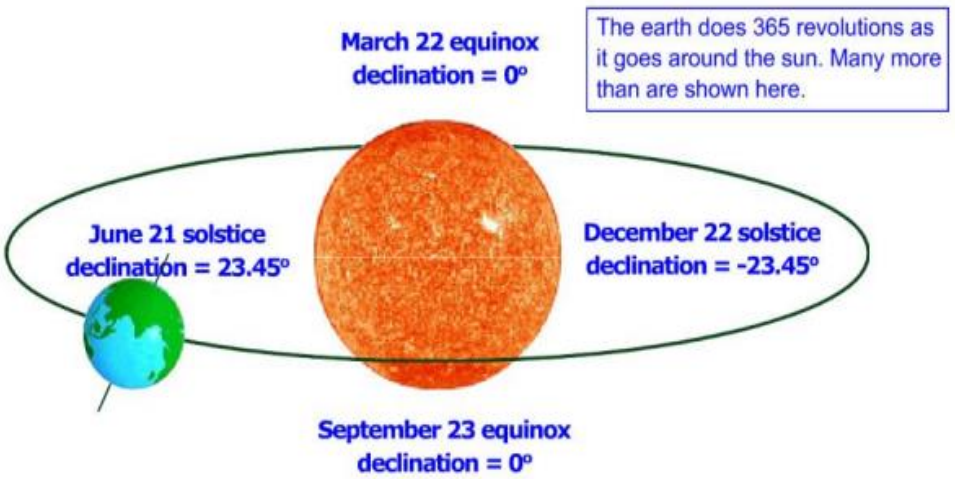

Figure I.3. declination angle for one year. [11]

I.5.1.c. Hour angle

In astronomy, the angle between an observer's meridian (a great circle passing over his head and through the celestial poles) and the hour circle (any other great circle passing through the poles) on which some celestial body lies. This angle, when expressed in hours and minutes, is the time elapsed since the celestial body's last transit of the observer's meridian. The hour angle can also be expressed in degrees, 15° of arc being equal to one hour.

I.5.2. Geographic coordinates

I.5.2.a. Latitude and longitude

In cartography, a coordinate system used to determine and describe the position of any place on Earth's surface.

• ***Latitude:*** is a measurement of a location north or south of the Equator. In contrast.

• ***Longitude***: is a measurement of location east or west of the prime meridian at Greenwich (an imaginary north-south line that passes through both geographic poles and Greenwich, London, England, U.K.).

Latitude and longitude together can describe the exact location of any place on Earth.

I.5.2.b. Altitude

Corresponds to the vertical distance between this point and a reference surface, the geoid, representing the mean sea level[13]

Figure I.4. Atitude and longitude of Washington, D.C. [12]

I.5.3. Horizontal coordinates

I.5.3.a. Height of the sun (h) :

Or The solar altitude angle it is the angle between the sun ′s rays and a horizontal plane as shown in Figure *I.5*. It is related to the solar zenith angle Φ, being the angle between the sun′s rays and the vertical. [12]

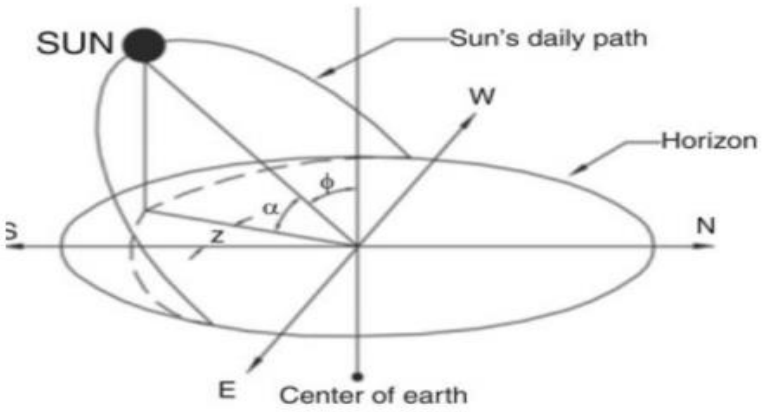

Figure.I.5. Apparent daily path of the sun across the sky from sunrise to sunset. [12]

Thus:

$$\boldsymbol{\phi + \alpha = \frac{\pi}{2} = 90^{\circ}} \quad \text{(I.11)}$$

The mathematical expression for the solar altitude angle is:

$$\boldsymbol{\sin\alpha = \cos\phi = \sin L \sin\delta + \cos L \cos\delta \cos h} \quad \text{(I.12)}$$

The mathematical expression for the height of sun :

$$sin\,h = sin\,\varphi sin\delta + cos\varphi cos\delta cos\,\omega \quad \text{(I.13)}$$

I.5.3.b. Azimuth (a)

The angular distance from the north or south point of the horizon to the foot of the vertical circle through a heavenly body. The azimuth of a horizontal direction is its deviation from the north or south.[14]

it is given by the relation:[15]

$$sin\alpha = \frac{cos\delta sin\omega}{cosh} \quad \text{(I.14)}$$

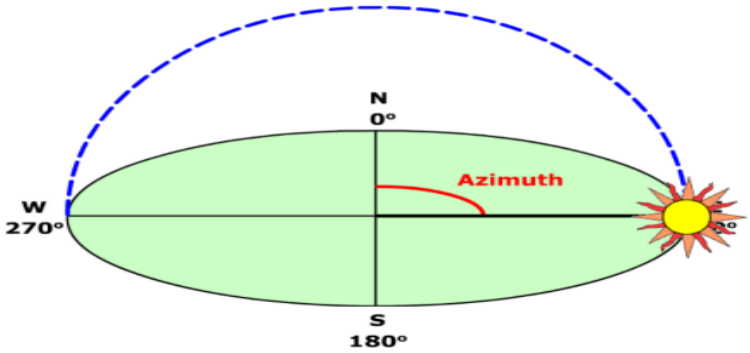

Figure.I.6. The azimuth angle. [13]

I.6. Solar Times

I.6.1. True Solar Time (T.S.V)

True solar time, at a given time and place, is the hourly angle of the sun:ω. It is given in the following form :

TSV = 12 + ω/15

I.6.2. Mean Solar Time (T.S.M) :

It is sometimes referred to as local time (TSM).[16]

TSV − ET = TSM

ET , the equation of time, which corrects for TSV versus TSM.

ET= 9.87 sin (2N') – 7.53 cos(N') – 1.5 sin(N') [min]

N' = (nj – 81) ×(360/365)

I.6.3. Universal Time (UTC)

This is the mean civil time of the Greenwich meridian (prime meridian) called GMT (Greenwich Mean Time).

TU=TSM+L/15

Or

L: is the longitude

L >0, for towns east of Greenwich

L <0, for towns west of Greenwich

TU = TSM, for Greenwich meridian

I.6.4 Legal Time (TL)

This is the official time of a state, it is given by:[17]

TL=TU+ ΔH

ΔH: the time difference between the Greenwich meridian and the state in question.

ΔH : 1 hour for Algeria.

I.7. Solar energy

Radiation from the Sun capable of producing heat, causing chemical reactions, or generating electricity. The total amount of solar energy incident on Earth is vastly in excess of the world's current and anticipated energy requirements. If suitably harnessed, this highly diffused source has the potential to satisfy all future energy needs. In the 21st century solar energy is expected to become increasingly attractive as a renewable energy source because of its inexhaustible supply and its nonpolluting character, in stark contrast to the finite fossil fuels coal, petroleum, and natural gas.

The Sun is an extremely powerful energy source, and sunlight is by far the largest source of energy received by Earth, but its intensity at Earth's surface is actually quite low. This is essentially because of the enormous radial spreading of radiation from the distant Sun. A relatively minor additional loss is due to Earth's atmosphere and clouds, which absorb or scatter as much as 54 percent of the incoming sunlight. The sunlight that reaches the ground consists of nearly 50 percent visible light, 45 percent infrared radiation, and smaller amounts of ultraviolet and other forms of electromagnetic radiation.

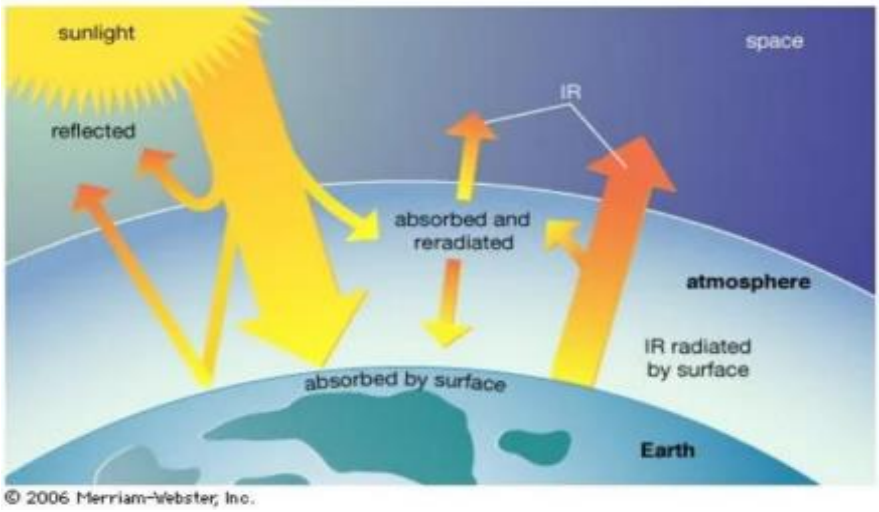

Figure.I.7. electromagnetic radiation of the sun to earth.[17]

Reflection and absorption of solar energy. Although some incoming sunlight is reflected by Earth's atmosphere and surface, most is absorbed by the surface, which is warmed.

The potential for solar energy is enormous, since about 200,000 times the world's total daily electric-generating capacity is received by Earth every day in the form of solar energy. Unfortunately, though solar energy itself is free, the high cost of its collection, conversion, and storage still limits its exploitation in many places. Solar radiation can be converted either into thermal energy (heat) or into electrical energy, though the former is easier to accomplish.[18]

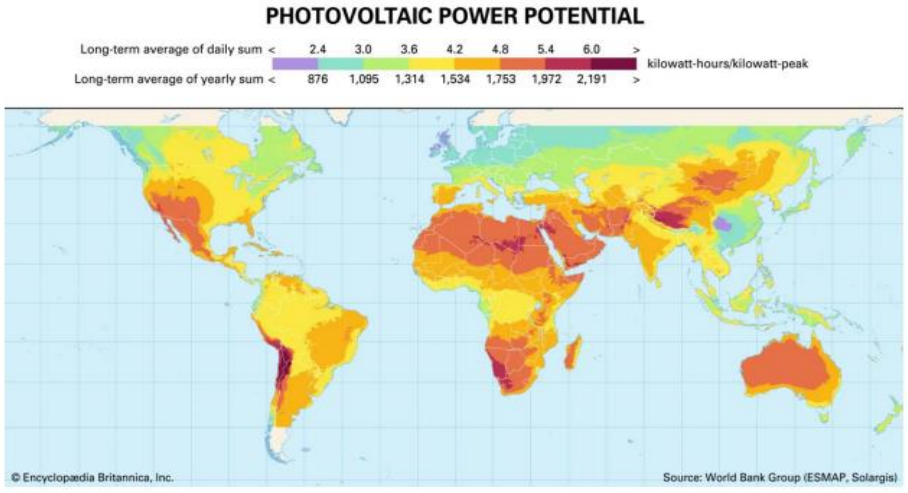

Figure.I.8. Earth's photovoltaic power potential. [16]

I.7.1. Solar energy in Algeria

Regarding solar power potential, Algeria is home to some of the world's highest solar irradiance levels, with the capacity to generate 1,850 to 2,100 kilowatts per hour and up to 3,500 hours per year in its desert regions .

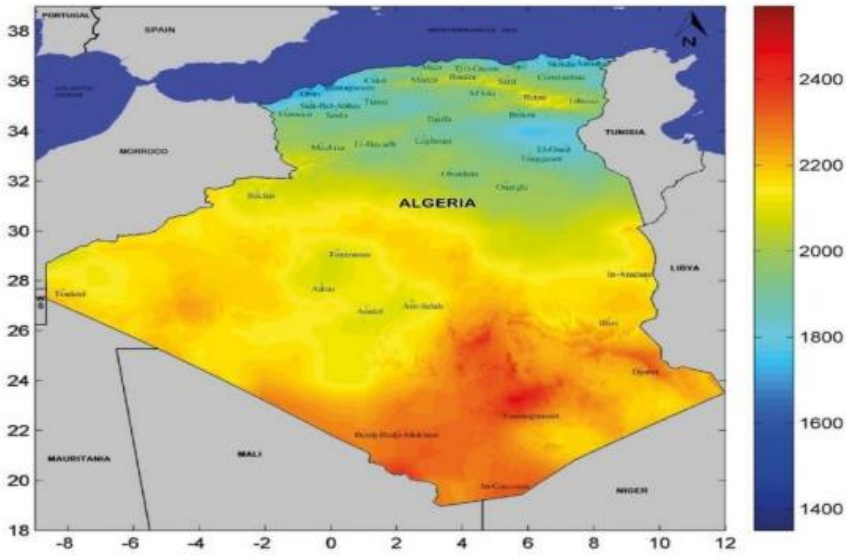

Figure.I.9. Solar radiation potential in Algeria. [18]

Algeria aims to produce 27 percent of its electricity from renewable resources by 2035, mostly from solar power. To reignite the country's energy transition, in 2021, the Algerian government made a new push to develop strategic partnerships in the field of renewable energies with multiple countries, including China, Germany, and the United States. More specifically, the government seeks to forge relationships with foreign suppliers in engineering services, storage systems, solar-tracking technologies, universal certification solutions, and solar application kits for agriculture. Towards this end, Algeria launched a tender for a onegigawatt solar energy project in 2021, comprised of building five power generation sites ranging from 50 to 300 MW each. Sonatrach, Algeria's national oil company, is also launching sizeable solar power projects to transition from oil and gas power generation for its off-grid oil and gas surface processing facilities.[19]

I.8. Solar collectors

I.8.1.Definition

Solar collectors are devices designed to capture sunlight and convert it into usable thermal or electrical energy. They are typically used in solar energy systems to harness the abundant energy from the sun for various applications, including heating water for domestic use, generating electricity, or providing space heating. Solar collectors come in various forms, such as flat-plate collectors, evacuated tube collectors, and concentrating collectors, each tailored to maximize the absorption of sunlight and conversion efficiency for specific purposes.

I.8.2. Different types and the operating principle of solar collectors

I.8.2.a. Photovoltaic solar collectors

These devices consist of photovoltaic cells formed by semiconductors in two layers doped positively (P) and negatively (N) which convert the energy of radiation into electrical energy through the photovoltaic effect.

I.8.2.a.1. Operating principle

A solar cell is an electronic component that converts sunlight into electricity through the photovoltaic effect.

The principle of photovoltaic conversion can be described by the following mechanisms:

- Absorption of incident photons and creation of electron-hole pairs if the energy of the incident photon is greater than the material's bandgap.

- Diffusion of minority charge carriers to the space charge region. Transfer of electric charges to the region where they will be majority due to the electric field present at the space charge region of the PN junction and collection. During the diffusion of charges to the space charge region, electric charges can recombine and be lost.
- Power dissipation in the load and in parasitic resistances.[20]
- Haut du formulaire

I.8.2.b. Solar thermal collectors

Which absorbs solar radiation to convert it into thermal energy transmitted using a heat transfer fluid. It supplies power to your central heating network.

I.8.2.b.1. Operating principle

✓ Solar thermal collectors consist of absorbers, in other words, tubes placed between a glass plate and a layer of insulation.
✓ They capture heat calories from the sun. This heat heats a heat transfer fluid which circulates in the absorber tubes.
✓ The heat transfer liquid is then transported to your water heater or central heating circuit.[19]

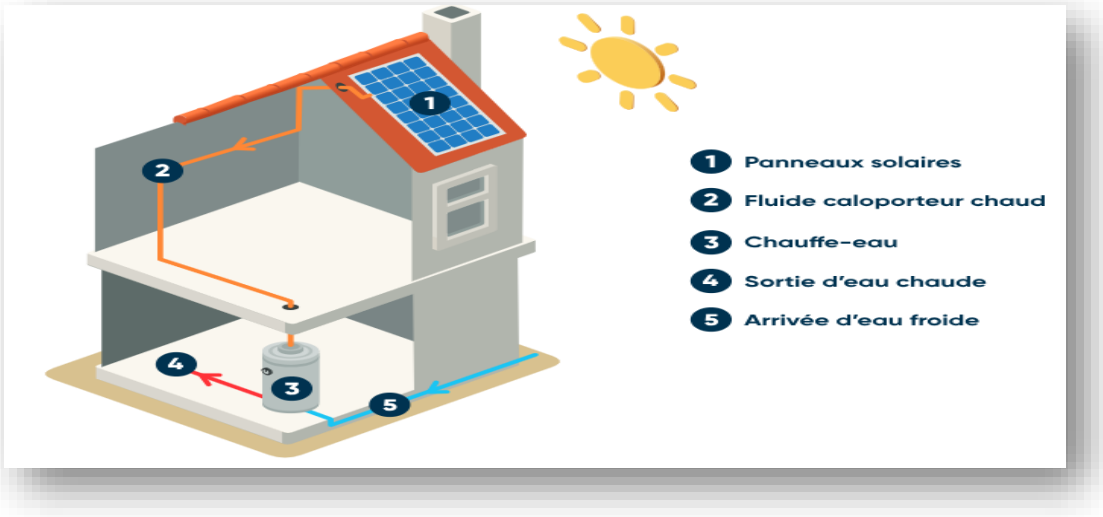

Figure.I.10. Installation of solar thermal collector[19]

I.8.2.c. Solar concentrators

✓ Solar concentrators are devices designed to concentrate sunlight onto a small area, there by increasing the intensity of the light and allowing for more efficient conversion of solar energy into heat or electricity. These devices are used in solar energy harvesting systems to increase energy efficiency and reduce costs. They can take different forms, such as parabolic concentrators, lens concentrators, or parabolic trough concentrators, each tailored to specific applications depending on concentration needs and solar energy use objectives. [19]

I.8.3. Thermal solar collectors

I.8.3.1. Different types of solar thermal collectors

I.8.3.1.a. Planar solar collectors

The flat panel solar collector is a type of thermal solar panel whose purpose is to transform solar radiation into thermal energy. This type of thermal solar panels is cost-effective in temperate climates and is well suited for a wide range of thermal applications, such as:

- ✓ Production of domestic hot water (DHW).
- ✓ Pool heating.
- ✓ Solar thermal heating aid.
- ✓ Preheating of industrial fluids.

The operation of a flat panel solar collector is based on heat transfer.

The sun's rays fall on the heat absorber of the collector. When radiation hits the surface of the absorber, some of its energy is converted into heat. As a result, the temperature of the solar collector increases. [19]

If a fluid is passed through the thermal solar panel, some of this heat is transferred to the liquid according to the first and second laws of thermodynamics. The rest of the energy is still lost as radiation from the solar thermal collector to the outside environment.

✓ If you want to achieve good performance and reduce energy consumption, you need to work the sensors at the lowest possible temperature.[19]

I.8.3.1.b. Vacuum Tube Sensors

A vacuum tube solar collector is a type of solar thermal collector that improves flat panel collectors. Solar collectors aim to convert solar radiation into thermal energy by reducing heat loss.

✓ The vacuum tube solar collector consists of a set of cylindrical tubes. The tubes consist of a selective absorber on a reflective seat and surrounded by a transparent glass cylinder. [19]

Figure.I.11.Vacuum Tube Sensors[19]

I.8.3.1.c. Concentrating solar collectors

A solar concentrator is a device designed to focus and concentrate solar radiation, and its application can involve both solar thermal power generation and solar photovoltaic power generation. Its operation is based on the use of reflective surfaces, usually formed by a series of mirrors arranged in an aligned manner. The main purpose of these solar concentrators is to capture as much solar radiation as possible and direct it to a small receiver.[19]

I.8.3.1.d. Hybrid Solar Collectors

Hybrid solar panels are devices that combine solar photovoltaic and thermal energy. Through them, you can get both electricity and heat. In other words, a PVT panel is capable of generating electrical energy and hot water.

For example, a hybrid solar panel consists of a photovoltaic collector with a heat exchanger. This exchanger is able to heat a fluid thanks to the part of the solar radiation that is not converted into electrical energy. [19]

I.8.3.2. Parabolic trough collectors

I.8.3.2.1. Définition

Parabolic trough collectors are another type of solar thermal collector. They use parabolic cylinders to concentrate all the sun's energy into a single point.

Instead of heliostats, this type of thermal solar panel uses rows of cylinder-shaped parabolic mirrors. Through the focus of the dish runs a pipe that receives concentrated rays from the sun, where the heat transfer fluid is heated through thermodynamic processes, normally a thermal oil. Currently, the fluid reaches temperatures close to 400 degrees Celsius.

Figure.I.12.Parabolic trough collectors[19]

I.8.3.2.2. The components of a Parabolic trough collectors

The main components of a Parabolic trough collectors are:[21]

- ✓ The metal structure to give rigidity to the whole.
- ✓ **The Parabolic Reflector:** The function of the parabolic receiver is to concentrate the sun's radiation on the absorbing tube. For this, it is built with reflective materials.
- ✓ **The absorber tube:** The solar concentration absorber tube consists of two concentric tubes separated by a layer of vacuum. The interior, through which the heated fluid circulates, is metallic and the exterior is made of glass.
- ✓ The working fluid that flows through the inner tube is different depending on the technology.
- ✓ **The Sun Tracking System:** The most common tracking system consists of a device that rotates the parabolic trough reflectors of the solar collector around an axis.

I.8.3.3. Parabolic sensors

Parabolic sensors are based on the well-known optical property of the paraboloid. Indeed, any incident ray orthogonal to the principal plane is reflected on the paraboloid towards the focal point, which can thus collect all the heat flux harvested by the paraboloid (again, minus the reflection efficiency). The concentration factor is therefore much higher than that of a CCP (it can reach 230°C).[19]

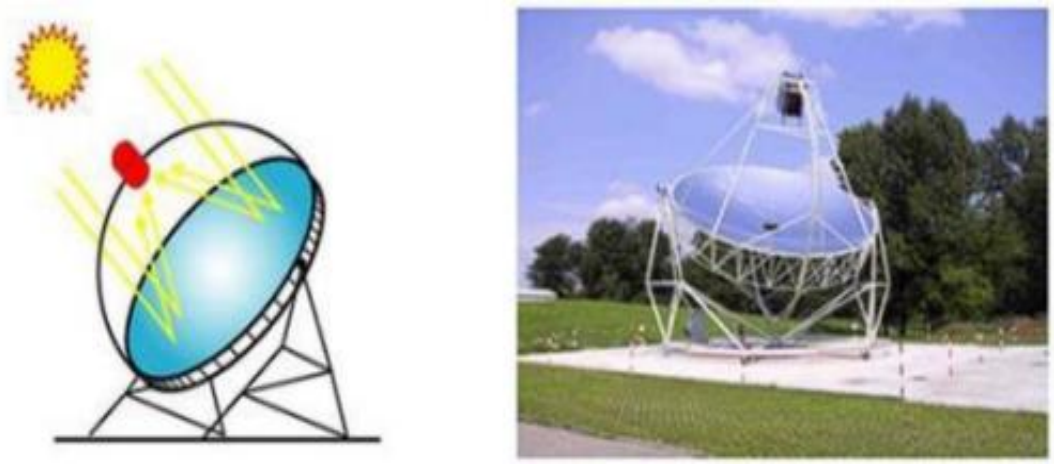

Figure.I.13.a parabolic sensor[19]

I.9.Different modes of heat transfer in parabolic cylindrical solar collector

Parabolic cylindrical solar collectors primarily utilize three modes of heat transfer: conduction , convection , radiation .

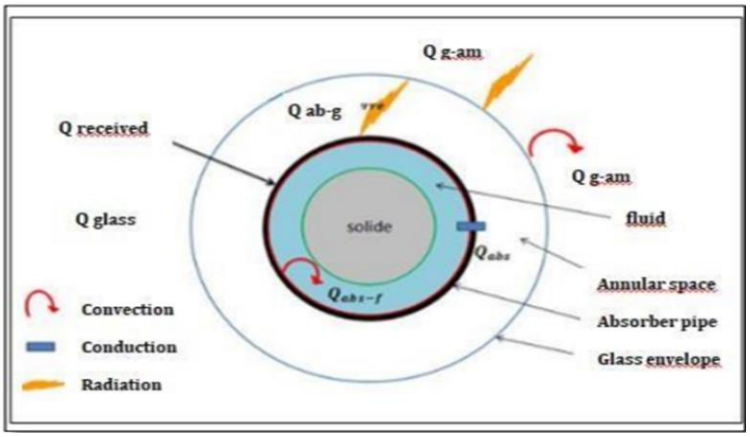

Figure.I.14.Simulation of different modes of heat transfer on a parabolic trough solar collector. [20]

1.9.1. Conduction through the absorber

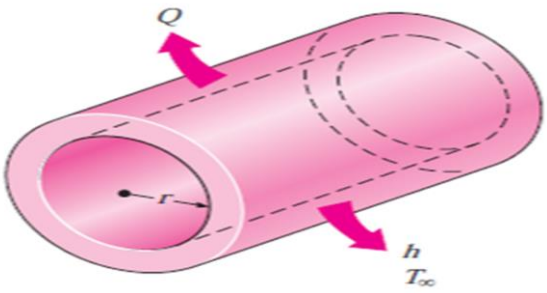

Figure.I.15. Conduction through the absorber[20]

Heat is lost from a hot-water pipe to the air outside in the radial direction, and thus heat transfer from a long pipe is one-dimensional[20]

Fourier's law of heat conduction for heat transfer through the cylindrical layer can be expressed as :

$$\boldsymbol{Q_{cond,cyl} = -kA\frac{dT}{dr}(W)} \quad \text{(I.15)}$$

where A=2πrL is the heat transfer area at location r. Note that A depends on r, and thus it varies in the direction of heat transfer. Separating the variables in the above equation and integrating from r = r_1, where T(r_1)=T_1, to r = r_2, where $T(r_2) = T_2$, gives :

$$\boldsymbol{\int_{r=r_1}^{r_2} \frac{Q_{cond.cyl}}{A} dr = \int_{T=T_1}^{T_2} kdT} \quad \text{(I.16)}$$

since $Q_{cond,cyl}$= constant. This equation can be rearranged as :

$$\boldsymbol{Q_{cond.cyl} = 2\pi Lk\frac{T_1-T_2}{Ln(r_{2/r_1})}(W)} \quad \text{(I.17)}$$

since $Q_{cond,cyl}$= constant. This equation can be rearranged as :

$$\boldsymbol{Q_{cond.cyl} = \frac{T_1-T_2}{R_{cyl}}(W)} \quad \text{(I.18)}$$

Where :

$$\boldsymbol{R_{cyl} = \frac{ln(r_{2/r_1})}{2\pi Lk} = \frac{ln(outer\ radius/inner\ radius)}{2\pi(length)(thermal\ conductivity)}} \quad \text{(I.19)}$$

Rcyl: is the thermal resistance of the cylindrical layer against heat conduction, or simply the conduction resistance of the cylinder layer.

I.9.2. Convection through the absorber

Convective heat transfer occurs whenever an object is either hotter or colder than a surrounding fluid. Convection only occurs in a moving liquid or a gas, never in a solid. The basic equation for the rate of convection heat transfer is known **as Newton's Law of Cooling**:

$$\boldsymbol{Q_{conv} = hA(T_\infty - T_S)} \quad \text{(I.20)}$$

where Q_{conv} is the convective heat transfer rate, h is the convective heat transfer coefficient, A=πDL is the surface area of the object being cooled or heated, T_∞ is the temperature of the surrounding fluid, and Ts is the surface temperature of the object. In English units h is expressed in units of Btu/(h·ft2·R), and in SI units it is W/(m^2·K). The algebraic sign

of Newton's law of cooling is positive for T∞ > Ts (heat transfer into the object) and negative when T∞ < Ts (heat transfer out of the object).

There are two types of convection: natural convection and forced convection. Natural convection is produced by density differences in a fluid produced by temperature differences in the fluid (e.g., as in "hot air rises"). Global atmospheric circulation and local weather phenomena (including wind) produce convective heat transfer.[22]

I.9.3 . Radiation Heat Transfer Coefficients

The heat transfer coefficient by radiation between the absorber tube and the glass envelope ($\boldsymbol{h_{r,int}}$) is deduced the following expression:

$$\boldsymbol{h_{r,int}} = \frac{\boldsymbol{\delta\left((T_A)^2+(T_v)^2(T_A+T_v)\right)}}{\frac{\boldsymbol{1}}{\boldsymbol{\varepsilon_A}}+\frac{\boldsymbol{1-\varepsilon_v}}{\boldsymbol{\varepsilon_v}}\left(\frac{\boldsymbol{D_{A,ext}}}{\boldsymbol{D_{V,int}}}\right)} \quad \text{(I.21)}$$

The heat transfer coefficient by radiation between the glass envelope and the sky ($h_{r,ext}$) is given as follows:[23]

$$\boldsymbol{h_{r,ext}} = \boldsymbol{\sigma\varepsilon_v}\left((\boldsymbol{T_V})^2 + \left(\boldsymbol{T_{sky}}\right)^2\left(\boldsymbol{T_{sky}} + \boldsymbol{T_V}\right)\right) \quad \text{(I.22)}$$

CHAPTER II

Nanofluids

CHAPTER II

Nanofluids

II.1 . Introduction

Currently, working fluids are used throughout the world through many different applications. These working fluids can consist of water, ethylene glycol, and various oils. They are used in many industries which include, but are not limited to: power generation, aerospace, medical field, and transportation. However, these fluids have a strong limiting factor when it comes to their ability to transfer heat. This is why there is a lot of research being done to try and improve this limiting factor. One of the main ways these working fluids are being modified is by the addition of nanoparticles to create what are called nanofluids.

II.2. Definition of nanofluid

A nanofluid is a mixture of nanoparticles within a base fluid. Nanoparticles change the physical properties of the working fluids including the thermal conductivity and viscosity. Initially, attempts were made to increase the thermal properties of working fluids with the millimeter and micrometer sized particles. These fluids had many problems though such as clogging of fluid paths, abrasion, and pressure drop . In an effort to create a working fluid without these problems in 1995, Choi first added nanoparticles to working fluids to create a nanofluid. A significant increase in the thermal conductivity of the fluids was observed. Most metals almost always have a higher thermal conductivity than liquids, therefore introducing a metal to a working fluid improves the ability of that fluid to transfer heat.

A significant amount of research has been done to identify the specific parameters that determine the thermal conductivity and viscosity of a nanofluid. Such parameters include the concentration of nanoparticles, size of nanoparticles, surfactants, temperature, base fluid, shape of nanoparticle, and using a hybrid nanofluid. Less research has been done examining the effect of these parameters on viscosity, but viscosity is an important concern in the design of nanofluids. The resistance of a fluid to flow and random motion of particles and molecules is directly tied to the viscosity of that fluid. Therefore, the heat transfer and pumping power required to pump a nanofluid could be greatly influenced by the characteristics of the nanofluid. This could have serious implications on the design of devices that utilize nanofluids.[24]

II.3. Classification of nanofluids

Nanofluids based on the composition of the nanomaterial dispersed can be classified into conventional and hybrid nanofluids :

II.3.1. Conventional or mononanofluids

Nanofluids as discovered, typically consisting of a single most nanomaterials component dispersed throughout the fluid phase are the conventional type of nanofluids known as mononanofluids. It may consist of any of the nanomaterials. This involves simplicity and the nature, rather behavior of the nanomaterials, is bound to the only component present.[25]

II.3.2. Hybrid nanofluids

The increasing need for enhanced properties of nanofluids has led to the discovery of "hybrid nanofluid" that involve the use of two or more components either separately present in the nanofluid or bound to each other. In addition, the limitations of a few systems like agglomeration in pure metal-based nanofluids and lesser thermal transport in metal oxide-based nanofluids are among the main reasons for propagation of the idea of nanofluids toward the development of hybrid nanofluids.

II.3.2.1. Nanomaterial mixture-based

Nanofluid prepared by simply physically mixing two or more types of nanomaterials in a base fluid can be called as mixture-based hybrid nanofluids. This is simply done so as to impart properties of both the components to the fluid. Mostly, these kinds of nanofluids contain binary mixtures of nanoparticles. Various researchers have dispersed different types of nanomaterials in a base fluid in varying ratios and studied their effect on various properties of the nanofluid. [26]

Table.II.1. details of a few Nanomaterial[25]

Nanomaterial	Base fluid	Avg. particle size of nanomaterials	Ratio of nanomaterial	Nanofluid concentration
Carbon nanotubes and gold nanoparticles	Water	Carbon nanotubes: 150–200nm Au: 15nm	–	0.3vol.% CNT + 1.4vol.% Au and 0.5vol.% CNT + 1.4vol.% Au
Carbon nanotubes and copper nanoparticles	Water	Carbon nanotubes: 150–200nm Cu: 35–50nm	–	0.5vol.% CNT + 0.05vol.% Cu, 0.5vol.% CNT + 0.1vol.% Cu, 0.5vol.% CNT + 0.2vol.% Cu, and 0.5vol.% CNT + 0.3vol.% Cu
Alumina nanoparticles and copper oxide nanoparticles	Water	–	Alumina=2.5mg and copper oxide=2.5mg	0.25, 0.5, and 1.0vol.%

II.3.2.2. Nanocomposite-based

Nanocomposites, on the contrary, are composites of two or more materials out of which one is in nanoscale. It can be combinations of any of the nanomaterials. Apart from achieving the synergism out of such materials, there are many purposes that drive the development of such materials for nanofluid applications. For example, due to the attraction forces between two sheets of graphene, nanofluids containing graphene are prone to sheet-restacking and consequently agglomeration leading to deterioration of the uniformity and stability of the nanofluid. [27]

II.4. Different Types of Nanoparticles

Studies have revealed the thermo-physical properties of several fluids can be improved by the addition of small concentrations of nanoparticles. Types of nanoparticles investigated include pure metals (Au, Ag, Cu, Al, and Fe), metal oxides (Al2O3, CuO, Fe3O4, SiO2, TiO2, and ZnO), Carbides (SiC, TiC) and a variety of carbon materials (diamond, graphite, single/multi wall carbon nanotubes). Many of these nanoparticle types have been incorporated into fluids such as water, water/ethylene glycol, ethylene glycol and oils. In terms of pure metals, both Au and Ag nanoparticles have been studied because of their unusual optical, electronic and chemical properties.[28]

Table.II.2. The thermo-physical properties of Nanoparticles and based fluid[27]

	Nanoparticule et fluide de base	K $(W/m.k)$	ρ (kg/m^3)	C_p $(J/kg.k)$	μ $(Pa.s)$
Métallique (solides)	**Cu**	400	8954	383	
	Fe	80.2	7870	447	
	Ni	90.7	8900	444	
	Au	317	19.300	129	
	Ag	429	10.500	235	
	C(diamant)	2300	3500	509	
Oxyde métallique (solides)	**SiO_2**	1.38	2220	745	
	TiO_2	8.4	4157	710	
	Al_2O_3	63	3970	765	
	CuO	69	6350	535	
	SiC	490	3160	675	
Liquides non métallique	L'eau	0.613	1000	4183	0.0008513
	Ethylène-glycol (EG)	0.258	1132	2349	0.0157

Table.II.3. Basic fluid combination/nanoparticles available in literature. [27]

Nanocomposite	Type of nanocomposite	Synthesis method	Base fluid
Silver-decorated hydrogen-exfoliated graphene (Ag/HEG)	Binary (metal/carbon)	Chemical reduction method	Water and ethylene glycol
Alumina-copper (Al_2O_3-Cu)	Binary (metal/metal)	Thermochemical synthesis method	Water
Cu nanoparticles decorated on graphene-carbon nanotube (Gr-CNT/Cu)	Tertiary (metal/carbon)	Chemical reduction method	Ethylene glycol
Copper-titanium dioxide (Cu-TiO_2)	Binary (metal/metal oxide)	Chemical reduction method	Ethylene glycol-water mixture
Alumina-copper (Al_2O_3-Cu)	Binary (metal oxide/metal)	Thermochemical synthesis method	Water

Table.II.4.a selection of thermal conductivity measurements from several nanofluid studies.

Nanoparticle	Particle Size (nm)	Working Fluid	Fraction	Thermal Enhancement (%)
Metals				
Ag	<100	Water	0.3–0.9 vol %	30 at 50 °C
Ag	100–500	Ethylene Glycol	0.1–1.0 vol %	18
Cu	50–100	Water	0.1 vol %	24
Cu	<10	Ethylene Glycol	0.01–0.05 vol %	41
Fe	10	Ethylene Glycol	0.1–0.55 vol %	18
Metal Oxides				
Al_2O_3	9	Water	2–10 vol %	29
Al_2O_3	28	Water/Ethylene Glycol	3–8 vol %	41
Al_2O_3	650–1000	Transformer oil	0.5–4 vol %	20
CuO	100	Water	7.5 vol %	52
TiO_2	15	Water	0.5–5 vol %	30

II.5. Methods of preparing nanofluids

Nanofluids are produced by several techniques first step, second step, and other techniques. To avoid the sedimentation of nanoparticles during its operation, surfactant may be added to them. Nanofluid preparation is the first step ahead of any implementations. Therefore, it entails more focus from researchers to obtain a good stage of stability. Colloidal theory states that sedimentation in suspensions ceases when the particle size is below a critical radius due to counterbalancing gravity forces by the Brownian forces. Nanoparticles of a smaller size may be a better size in the different applications. However, it has a high surface which leads to the formation of agglomerates among them. Therefore, to obtain a stable nanofluid with optimum particle diameter and concentration, it is considered a big challenge for researchers. Two common methods are used to produce nanofluids, the two-step method and the one step method, and others have worked up some innovations.[29]

II.5.1. The two-step method

The two-step method is the common method to produce nanofluids. Nanoparticles of different materials including nanofibers, nanotubes, or other nanomaterials are first produced as nanosized from 10 to 100 nm by chemical or physical methods. Then, the nanosized powder will be dispersed in base fluids with the help of intensive magnetic force agitation, ultrasonic agitation, high-shear mixing, homogenizing, and ball milling. As resulting from high surface area and surface activity, nanoparticles tend to aggregate reflecting adversely on the stability of nanofluid . To avoid that effect, the surfactant is added to the nanofluids.

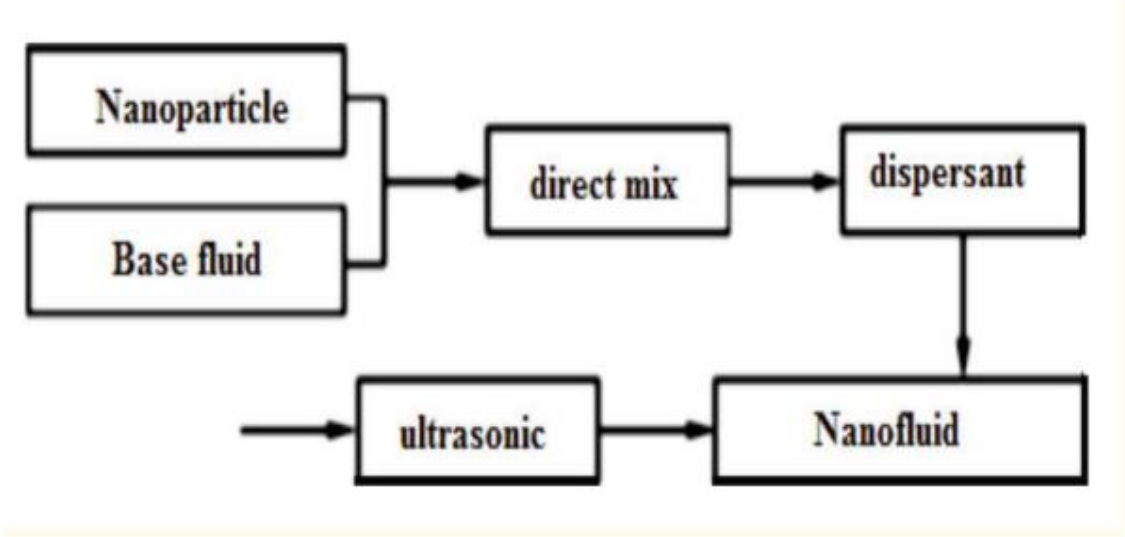

Figure.II.1. Shows a block diagram of preparation of two-step method. [28]

II.5.2. One-step method

The one-step process is simultaneously making and dispersing the particles in the base fluids which could be reduced to the agglomeration of nanoparticles. This method makes the nanofluid more stable with a limitation of the high cost of the process.[30]

II.6. Applications of nanofluids for heat transfer process

Nanofluids as a combination of base fluid and a low concentration of nano-sized particles of metal or metal oxides are used in different fields of human activity, including engineering devices in power and chemical engineering, medicine, electronics, and others. The main reason for such huge variety of nanofluid applications is the possibility, from one side, to enhance the heat and mass transfer due to the low concentration of nano-sized particles andfrom the other side, to control the transport processes that can be used, e.g., in the drag delivery systems.[31]

Now, nanofluids are promising mediums as alternatives to the base fluids, and hence the researches are still under investigation to improve and develop the heat transfer equipment systems .[29]

•Other applications :

•The heat exchanger.

• Cooling of electronic components (producing a stable nanofluid that is compatible with electronic circuits and components).

• Nanoparticles for refrigerator efficiency (formulation of lubricants and coolant liquids mixed with nanoparticles could lead to an increase in the energy efficiency of refrigerators).

• Aerospace and space.

• Cooling of nuclear systems.

• Transportation (cooling management / Thermal engine vehicle).

• Other applications (fuel cells, solar water heating, drilling, thermal storage).[30]

II.7 . The advantages and The disadvantages of Nanofluids

-The advantages

High specific surface area and hence more heat transfer surface between particles and fluid. Nanofluids show high dispersion stability with predominant Brownian motion of particles. Presence of nanofluids results in reduction of particle clogging as compared to conventional fluids thus promoting system miniaturization. These new engineered fluids have adjustable properties including thermal conductivity and surface wet ability, by varying particle concentrations. [30]

-The disadvantages

-High pressure losses.

- Erosion.

- Sedimentation.

- Flow blockages.

- The high cost of nanofluids.

- Challenges in the production process.[30]

II.8. Thermophysical properties of nanofluids

II.8.1 volume fraction

The volume fraction is the most important property for a nanofluid because the calculations of all other properties are based on the volume fraction of the nanofluid. The volume fraction can be defined as the volume of solid particles (nanoparticles) divided by the total volume (nanoparticles + base fluid). The value of the volume fraction varies between 0 (pure base fluid) and 1. The volume fraction isgiven by the following relation :

$$\varphi = \frac{v_s}{v_s + v_f} \qquad (II.1)$$

"Vs" and "Vf" are respectively the volume of nanoparticles and the volume of the base fluid $[m^3]$.

II.8.2 Density

The density of nanofluids is proportional to the volume fraction of particles and increases with the addition of nanoparticles. In the literature, and in the absence of experimental results, the density of nanofluids is often calculated using a mixing law in which the nanofluid is assumed to be homogeneous. This approach was introduced by Pak (1998).[32]

$$\boldsymbol{\rho_{nf} = (1 - \phi)\rho_{bf} + \phi\rho_{sp}} \quad \boldsymbol{(II.2)}$$

With:

$\boldsymbol{\rho_{nf}}$: The density of the nanofluid

$\boldsymbol{\rho_{bf}}$: The density of the base fluid

$\boldsymbol{\rho_{sp}}$**:**the density of nanoparticles

II.8.3. Theoretical Models

These following theoretical models being presented are based on a single nanofluid and not hybrid nanofluids.

II.8.3.1. Effective Medium Theory

The effective medium theory (EMT) is a method used to predict the thermophysical properties of a fluid mixture. EMT models rely on the volume fraction of the solute and the properties of the particle and base fluid. EMT models assume a stationary and homogenous dispersion of particles within the base fluid as shown in Figure.II.2

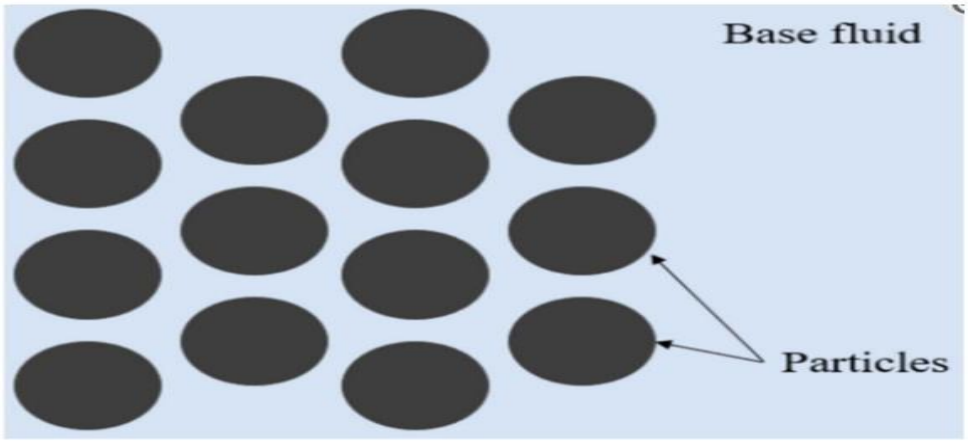

Figure.II.2.Particles in Fluid base [31]

II.8.3.2. Thermal conductivity

Thermal conductivity is the ability of a material to conduct or transmit heat. It's a crucial property for enhancing the thermal performance of a heat transfer fluid. The synthesis of nanofluids addresses the need to improve and enhance the thermal conductivity of liquids. There are several theoretical models available to estimate, under certain conditions, the thermal conductivity of suspensions. In this section, we will present the most commonly used models for nanofluids :

-Maxwell Model

This static based theory was first developed by Maxwell in 1873 where Maxwell experimented with micro sized particles and channels. His research resulted in the formulation of the following equation shown below in Equation :

$$k_{nf} = \frac{k_p + 2k_{bf} + 2\phi(k_p - k_{bf})}{k_p + 2k_{bf} - \phi(k_p - k_{bf})} k_{bf} \qquad \text{(II.3)}$$

Where k_p is the thermal conductivity of the nanoparticle, k_{bf} is the thermal conductivity of the base fluid, k_{nf} is the thermal conductivity of the nanofluid and ϕ the volume concentration of particles within a base fluid. This model is effective for calculating thermal conductivity of mixtures using micro and milli sized particles within a base fluid under relatively low concentrations of less than 2% .

-Hamilton & Crosser Model

It is known that nanoparticles can form agglomerates due to interacting particles when dispersed in a liquid and Hamilton Crosser believed that the shape of the agglomerates formed could impact the thermal conductivity of the nanofluids. Hamilton and Crosser proposed considered the agglomerate shape and proposed the following equation:

$$k_{nf} = k_{bf}\left[\frac{k_p + (n-1)k_{bf} - (n-1)(k_{bf} - k_p)\phi}{k_p + (n-1)k_f + (k_{bf} - k_p)\phi}\right] \qquad \text{(II.4)}$$

Where n is an empirical constant based on the shape of the nanoparticle agglomerates formed. It was determined that n can be calculated based on the sphericity of the agglomerates. It was determined that n is three for spherical particles and six for cylindrical particles. A model was also created by Wasp which reduces down to the Hamilton Crosser model when the particle agglomerates are described as spheres given as :

$$k_{nf} = k_{bf} \frac{k_p + 2k_{bf} - 2\phi(k_{bf} - k_p)}{k_p + 2k_{bf} + \phi(k_{bf} - k_p)} \qquad \text{(II.5)}$$

Based on experimental work done using Ag–water nanofluids, Godson proposed the following model for the thermal conductivity of nanofluids as the other models that have been proposed predicted a thermal conductivity which was lower than the measured thermal conductivity. The model is given as:

$$\mathrm{k_{nf}} = \mathrm{k_{bf}}(0.9692\phi + 0.9508) \qquad \text{(II.6)}$$

Sundar Model

Sundar worked on looking at the effect of thermal conductivity with temperature. Sundar created his own experiment to analyze the effect of changes in temperature. a correlation was given to show his experimental empirical equation shown as:

$$k_{nf} = k_{bf}(1 + 10.5\phi)^{0.1051} \qquad \text{(II.7)}$$

Yu and Choi Model

Yu and Choi (2003) proposed a modified model that is more complex than the Hamilton-Crosser, which takes into account the interface effect between particles and the fluid of base but it is only valid for spherical shaped particles.

$$k_{nf} = \frac{k_s + 2k_f - 2(k_s - k_f)(1+\mathcal{B})^3\varphi}{k_s + 2k_f - (k_s - k_f)(1+\mathcal{B})^3\varphi} k_f \qquad \text{(II.8)}$$

Where β : is the ratio of the nanometric layer to the particle radius.

II.8.3.3. Empirically Determined Viscosity Models

-Einstein Model

While increasing thermal conductivity of a nanofluid is desirable to improve the heat transfer capabilities of the nanofluid, the effect on viscosity of the nanofluid must also be considered. The pumping power required for a working fluid is related to the viscosity of the fluid. Therefore, understating the viscosity of a fluid is necessary to optimize the system in which it will be used. Several of the theoretical models to describe the viscosity of a nanofluid will be discussed in this section.

One of the first attempts to model the viscosity of a fluid-particle mixture was done by Einstein in the 1900s. This early model was used to predict the effective viscosity of mixture fluids and was applicable in limited low volume concentration applications $\phi < 0.02\%$.

$$\mu_{nf} = (1 + 2.5\phi)\mu_{bf} \qquad (II.9)$$

-Brinkman Model

The model proposed is most accurate at low particle concentrations. Brinkman attempted to expand on the model proposed by Einstein based on the work done by in the following model:[33]

$$\mu_{nf} = \mu_{bf}\left(\frac{1}{(1-\phi)^{2.5}}\right) \qquad (II.10)$$

μ_{nf} : is the viscosity of the nanofluid and μ_{bf} is the viscosity of the base fluid.

-Batchelor Model

$$\mu_{nf} = \mu_f(1 + \eta\varphi + k_h\varphi^2 + \cdots) \qquad (II.11)$$

II.8.3.4. Specific heat capacity

Thermal conductivity and dynamic viscosity are the two most studied thermophysical properties in the case of nanofluids. Specific heat capacity of nanofluids, on the other hand, is rarely studied, especially experimentally. Specific heat capacity, or mass heat capacity, is defined as the amount of energy required per unit mass to raise the temperature of a substance

by one Kelvin. This quantity is incorporated into the energy equation and therefore requires rigorous determination. Most studies in the literature use one of the two models defined by:

-Pak and Cho(1998) Model [34]

$$(C_p)_{nf} = (1 - \varphi)(C_p)_f + \varphi(C_p)_s \qquad (II.12)$$

-Xuan (2000) Model

$$(\rho C_p)_{nf} = \frac{(1-\varphi)(\rho C_p)_f + \varphi(\rho C_p)_s}{(1-\varphi)\rho_f(C_p)_f + \varphi\rho_s} \qquad (II.13)$$

II.8.3.5. Thermal expansion coefficient

The variation in density under the influence of temperature is characterized by the thermal expansion coefficient, also known as the isobaric expansion coefficient.

$$\beta = \frac{1}{\rho}\left(\frac{\partial\rho}{\partial T}\right) \qquad (II.14)$$

II.9. Syltherm 800

Syltherm 800 fluid is a highly stable, long-lasting, silicone fluid designed for high-temperature liquid phase operation. It has a recommended operating temperature range of -40°F (-40°C) to 750°F (400°C). Operating continuously at the upper end of this range, SYLTHERM

800 fluid exhibits low potential for fouling and can often remain in service for 10 years or more.

The fluid is essentially odorless and is low in acute oral toxicity.[33]

Include:

■ Low fouling potential

■ Low freeze point

■ High-temperature stability

■ Long life

■ Noncorrosive

■ Low acute oral toxicity

Thermophysical properties of Syltherm 800 as a function of temperature are given by following equations :

$\mu = 8.47 * 10^{-2} - 5.54 * 10^{-4}\ T + 1.39 * 10^{-6}\ T^2 - 1.57 * 10^{-9}\ T^3 + 6.67 * 10^{-13}\ T^4$

$\lambda = 1.90 * 10^{-1} - 1.87 * 10^{-4}\ T - 5.75 * 10^{-10}\ T^2$

$C = 1.1078 * 10^3 + 1.7080\ T$

$\rho = 1.1057 * 10^3 - 4.1535 * 10^{-1} T - 6.0616 * 10^{-4} T^2$

Table.II.5. Saturated Liquid Properties of SYLTHERM 800 Fluid (SI Units) .[33]

Temp. °C	*Specific Heat* kJ/kg K	*Density* kg/m³	*Thermal Conductivity* W/m K	*Viscosity* mPa•s	*Vapor Pressure* kPa
-40	1.506	990.61	0.1463	51.05	0.0
-30	1.523	981.08	0.1444	35.45	0.0
-20	1.540	971.68	0.1425	25.86	0.0
-10	1.557	962.37	0.1407	19.61	0.0
0	1.574	953.16	0.1388	15.33	0.0
10	1.591	944.04	0.1369	12.27	0.0
20	1.608	934.99	0.1350	10.03	0.0
30	1.625	926.00	0.1331	8.32	0.0
40	1.643	917.07	0.1312	7.00	0.1
50	1.660	908.18	0.1294	5.96	0.20
60	1.677	899.32	0.1275	5.12	0.42
70	1.694	890.49	0.1256	4.43	0.81
80	1.711	881.68	0.1237	3.86	1.46
90	1.728	872.86	0.1218	3.39	2.47
100	1.745	864.05	0.1200	2.99	4.00
110	1.762	855.21	0.1181	2.65	6.22
120	1.779	846.35	0.1162	2.36	9.30
130	1.796	837.46	0.1143	2.11	13.5
140	1.813	828.51	0.1124	1.89	19.0
150	1.830	819.51	0.1106	1.70	26.1
160	1.847	810.45	0.1087	1.54	35.0
170	1.864	801.31	0.1068	1.39	46.0
180	1.882	792.08	0.1049	1.26	59.5
190	1.899	782.76	0.1030	1.15	75.6
200	1.916	773.33	0.1012	1.05	94.6
210	1.933	763.78	0.0993	0.96	116.8
220	1.950	754.11	0.0974	0.88	142.4
230	1.967	744.30	0.0955	0.81	171.7
240	1.984	734.35	0.0936	0.74	204.8
250	2.001	724.24	0.0918	0.69	242.1
260	2.018	713.96	0.0899	0.63	283.6
270	2.035	703.51	0.0880	0.59	329.6
280	2.052	692.87	0.0861	0.54	380.2
290	2.069	682.03	0.0842	0.50	435.4
300	2.086	670.99	0.0824	0.47	495.5
310	2.104	659.73	0.0805	0.44	560.5
320	2.121	648.24	0.0786	0.41	630.5
330	2.138	636.52	0.0767	0.38	705.6
340	2.155	624.55	0.0748	0.36	785.7
350	2.172	612.33	0.0729	0.33	870.9
360	2.189	599.83	0.0711	0.31	961.2
370	2.206	587.07	0.0692	0.29	1057
380	2.223	574.01	0.0673	0.28	1157
390	2.240	560.66	0.0654	0.26	1262
400	2.257	547.00	0.0635	0.25	1373

Chapter III

Mathematical Formulation

Chapter III

Mathematical Formulation

III.1 Introduction

In this chapter we will present the configurations studied, the hypotheses simplifying equations, as well as the continuity and momentum equations coupled with the energy equation for the fluid, which governs the phenomenon of thermal convection incompressible and stationary in a parabolic trough solar collector.

III.2 The geometries of the problem studied

The geometrical model used in this study includes of the receiver of a cylindrical-parabolic trough solar collector as schematized in Figure III.1. The receiver consists of two coaxial tubes, one of which is made of copper metal and is called an absorber with an inner and outer diameter $D_{ai} = 65mm$, $D_{ae} = 70mm$, and the other is made of glass with an inner and outer diameter $D_{gi} = 109mm$, $D_{ge} = 115mm$, The space between the two is filled with air. Both tubes are subjected to direct and diffuse solar radiation as well as radiation reflected and concentrated by the cylindrical-parabolic mirror. The reflector has a length $L_r = 4m$ and aperture width $W_a = 5,77m$, at a focal distance $F = 1,71m$ from the absorber .

The absorber tube of a parabolic solar collector is equipped with twisted tape. In this model, the twisted ratio (y/W) is 8 and the twisted tape thickness is 2 mm (Figure III. 1). The geometrical specifications of the model can be seen in Table 1. In the current work, copper (Cu) nanoparticles with different volume percentages (from one to four percent) are added to Syltherm 800 to enhance the rate of heat transfer inside the collector adsorbent tube.

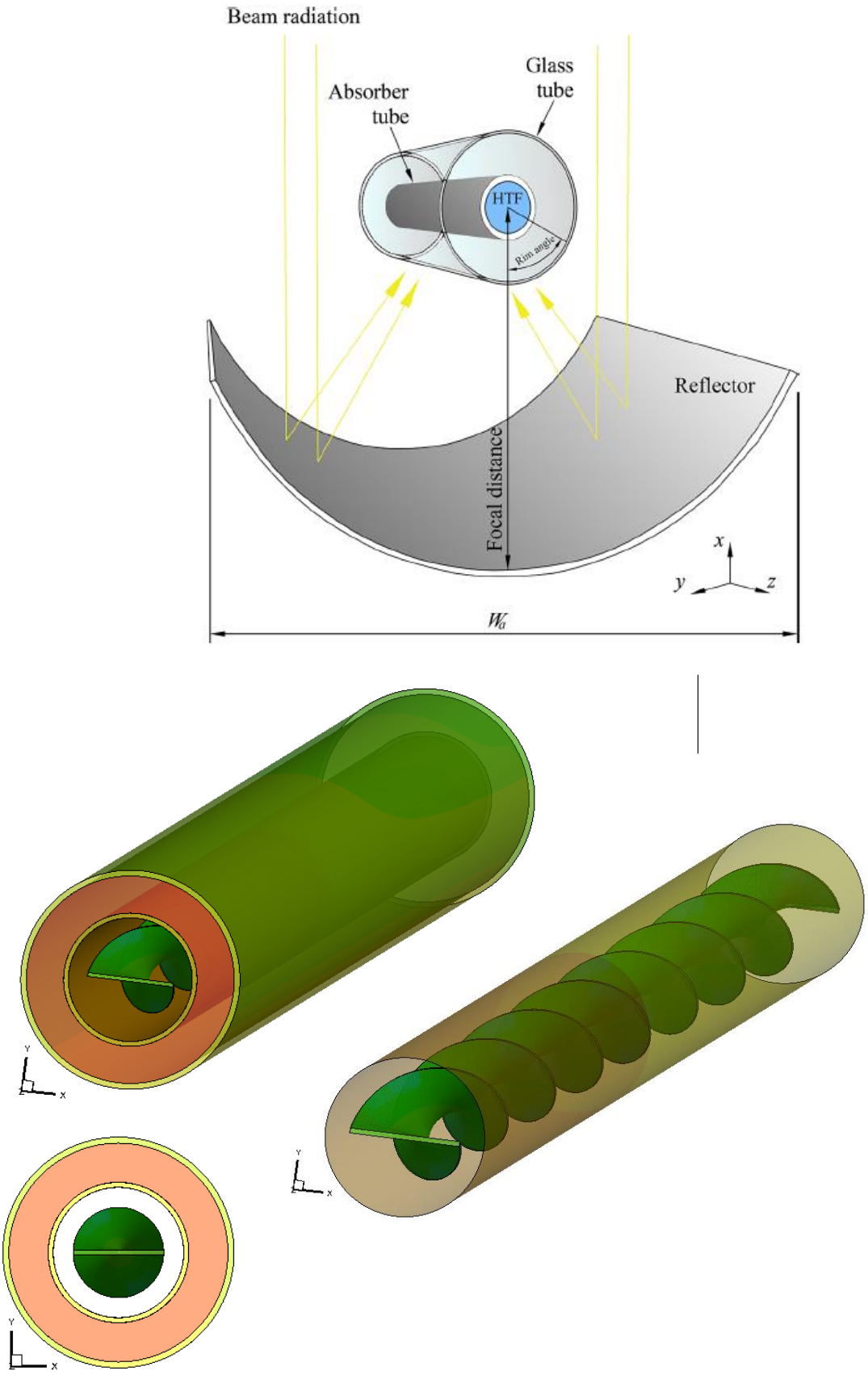

Figure.III.1. The cylindrical-parabolic trough solar collector, absorber tube equipped with twisted tape.

Table.III.1.Dimensions of the cylindrical-parabolic trough solar collector

Items	Parameter
Aperture width	5.77m
Focal length	1.71m
Length	4m
Inner / outer diameter of absorber tube	65/70 mm
Inner/outer diameter of glass envelop	109/115
Mirror reflectivity	0.94
Glass envelope transmissivity	0.96
Coating absorptivity	0.95

III.3. Simplifying assumptions

For the simplification of numerical analysis, the following assumptions are made

1. Three-dimensional flow (along x, y, z).
2. The heat transfer phenomenon is assumed to be in steady state. ($\partial\partial t$ = 0).
3. The heat transfer fluid (HFT) is considered to be incompressible and laminar .
4. The working fluid's (Syltherm-800) physical properties are supposed to be dependent upon temperature, and therefore the physical properties are considered to be a polynomial function of temperature.

III.4. The Governing Equations of the Problem Under Study

After the introduction of the assumptions given above. We can establish the different equations necessary to solve the problem considered in this study as follows:

III.4.1.Continuity equation

$$\frac{\partial \mathrm{u}}{\partial \mathrm{x}} + \frac{\partial \mathrm{v}}{\partial \mathrm{y}} + \frac{\partial \mathrm{w}}{\partial \mathrm{z}} = 0 \qquad \text{(III.1)}$$

III.4.2.Equation for Conservation of Momentum

Following **x:**

$$\left[\frac{\partial uu}{\partial x} + \frac{\partial uv}{\partial y} + \frac{\partial uw}{\partial z}\right] = -\frac{1}{\rho_0}\frac{\partial p}{\partial x} + v\left\{\frac{\partial}{\partial x}\left[u\frac{\partial u}{\partial x}\right] + \frac{\partial}{\partial y}\left[v\frac{\partial u}{\partial y}\right] + \frac{\partial}{\partial z}\left[w\frac{\partial u}{\partial z}\right]\right\} \qquad \text{(III.2)}$$

Following **y :**

$$\left[\frac{\partial vu}{\partial x}+\frac{\partial vv}{\partial y}+\frac{\partial vw}{\partial z}\right]=-\frac{1}{\rho_0}\frac{\partial p}{\partial x}+v\left\{\frac{\partial}{\partial x}\left[u\frac{\partial v}{\partial x}\right]+\frac{\partial}{\partial y}\left[v\frac{\partial v}{\partial y}\right]+\frac{\partial}{\partial z}\left[w\frac{\partial v}{\partial z}\right]\right\}+\ g\beta(T-T_0) \quad \text{(III.3)}$$

Following **z :**

$$\left[\frac{\partial wu}{\partial x}+\frac{\partial wv}{\partial y}+\frac{\partial ww}{\partial z}\right]=-\frac{1}{\rho_0}\frac{\partial p}{\partial x}+v\left\{\frac{\partial}{\partial x}\left[u\frac{\partial w}{\partial x}\right]+\frac{\partial}{\partial y}\left[v\frac{\partial w}{\partial y}\right]+\frac{\partial}{\partial z}\left[w\frac{\partial w}{\partial z}\right]\right\} \quad \textit{(III.4)}$$

III.4.3. Energy Equation

$$\rho_0.C_{P.}\left[\mathrm{u}\frac{\partial \mathrm{T}}{\partial \mathrm{x}}+\mathrm{v}\frac{\partial \mathrm{T}}{\partial \mathrm{y}}+\mathrm{w}\frac{\partial \mathrm{T}}{\partial \mathrm{z}}\right]=\frac{\partial}{\partial \mathrm{x}}\left[\lambda\frac{\partial \mathrm{T}}{\partial \mathrm{x}}\right]+\frac{\partial}{\partial \mathrm{y}}\left[\lambda\frac{\partial \mathrm{T}}{\partial \mathrm{y}}\right]+\frac{\partial}{\partial \mathrm{z}}\left[\lambda\frac{\partial \mathrm{T}}{\partial \mathrm{z}}\right] \quad \text{(III.5)}$$

λ:The thermal conductivity

Cp : The specific heat at constant pressure.

ρ : The density.

β : The coefficient of isobaric expansion of the fluid.

μ : Dynamic viscosity of the fluid.

III.5. Radiation model

One of the useful features of Fluent is the solar load model. This capability can be used to calculate the effective radiation load based on the position on the Earth's surface (latitude and longitude), the orientation of the model relative to the north, the time of day, the season, and the conditions set for clear or cloudy weather.

Fluent provides radiation models that enable us to include radiation with or without participating medium in heat transfer simulations. These models are :

- Discrete Transfer Radiation Model
- Rosseland radiation model
- Discrete Ordinate radiation model

III.6. Radiative transfer equation

The radiative transfer equation for an absorbing, emitting, and scattering medium at position $\vec{r}$ in the direction $\vec{s}$ is :

$$\frac{dI(\vec{r},\vec{s})}{ds}+(a+\sigma_s)I(\vec{r},\vec{s})=an^2\frac{\sigma T^4}{\pi}+\frac{\sigma_s}{4\pi}\int_0^{4\pi}I(\vec{r},\vec{s}')\Phi(\vec{s},\vec{s}')d\Omega \quad \text{(III.6)}$$

I : The radiation intensity (it depends on the direction and position of the vector) ;

$\vec{r}$: The position vector ;

$\vec{s}$: The direction vector ;

$\vec{s'}$: The direction of the diffusion vector ;

a : The absorption coefficient ;

s : The path length ;

n : The refractive index ;

σs : The diffusion coefficient ;

σ : The Stefan-Boltzmann constant ($5.672x10^{-8}$ W/m^2K^4);

Φ : The phase function ;

T :The local temperature;

Ω : The solid angle;

III.7. The equations of the Rosseland model

The radiation flux **qr** is given by the following equation :

$$qr = -\frac{1}{3(a+\sigma_s)-G\sigma_s}\nabla G \qquad (\text{III.7})$$

a : The absorption coefficient ;

σs : The scattering coefficient ;

G is The incident radiation;

C is The coefficient of the linear-anisotropic phase function;

After introducing the parameter :

$$\Gamma = \frac{1}{(3(a+\sigma_s)-G\sigma_S)} \qquad (\text{III.8})$$

The equation (III.7) simplifies to :

$$qr = -\Gamma\nabla G \qquad (\text{III.9})$$

The transport equation of **G** is:

$$\nabla.(\Gamma\nabla G) - aG + 4a\sigma T^4 = S_G \qquad (\text{III.10})$$

Where **σ** is the Stefan-Boltzmann constant and $\mathbf{S_G}$ is a radiation source defined by the user.

Fluent solves this equation to determine the local radiation intensity when the Rosseland model is active.

By combining Equations (III.9) and (III.10), we obtain the following equation:

$$-\nabla.q_r = aG - 4a\sigma T^4 \qquad (\text{III.11})$$

III.8. Boundary conditions

The resolution of the system of equations obtained previously requires the incorporation of boundary conditions for each dependent variable. The boundary conditions for the entire governing set of equations are presented below:

- **The inlet:**

- velocity inlet :
uo, To=25°C

$$\mathrm{Re} = \frac{\rho.u_0.D_{ai}}{\mu} \Longrightarrow u_0 = \frac{\mathrm{Re}.\mu}{\rho.D_{ai}} \qquad \text{(III.12)}$$

- **The outlet: (pressure outlet) :**

$$P = P_{atm}, \ \frac{\partial T}{\partial x} = \frac{\partial T}{\partial y} = \frac{\partial T}{\partial z} = 0 \qquad \text{(III.13)}$$

- The wall-fluid interfaces are coupled: (inner wall of the glass and the air) and (inner wall of the absorber and the fluid :

$$k_s \frac{\partial T}{\partial n}\Big|_{paroi} = k_n \frac{\partial T}{\partial n}\Big|_{paroi} \qquad \text{(III.14)}$$

For the outer wall of the glass tube, a mixed boundary condition is used to account for both radiation and heat transfer by convection. There is heat exchange by radiation between this surface and the sky.

-The convective flux was calculated using **Newton's law** :

$$\varphi = h.S.\left(T_p - T_\infty\right) \qquad \text{(III.15)}$$

$$h = 4.V_v^{0.58}.D_{ve}^{-0.42} \qquad \text{(III.16)}$$

Where $\mathbf{V_v}$ is the wind speed and $\mathbf{D_{ve}}$ is the outer diameter of the glass tube.

For the M'sila region, the average annual wind speed is 4.5 m/s.

-The solar flux was modeled using the (Solar load Model) for the M'sila region.

III.9. Calculation of Hydrodynamic and Thermal Parameters

III.9.1.Reynolds number

Reynolds, an English engineer specialized in hydrodynamics, introduced this number, which bears his name and is constantly used in calculations. It is a function of three parameters: the diameter '**D**,' the velocity '"**uo**,' and the cinematic viscosity of the fluid **"ν".**

$$\mathrm{Re} = \frac{u_0 D_h}{vf} \qquad \text{(III.17)}$$

u_0 : Fluid inlet velocity [m/s] .

D_h : Hydraulic diameter [m].

vf : cinematic viscosity of the fluid [m^2 /s].

- ***Hydraulic dialeter[m]***

$$D_h = \frac{4V}{S} \leftrightarrow \frac{4\frac{\pi D^2}{4}L}{\pi D L} \qquad \text{(III.18)}$$

V : the volume in contact with the fluid**.**

S: the surface in contact with the fluid .

III.9.2. Convective heat transfer coefficient h

$$h = \frac{q_c}{A(Tw - Tm)} \quad [W/m^2K] \qquad \text{(III.19)}$$

qc : Amount of heat defined by the following expression:

$$q_c = \dot{m} C_p (T_{out} - T_0) \qquad \text{(III.20)}$$

T_{out} :Average outlet temperature [K].

T_0 : Inlet temperature [K].

ṁ : Mass flow rate [kg/s].

Cp : Specific heat capacity at constant pressure.

A : Surface for thermal exchange [m^2].

$$T_{out} = \frac{\iint A\, Tu\, dA}{\iint Tu\, dA} \qquad \text{(III.21)}$$

III.9.3.Nusselt number

The Nusselt number is a dimensionless number used to characterize heat transfer between a fluid and a surface, known as convective heat transfer. The average Nusselt number has been defined as follows:

$$Nu = \frac{h_m D_h}{kf} \qquad \text{(III.22)}$$

h_m :Average convection coefficient [W/m²K].

k_f :Thermal conductivity of the fluid [W/m K].

III.10.Conclusion

In this chapter, we presented the studied geometry, as well as the equations governing our problem. We also introduced the boundary conditions and simplifying assumptions. For solving the governing equations and creating the geometry and mesh, we will use the software Gambit and Fluent.

Chapter IV

Numerical Simulation Procedure

Chapter IV

Numerical Simulation Procedure

IV.1.Introduction

In our study, we used two software programs. Gambit and Fluent, in this chapter, we will provide an overview of these two software programs, and then we will explain the various main steps involved in creating the geometry studied using Gambit and the meshing process employed, as well as the simulation steps carried out with Fluent.

IV.2.Presentation of Fluent and Gambit Software

- **The software Gambit**

The software Gambit (Geometry And Mesh Building Intelligent Toolkit) is a 2D/3D meshing preprocessor that allows meshing geometry domains of a CFD problem. It can generate structured or unstructured meshes in Cartesian, polar, cylindrical, or axisymmetric coordinates. It can create complex meshes in two or three dimensions with mesh elements such as rectangles or triangles. The mesh generation options in Gambit provide flexibility in choice. One can decompose the geometry into several parts to generate a structured mesh. Alternatively, Gambit automatically generates an unstructured mesh suitable for the constructed geometry type. With mesh verification tools, defects are easily detected.

It can be used to construct geometry and generate mesh for it. Additionally, geometry from another CAD software can be imported into this preprocessor. It generates *.msh files for Fluent.

- **The software Fluent**

Fluent is a widely used commercial CFD code in the industry. It enables the solution of fluid flows and heat transfer for various types of problems. For example, it can calculate the lift of an aircraft wing, the drag of a car, the cooling of electronic circuits by ventilated air…

The use of Fluent is straightforward, simply follow the menu order generally from left to right and top to bottom. The main simulation steps in FLUENT are as follows:

- Importing the geometry (*.msh)
- Verification of the importedmesh
- Mesh smoothing (smooth and swap the grid)
- Scale verification
- Solver selection
- Grid display
- Turbulence model selection
- Fluid properties definition
- Operating condition
- Boundary conditions

- Convergence criteriaselection
- Calculation initialization
- Saving the *mesh .case file
- Simulation launch
- Solution post-processing

VI.3. Creation of the geometry in Gambit

The figures below represent the design steps carried out in Gmabit software. Let's begin with the creation of circles and the two arcs of the parabol, followed by the 3D extension, than the mesh.

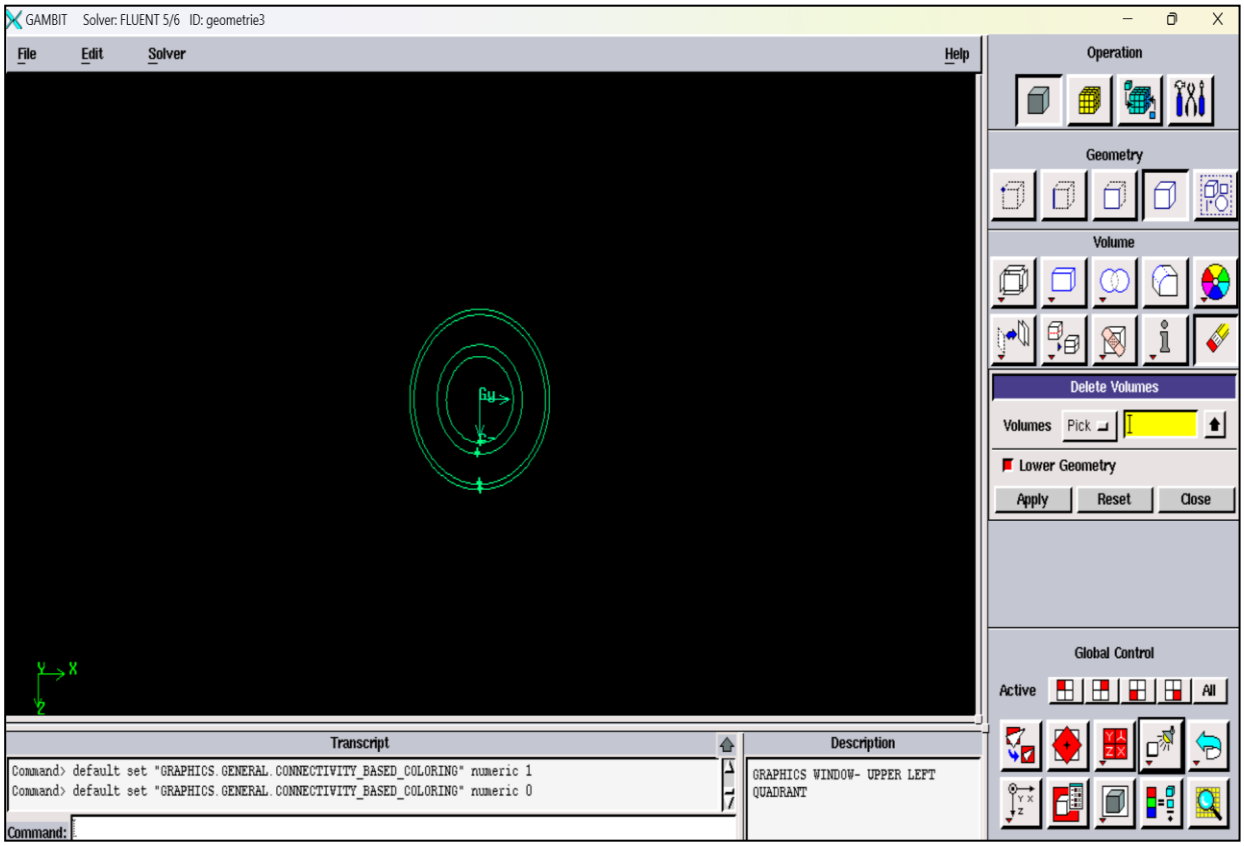

Figure VI.1. Drawing of 4 circles

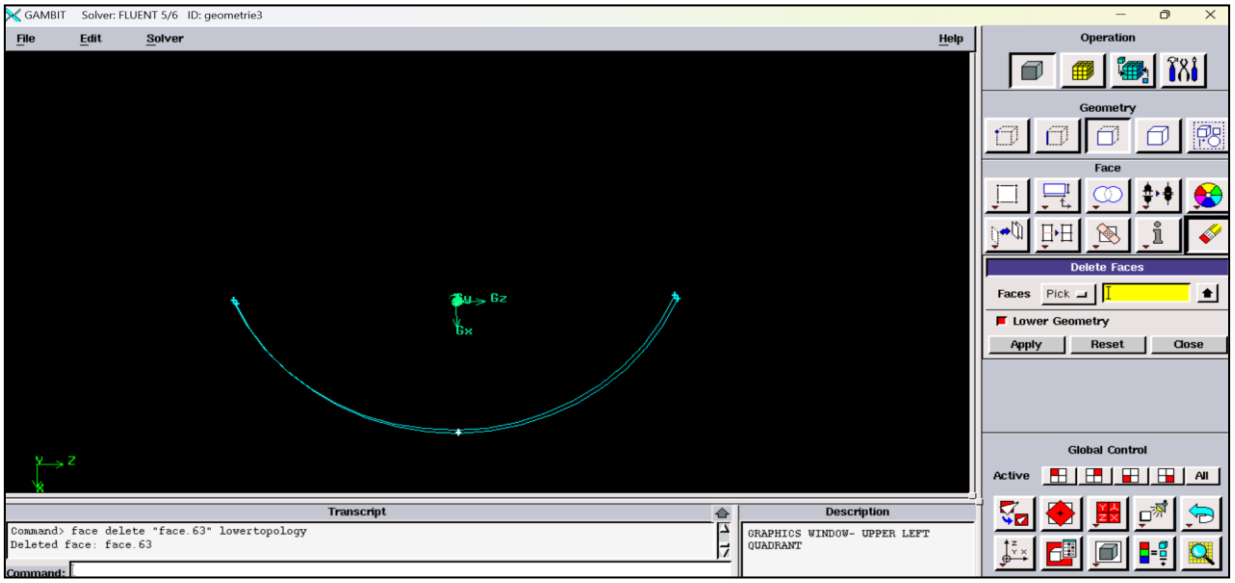

Figure VI.2. Creation of an arc

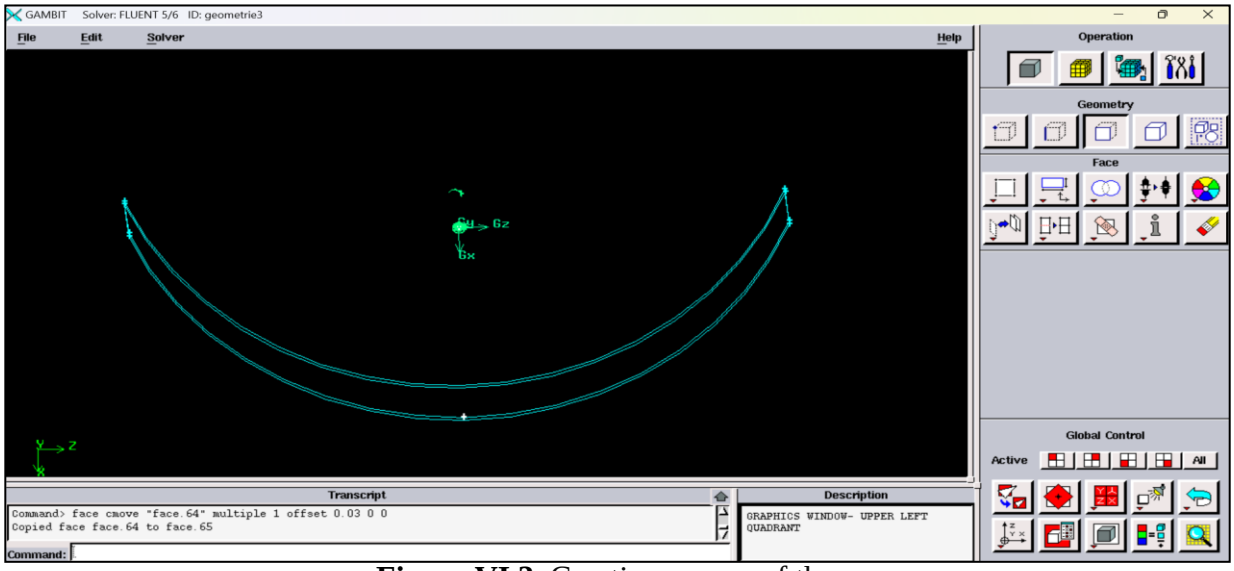

Figure VI.3. Creating a copy of the arc

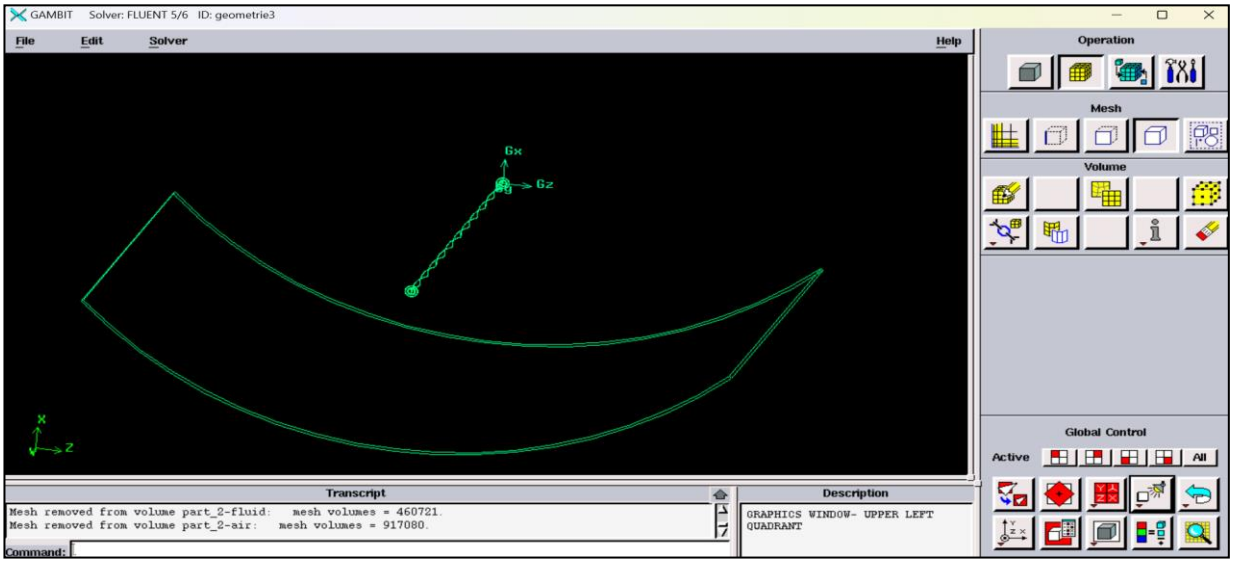

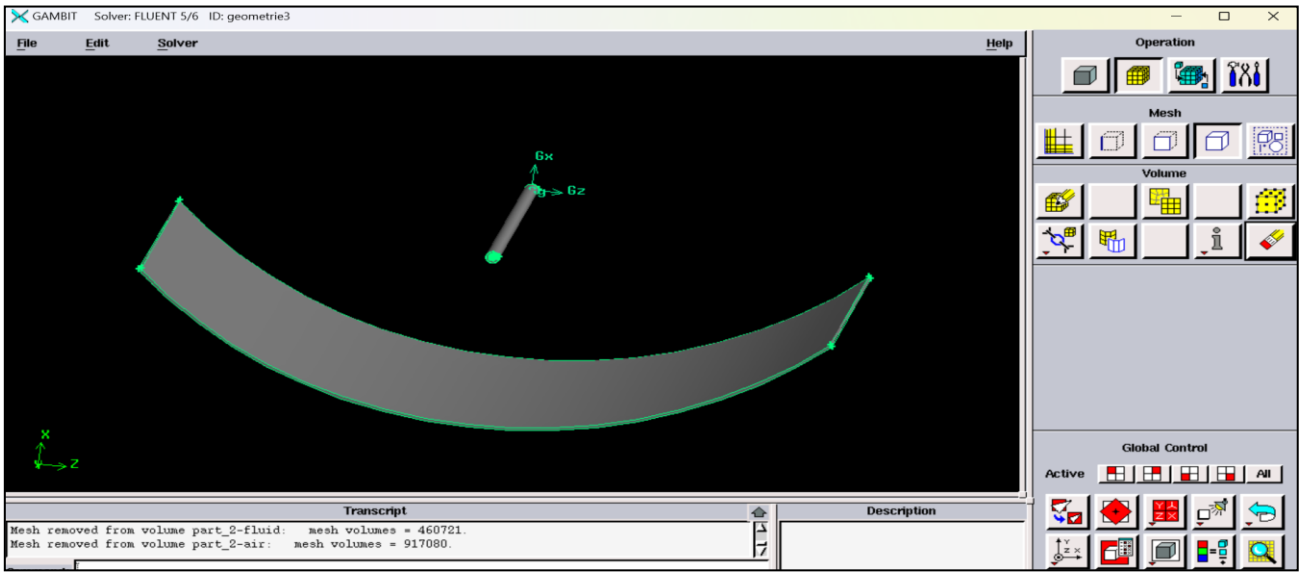

Figure VI.4. Converting the reflector arcs to volume

➢ ***The mesh :***

Mesh ⟹ ***volume***

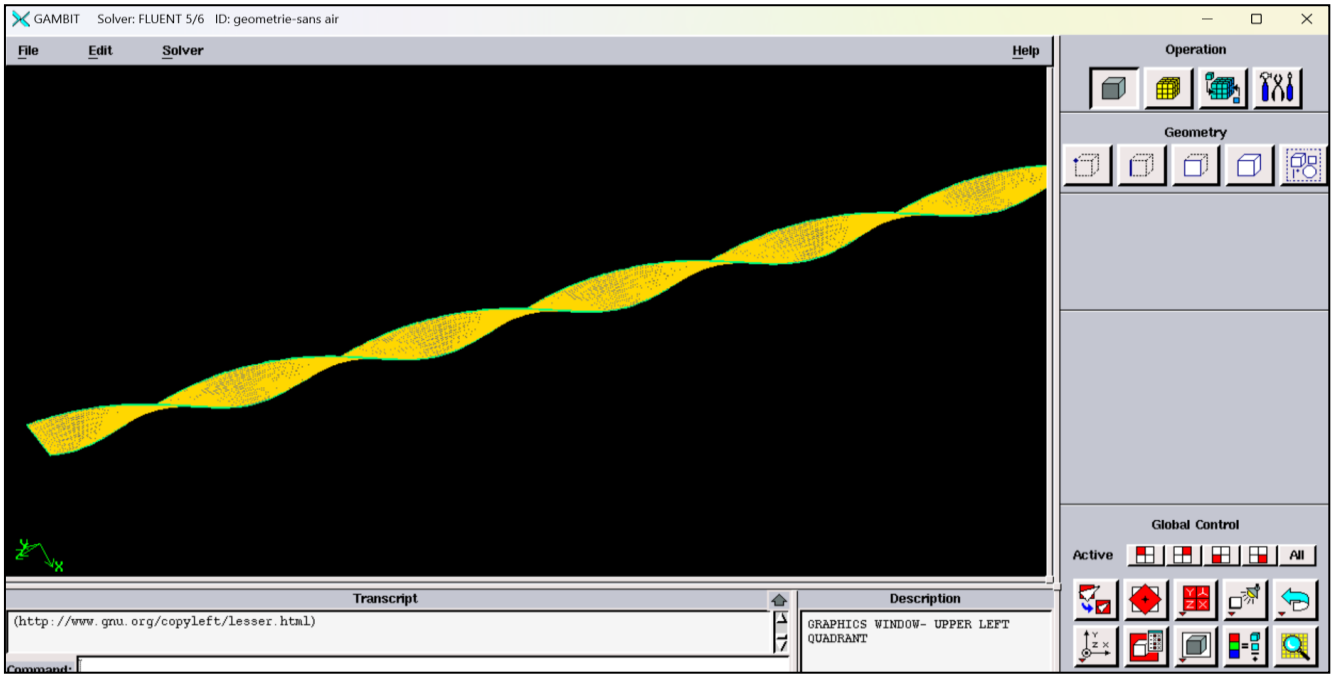

Figure VI.5.The mesh of twisted tape

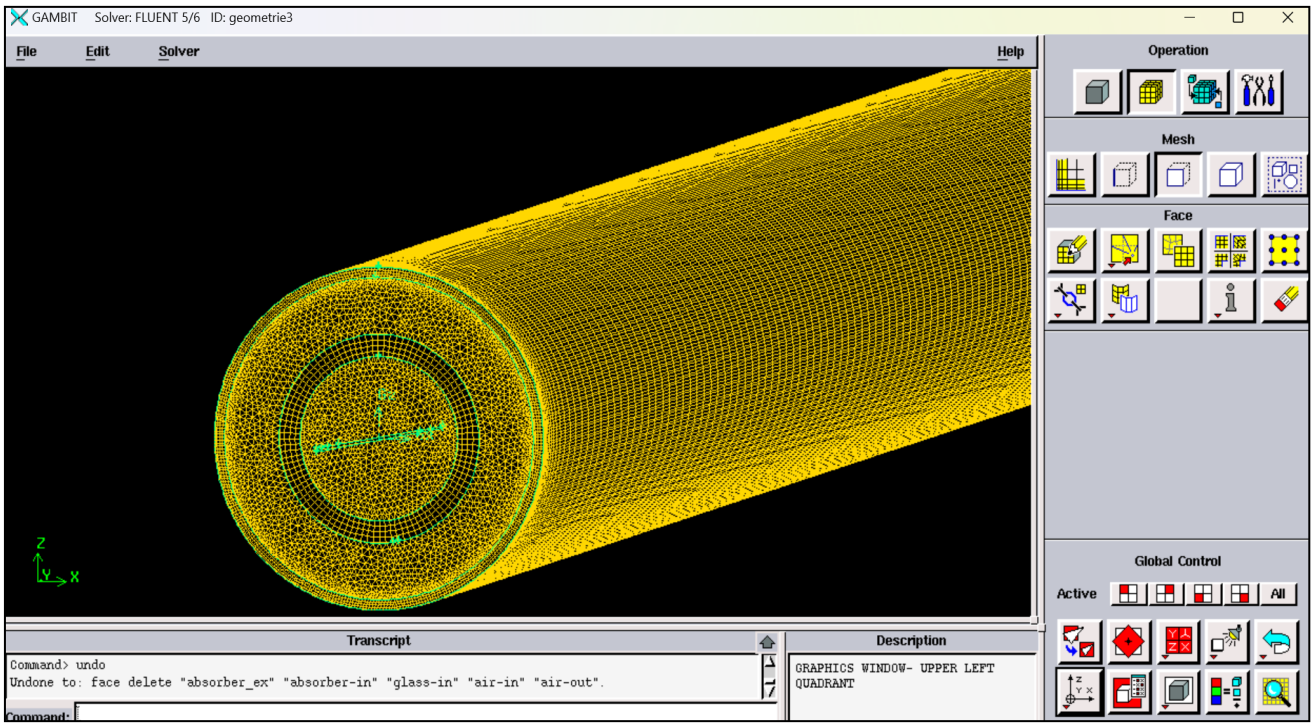

Figure VI.6. The mesh of volume of tube

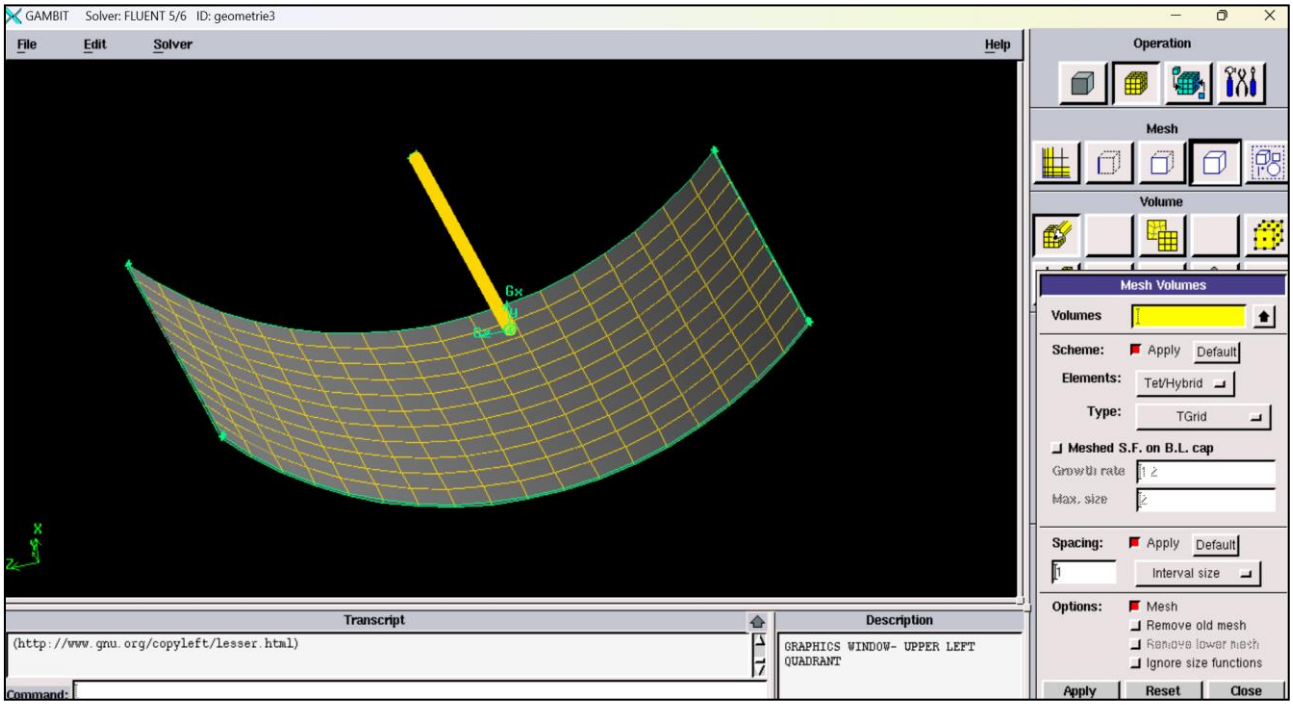

Figure VI.7. The mesh of cylindrical parabolic collector

➢ ***Boundary condition :***

Operation ⇨ ***Zones*** ⇨ ***Specify boundary types*** / ⇨ ***Specify continuum types***

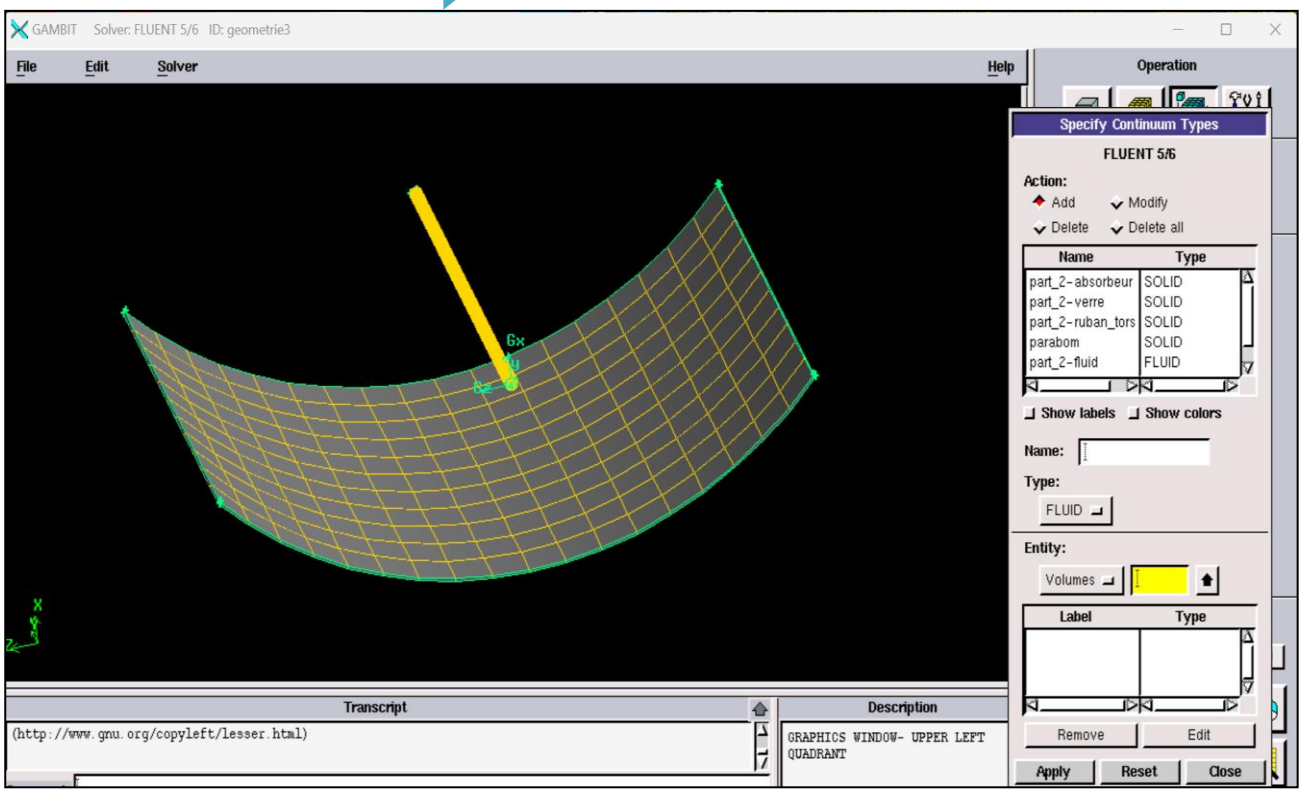

Figure VI.8. Specify continuum types

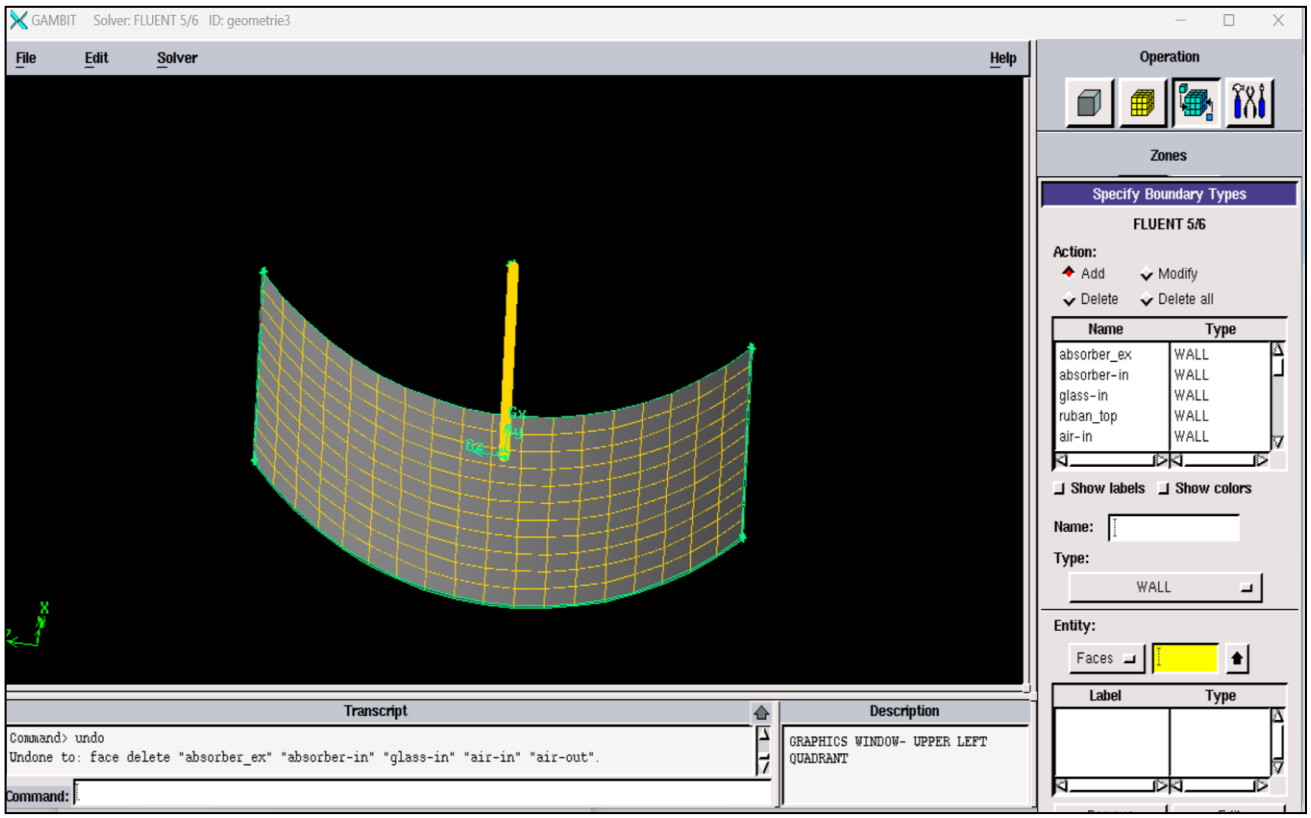

Figure VI.9. Specify boundary types

File ⇨ ***Export*** ⇨ ***Mesh***

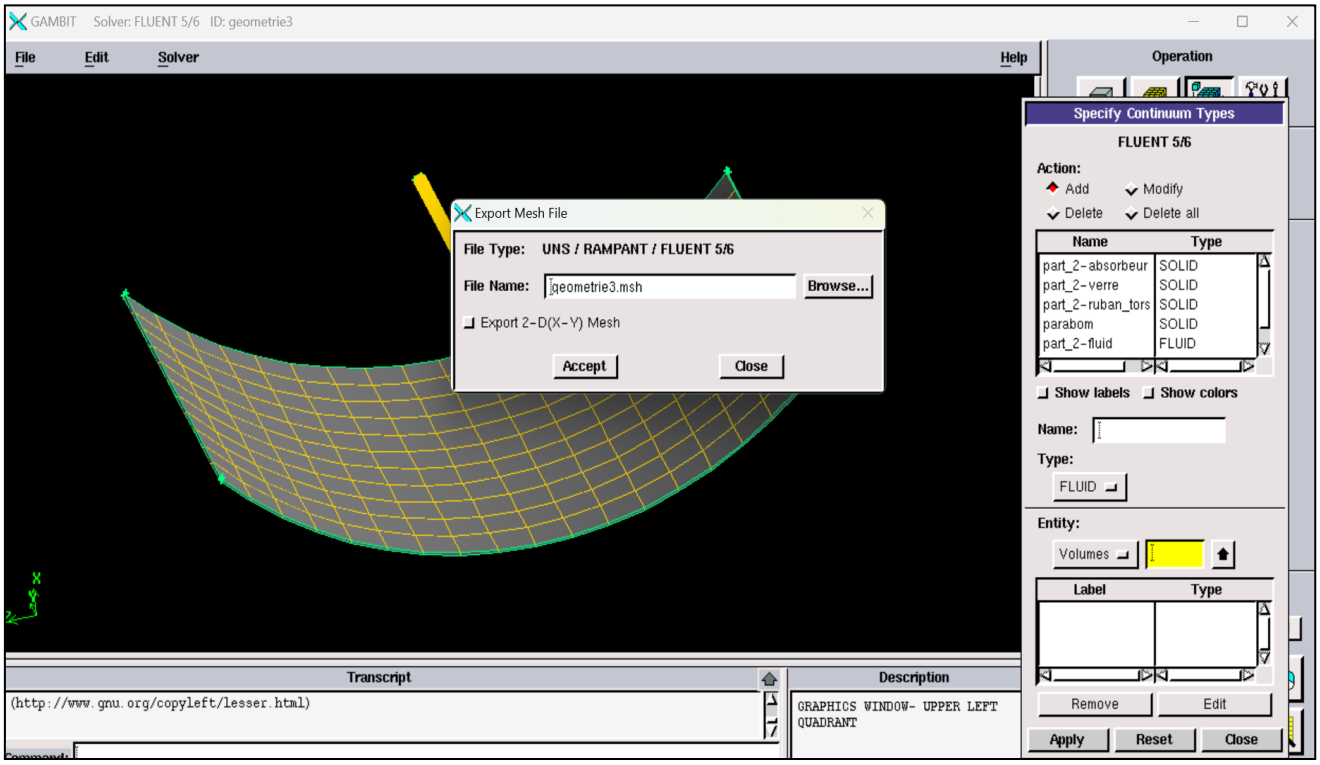

Figure VI.10.Export file mesh

VI.4. Simulation steps with Fluent software :

VI.4.1.Overview of Fluent

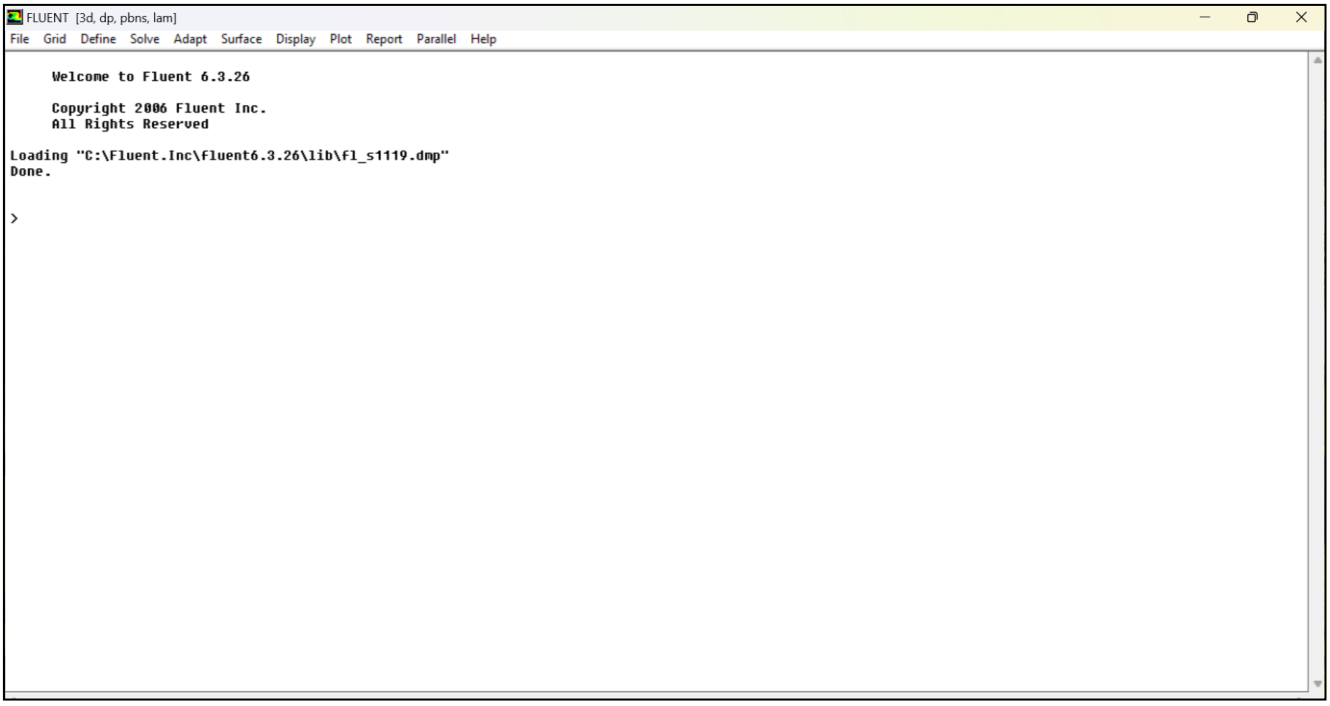

Figure VI.11. Overview of Fluent software

VI.4.2.Import the file mesh to fluent

File ⇨ ***Read*** ⇨ ***Case***

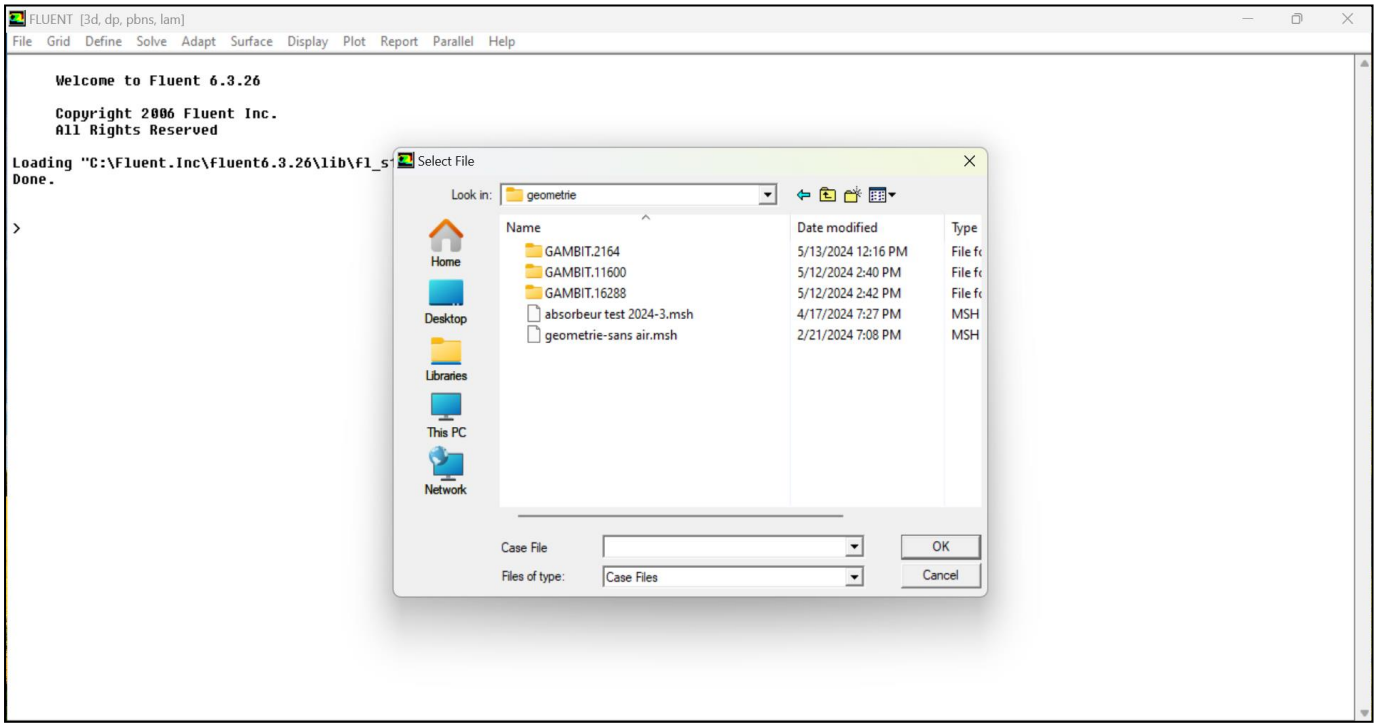

Figure VI.12. Import the file mesh

Grid ⇨ ***Check*** ⇨ ***Smooth/Swap…***

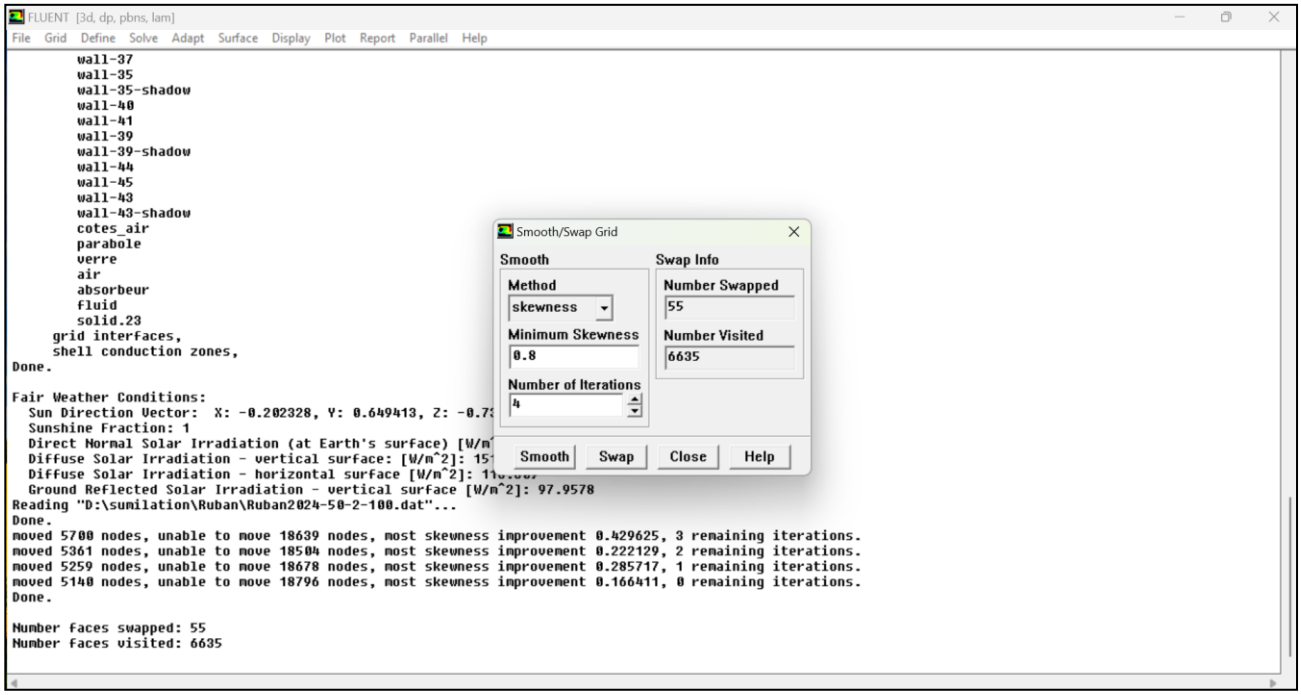

Figure VI.13. check and smooth/swap…

VI.4.3. Authorization of heat transfer

Difine ⇨ **Models** ⇨ **Energy**

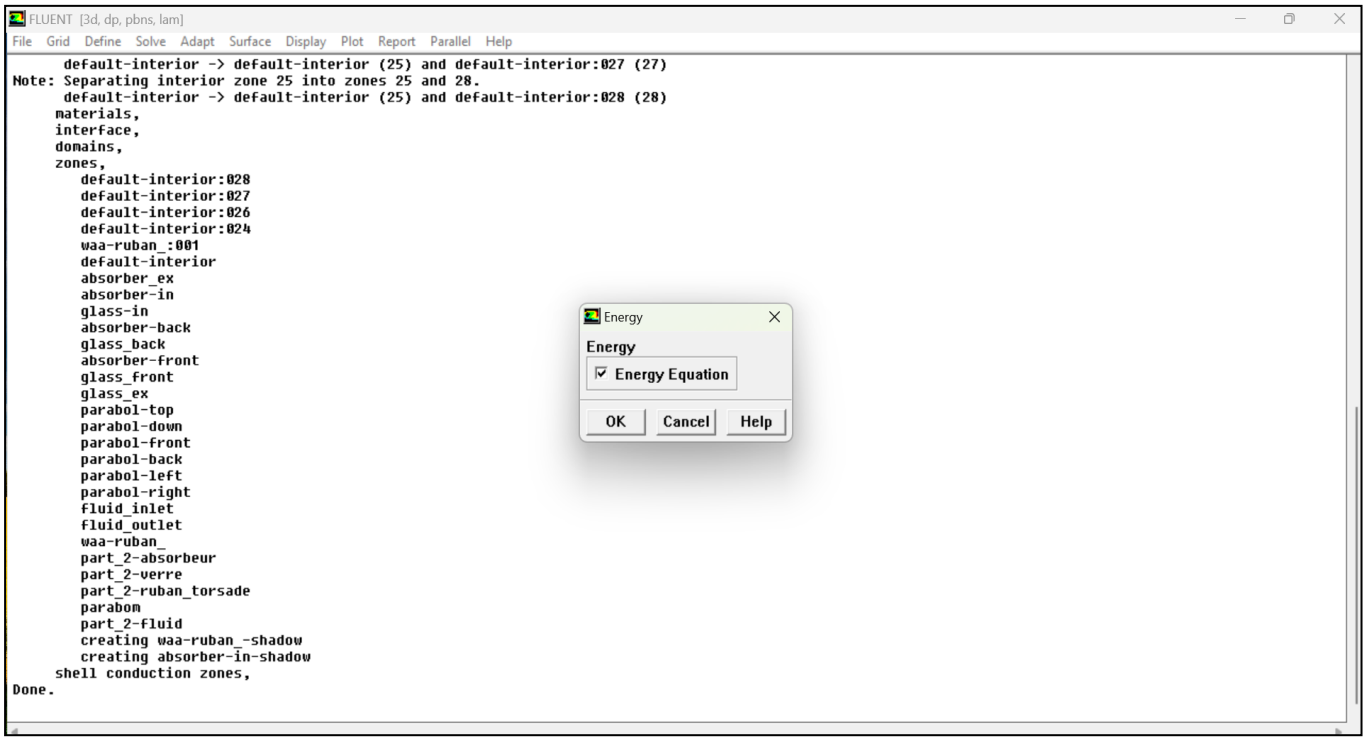

Figure VI.14. Authorization of the energy equation

VI.4.4. choose of the type of flow

Models ⇨ ***Viscous*** ⇨ **Laminar**

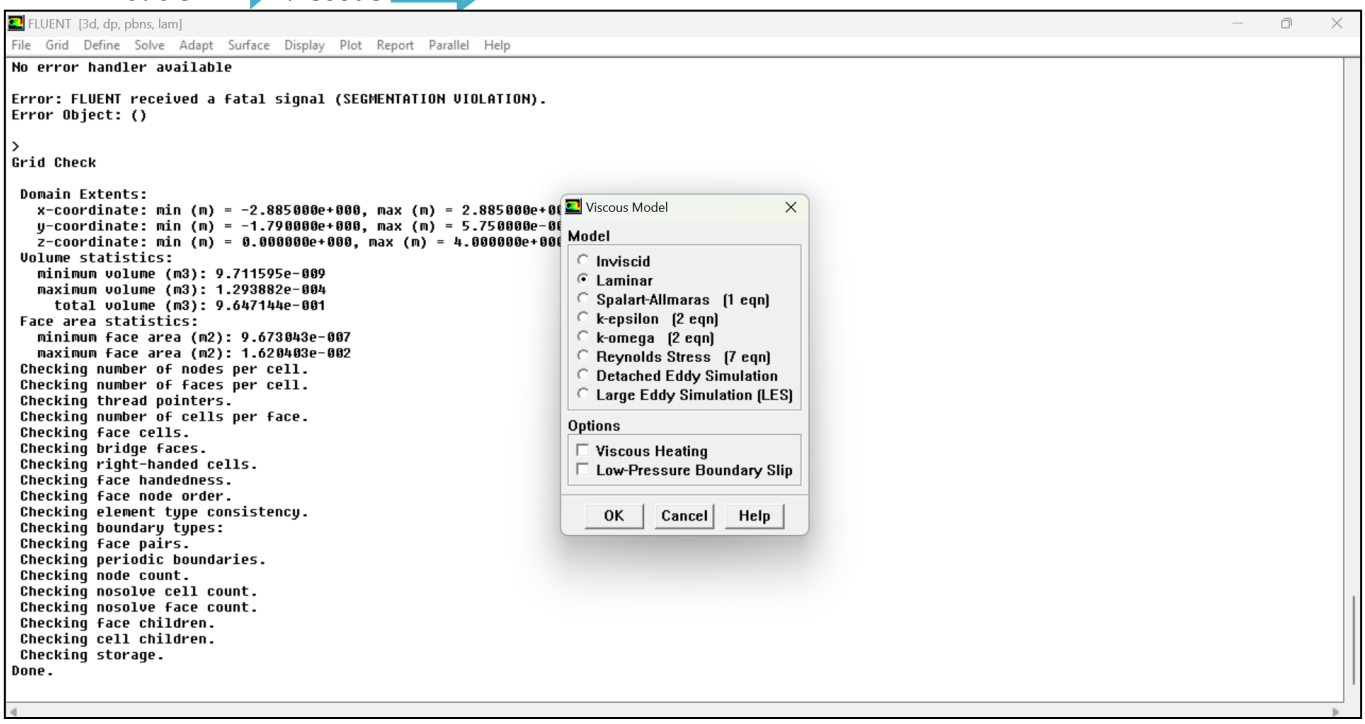

Figure VI.15. Choice of flow type

VI.4.5. Authorization and choice of the radiation model

Models ⇨ ***Radiation*** ⇨ ***Rosseland*** ⇨ ***Solar calculator***

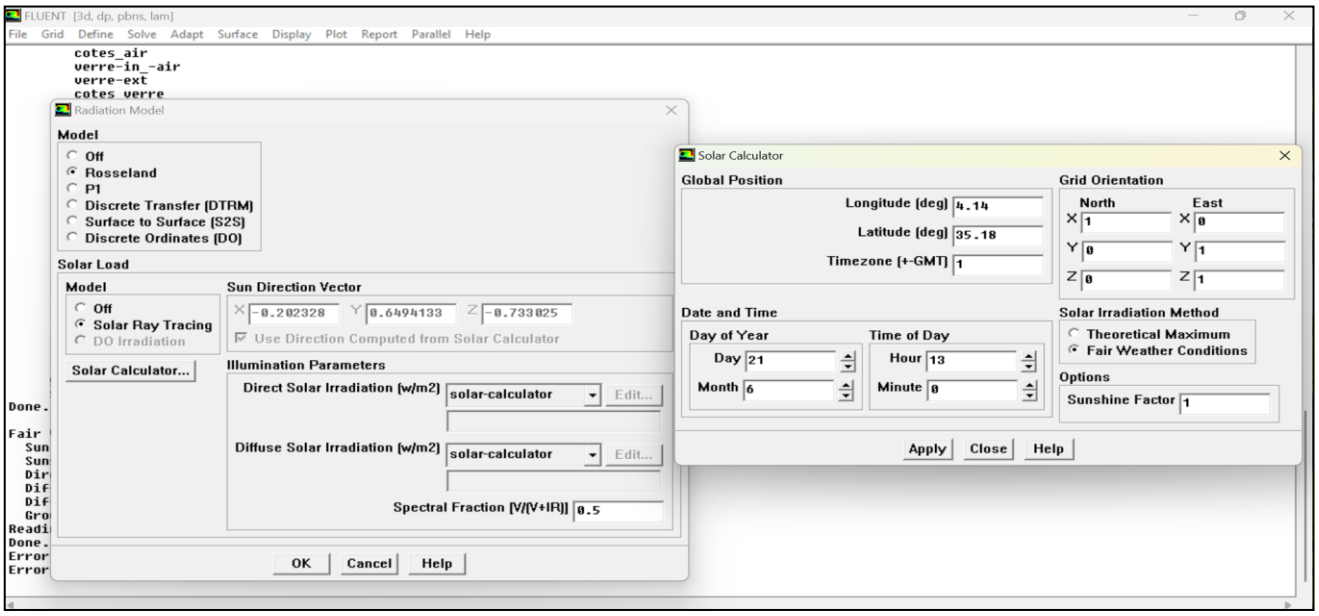

Figure VI.16.Authorization and choice of the radiation model

VI.4.6.Definition of material characteristics

Define ⇨ Materials

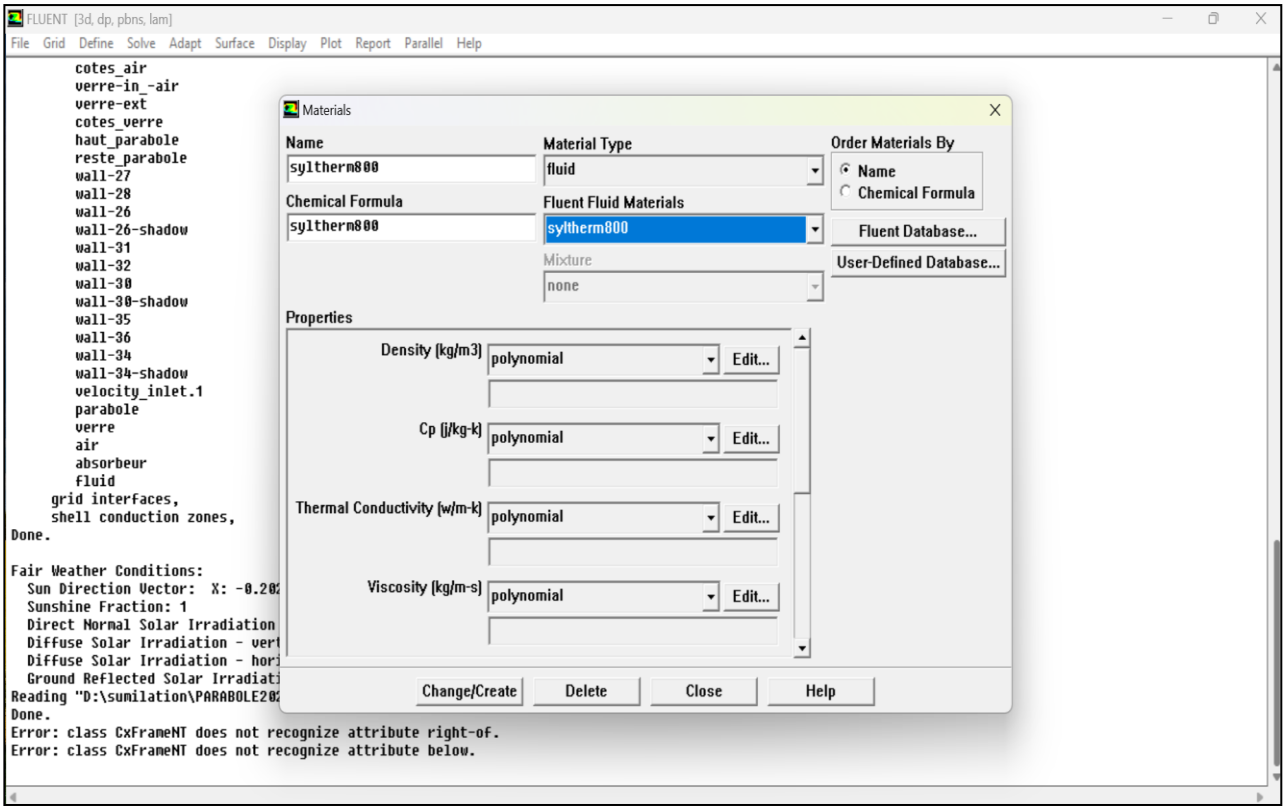

Figure VI.17. Definitionof material characteristics

VI.4.7. Definition of boundary condition

Define ⇨ Boundary condition

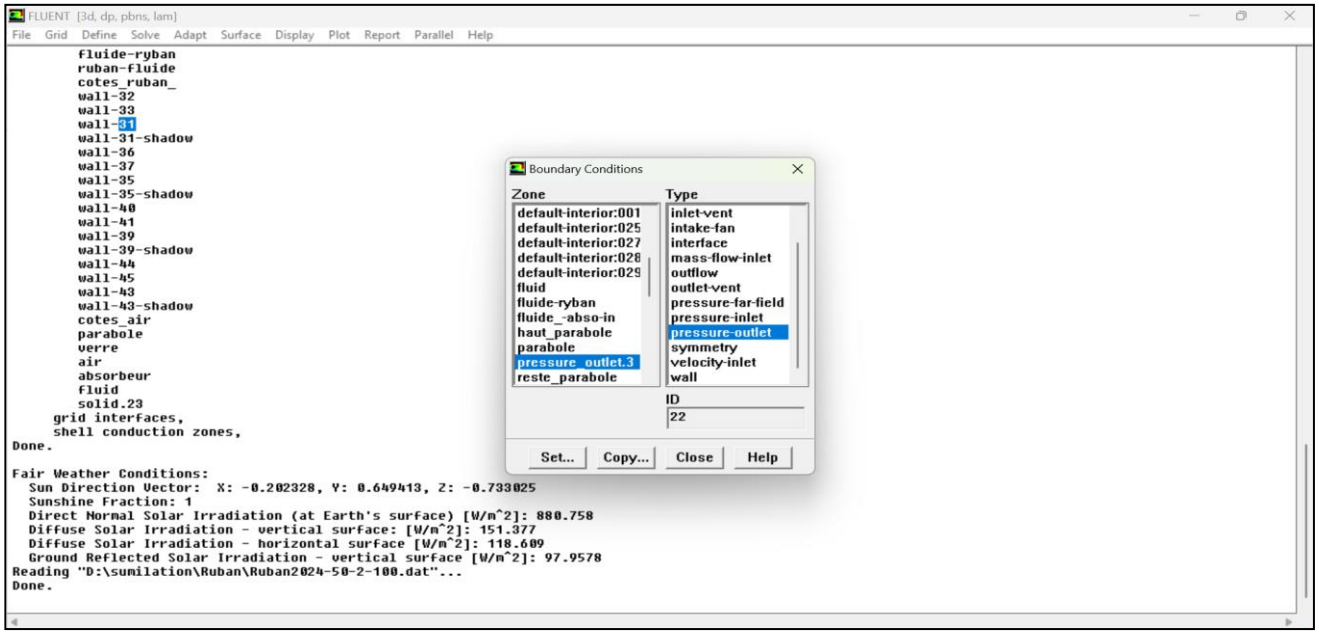

Figure VI.18.boundary condition

Boundary condition ⇒ velocity inlet

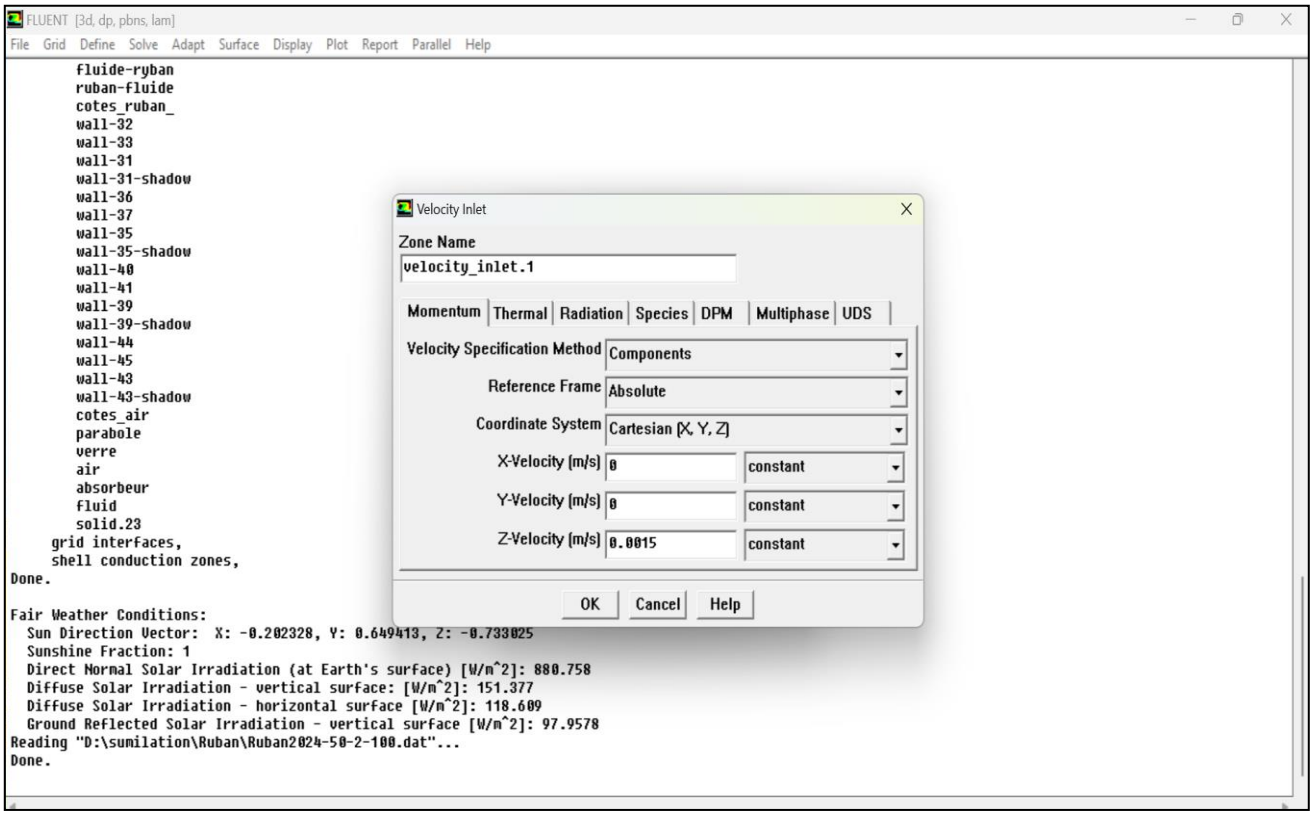

Figure VI.19.definition of velocity inlet

VI.4.8.Definition of interfaces

Define ⇒ Grid interfaces

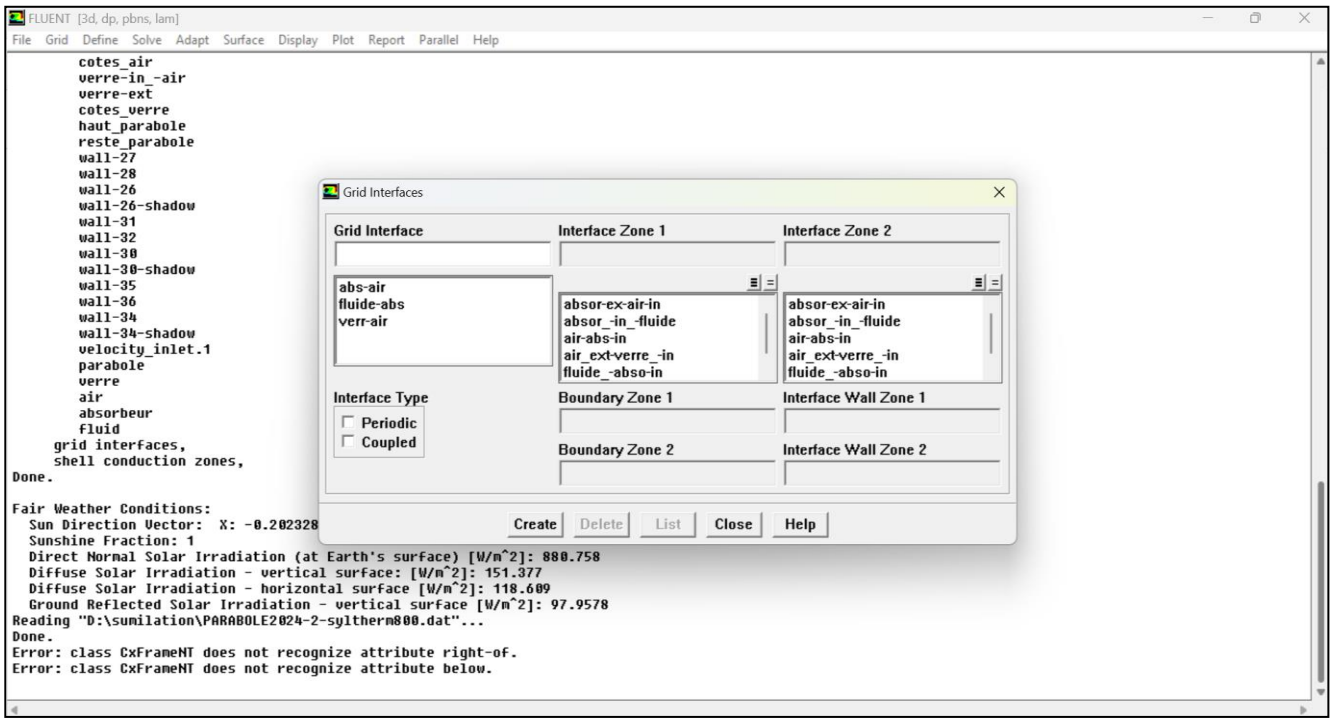

Figure VI.20.Grid interfaces

VI.4.9.Choose an solution controls

Solve ⇒ ***Solution of controls***

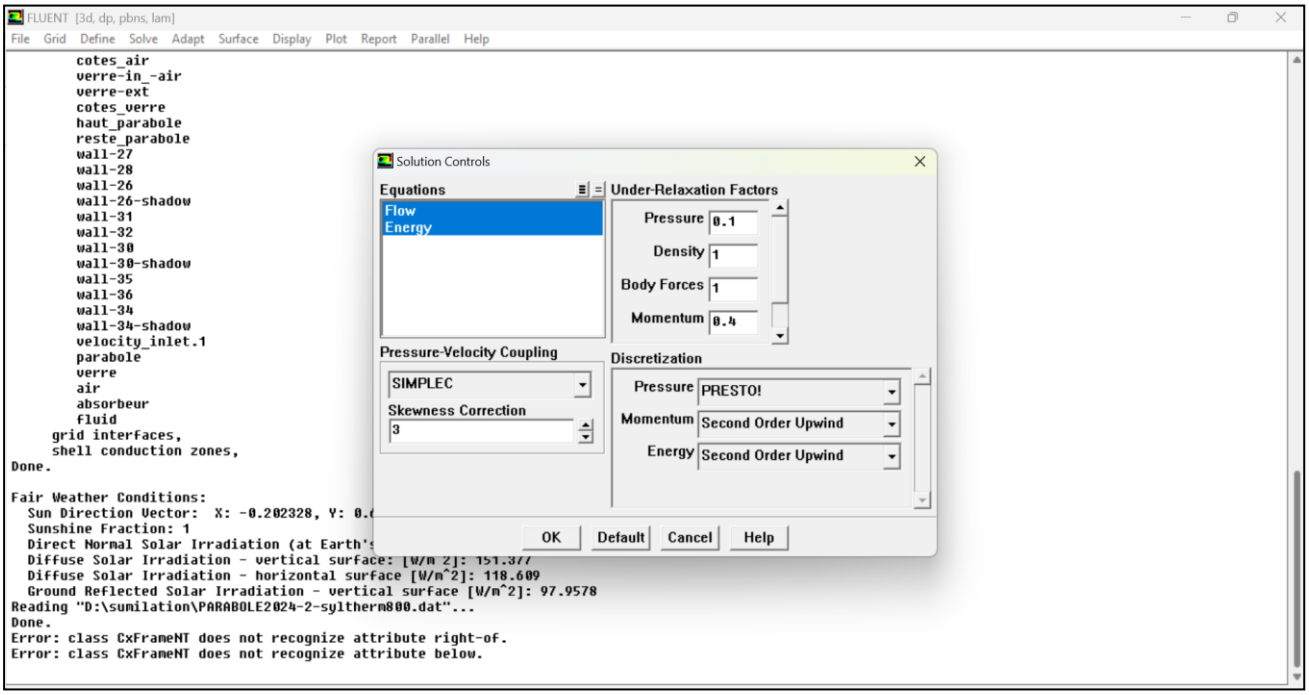

Figure VI.21.choice of solution controls

VI.4.10.Initialize

Solve ⇒ ***Initialize*** ⇒ ***Solution Initialize***

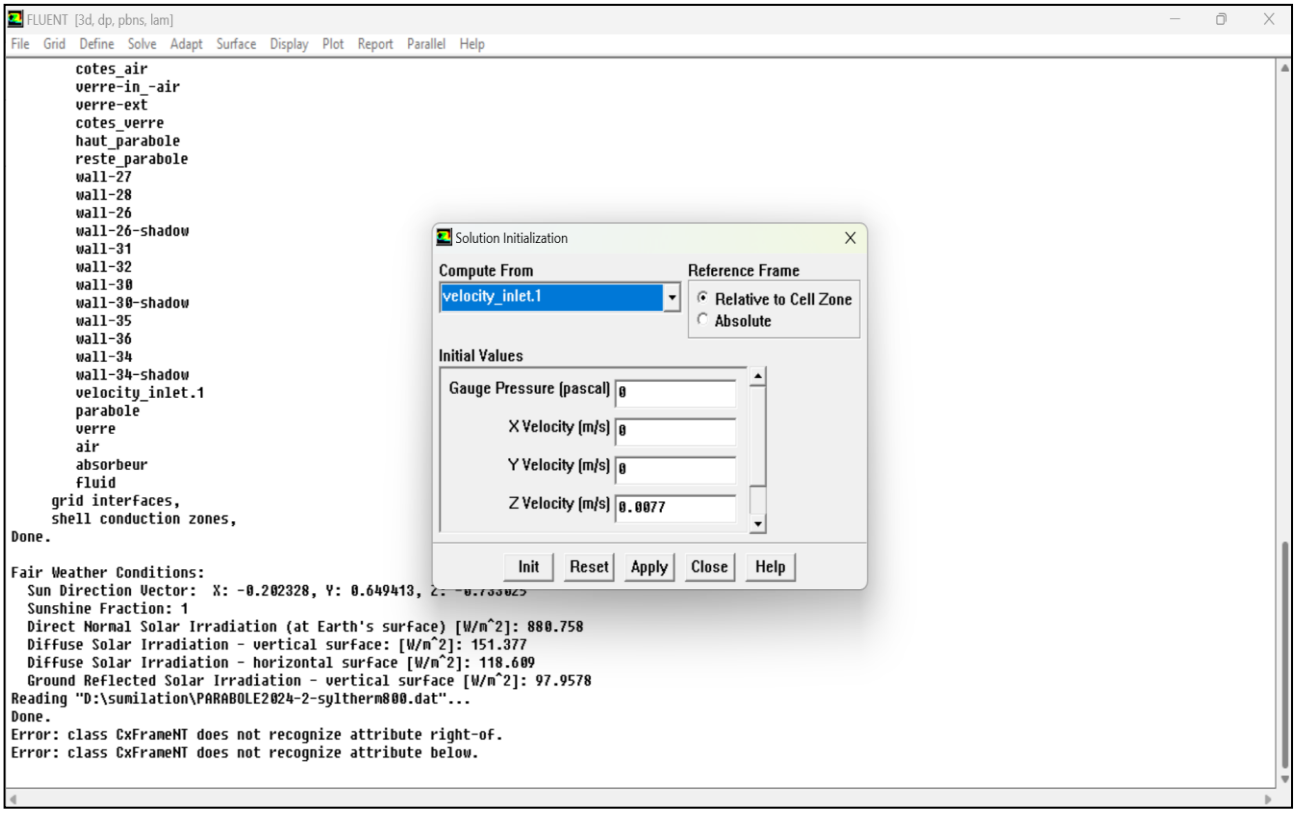

Figure VI.22.Initialize

Solve ⇒ Initialize ⇒ Patch

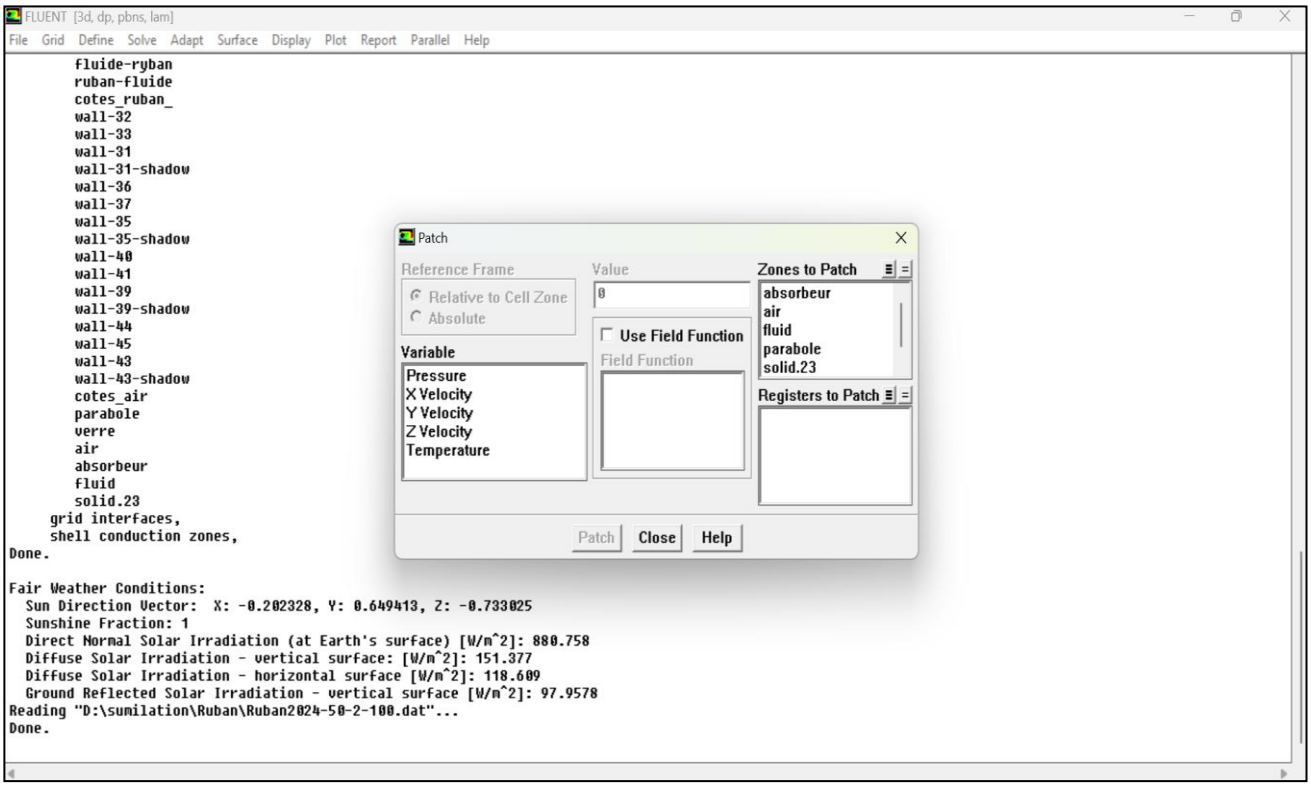

Figure VI.23.Patch

VI.4.11. choose residual

Solve ⇒ Monitors ⇒ Residual

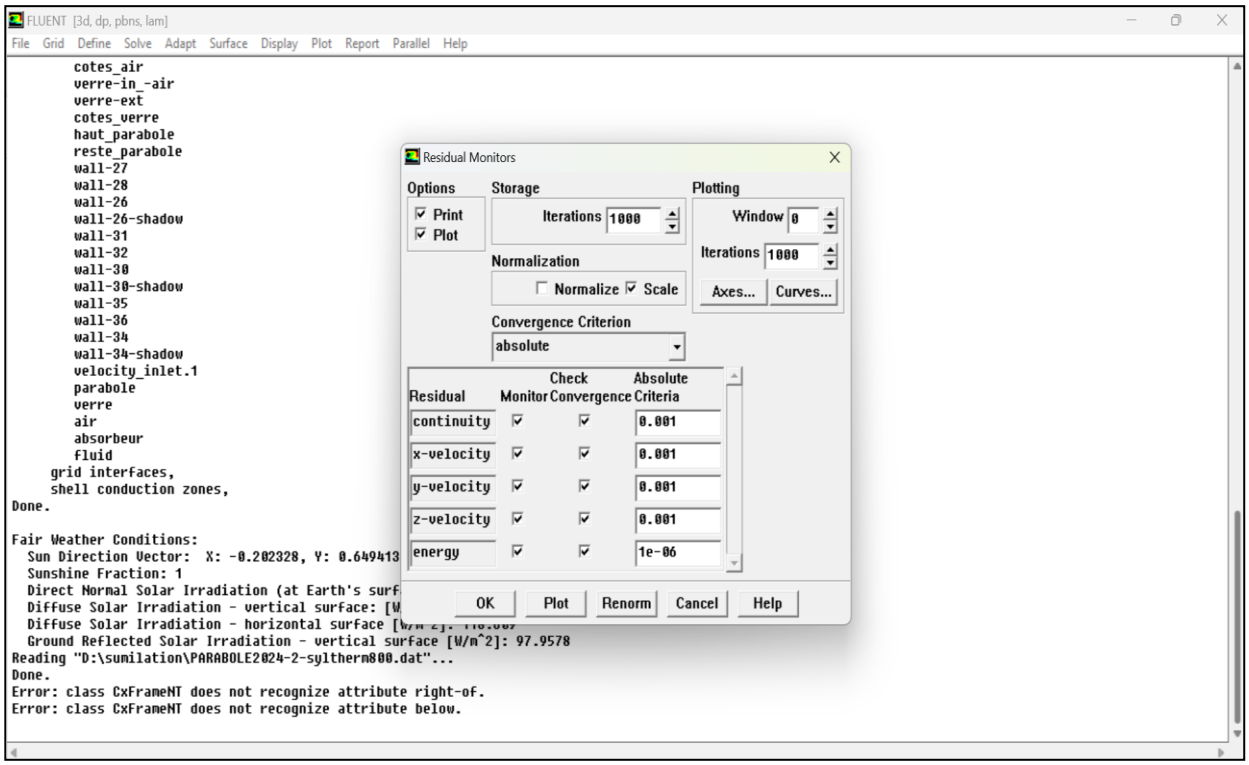

Figure VI.24.Residial monitors

VI.4.12.Iterate

Solve ⇒ Iterate

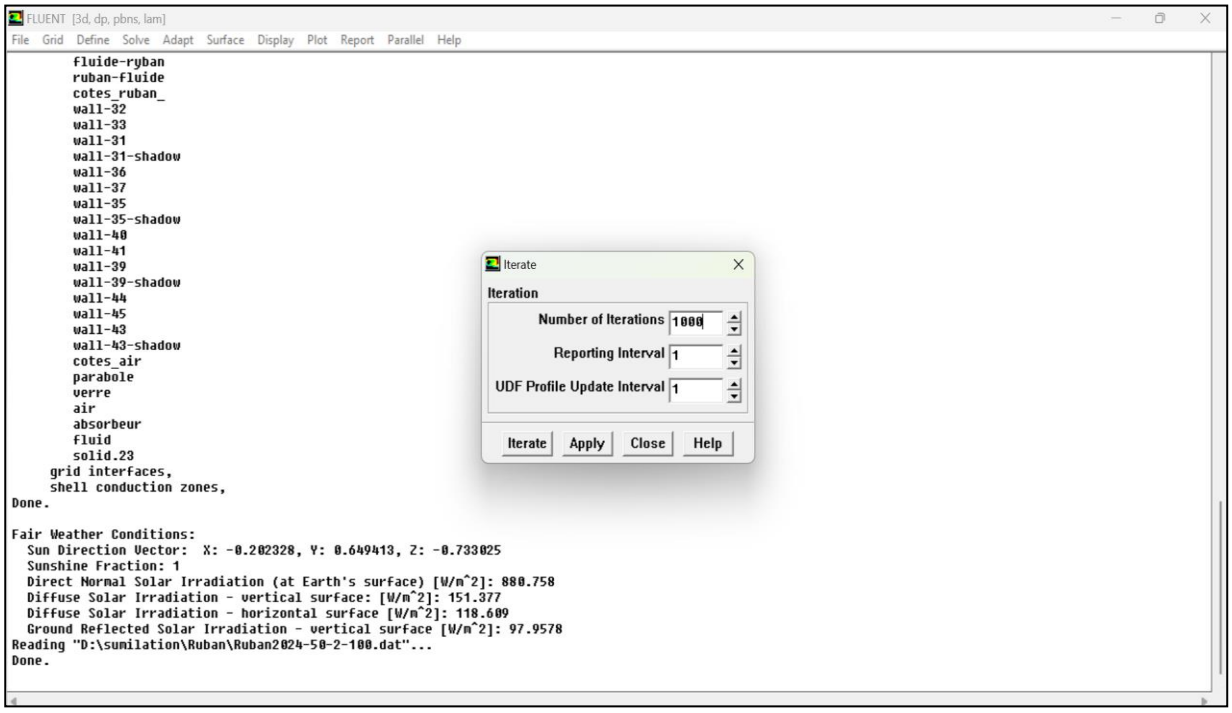

Figure VI.25.Iterate

VI.4.13.calculte of outlet temperature

Repports ⇒ surface integral ⇒ Area-Wheited average

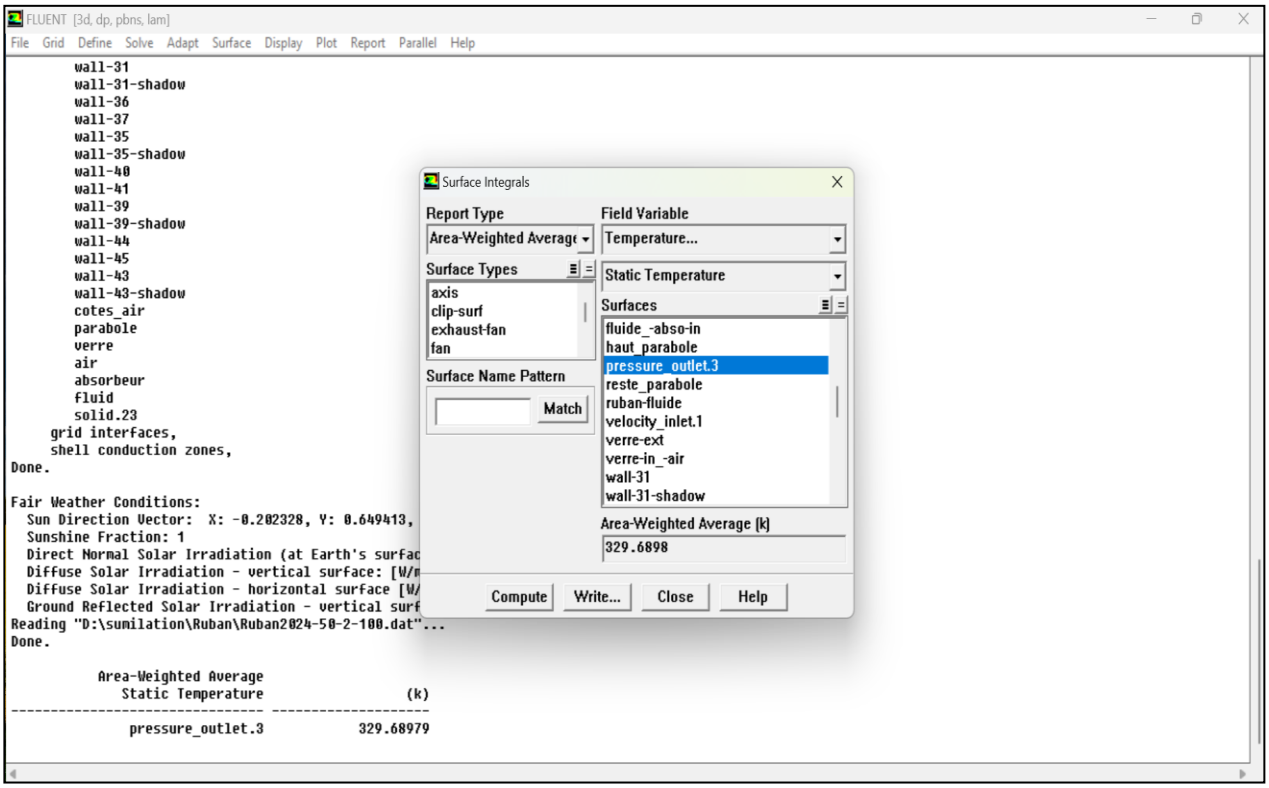

Figure VI.26. calculate of outlet temperature

VI.4.Conclusion

Through this chapter, we have outlined the various steps of using the geometry creation and meshing software using Gambit and solving the algebraic equations arising from the physical system using Fluent. The simulation results are presented in the following chapter.

Chapter V
Results and Discussions

Chapter V:Results and Discussions

V.1. Introduction

In this chapter, we present the different results of the numerical simulation obtained using the CFD code (Fluent) regarding steady-state laminar mixed convection in a cylindrical-parabolic collector in three studied cases. With Syltherm 800 and with nanofluid (Syltherm 800+ Cu) at different concentrations φ= 1%, 2%, 3%, 4% without and with twisted tape. Our numerical simulations were conducted for Reynolds numbers ranging from 100 to 500. For each case, we present temperature and velocity contours, streamlines, as well as the variation of the Nusselt number with the Reynolds number.

V.2 The parameters used

V.2.1. The physical properties of the fluids used -Syltherm 800 :

Density : **ρ**= $1.1057 * 10^{3} - 4.1535 * 10^{-1}T - 6.0616 * 10^{-4}T^{2}$

specific heat capacity : ***Cp*** =$1.1078 * 10^{3} + 1.7080\ \mathrm{T}$

thermal conductivity : $\boldsymbol{\lambda}$= $1.90 * 10^{-1} - 1.87 * 10^{-4}\mathrm{T} - 5.75 * 10^{-10}\mathrm{T}^{2}$

dynamic viscosity : $\boldsymbol{\mu}$ = $8.47 * 10^{-2} - 5.54 * 10^{-4}\mathrm{T} + 1.39 * 10^{-6}\mathrm{T}^{2} - 1.57 * 10^{-9}\mathrm{T}^{3} + 6.67 * 10^{-13}\mathrm{T}^{4}$

V.2.2. The physical properties of the materials used :

Aluminum :

Density: **ρ** =2719kg/m³

specific heat capacity : ***Cp*** = 871 (J/kg K)

thermal conductivity : $\boldsymbol{\lambda}$= 202.4(W/m K)

Copper **:**

Density: **ρ**=8978kg/m³

specific heat capacity : ***Cp*** = 381 (J/kg K)

thermal conductivity : $\boldsymbol{\lambda}$ = 387 (W/m K)

Glass :

Density : **ρ**=2800kg/m³

specific heat capacity : ***Cp*** = 750 (J/kg K)

thermal conductivity :$\boldsymbol{\lambda}$= 0.7 (W/m K)

Emissivity = 0.9

Absorption = 0.1

V.2.3.Location data

- Longitude : 4,14° N

- Latitude : 35,18° E

- Time zone (GMT) +1

- Day : 21 , Month : 6 hour : 13h

V.3. Results and Discussions

V.3.1.Without twisted tape

V.3.1.1 Case of sylherm 800

V.3.1.1.1 Temperature contours

The Figures (V.1 and V.2) show the temperature distributions on seven different cross-sections with z =0.2, 1, 1.5, 2, 2.5, 3 ,3.8 m for Reynolds numbers Re=200 , Re=500. It can be seen that the temperature is maximum at the outer circumference and is decreasing towards the center.

We notice that the temperature of the glass is maximum at the top than at the bottom of the glass tube, this is only due to a higher concentration of solar flux in the top half of the receiver than at the lower.

It can be seen also that the temperature of Syltherm 800 decreases as the Reynolds number increases. Increasing the Reynolds number results in an increase in the inlet velocity and consequently an increase in the mass flow rate, which causes a decrease in temperature. The radial distribution of temperature shows that the temperature is maximum on the inner wall of the tube, forming a thin thermal boundary layer, and it decreases towards the center. It is also observed that the fluid temperature gradually increases from the inlet to the outlet, reaching a maximum value at the absorber outlet.

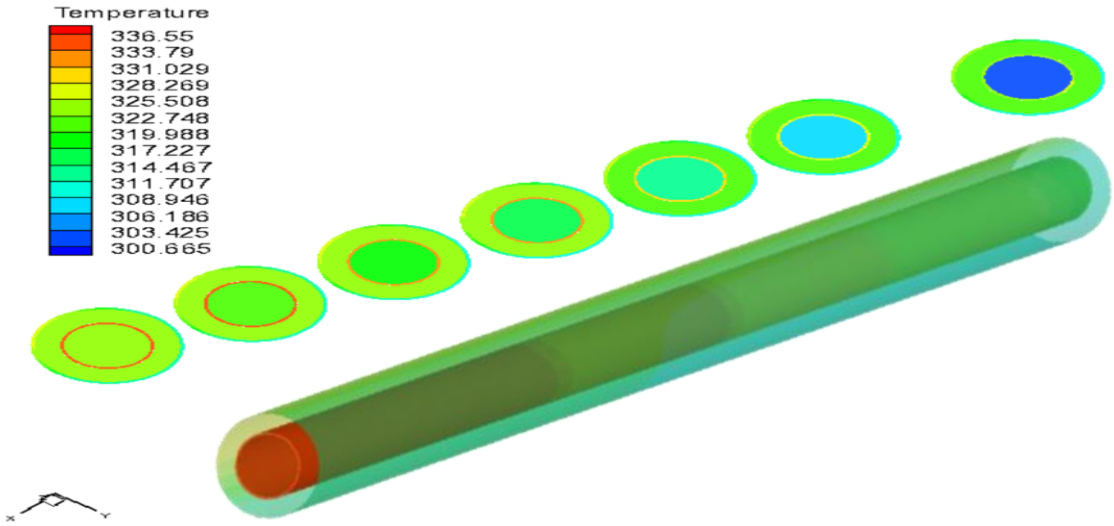

Figure V.1 : Temperature contours for Re = 200

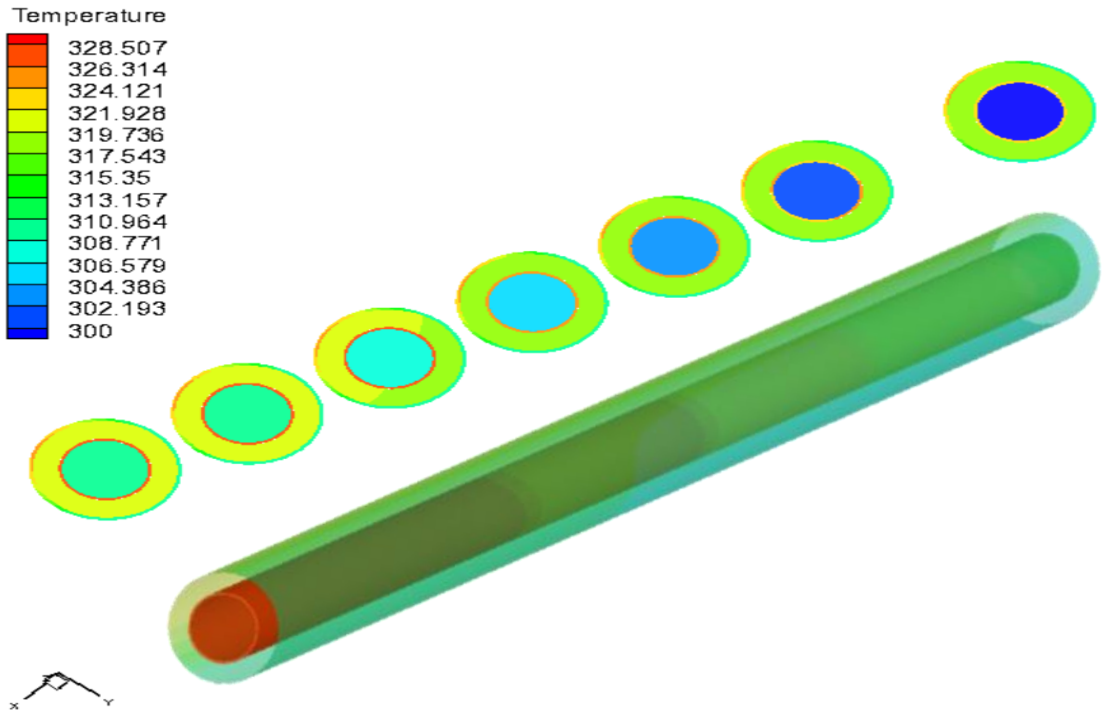

Figure V.2 : Temperature contours for Re = 500

V.3.1.1.2.Variation of outlet Temperature as a function of Reynolds number

Figure V.3 specifies that the outlet temperature of HTF decreases with an increase in Reynolds number. The increase in Re leads to increase in velocity; the HTF will get less time for interacting with the metallic absorber tube.

The decrease in outlet temperature is more significant at low Reynolds; decreases from 64.76 °C to 32.13 °C when the Reynolds number increases from 200 to 1000 and becomes lower when the Reynolds number is higher.

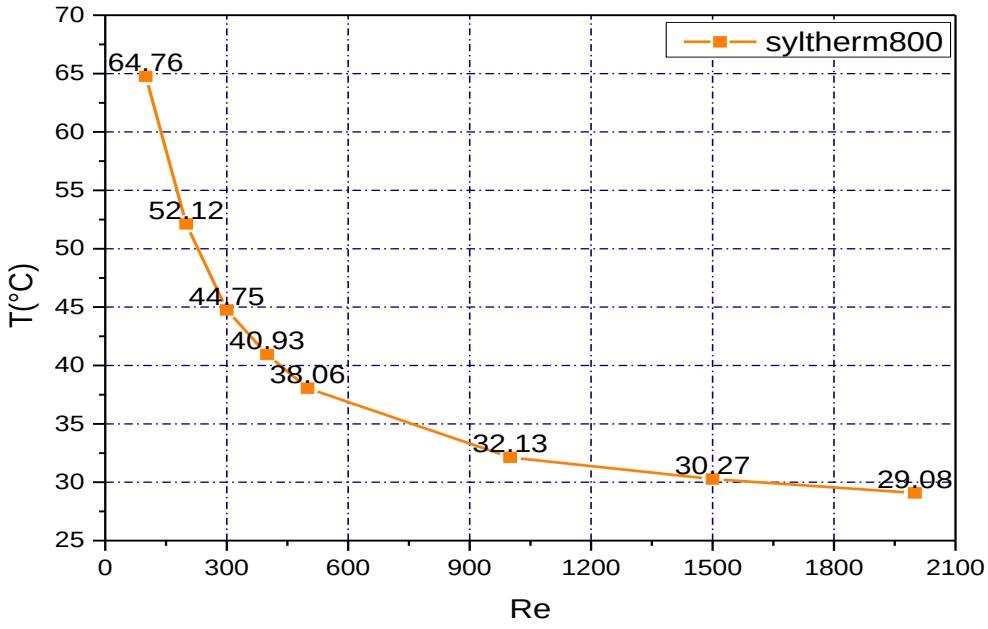

Figure V.3.The temperature differences in the case of Syltherm 800 as a function of Re

V.3.1.1.3. Variation of the Nusselt number as a function of the Reynolds number:

Figure V.4 shows the variation of the Nusselt number with Reynolds number, It is clear that the mean Nusselt number deacreases with Reynolds number augmentation, which supports moreover the conduction-convective phenomenon between the wall and the fluid flow absorber.

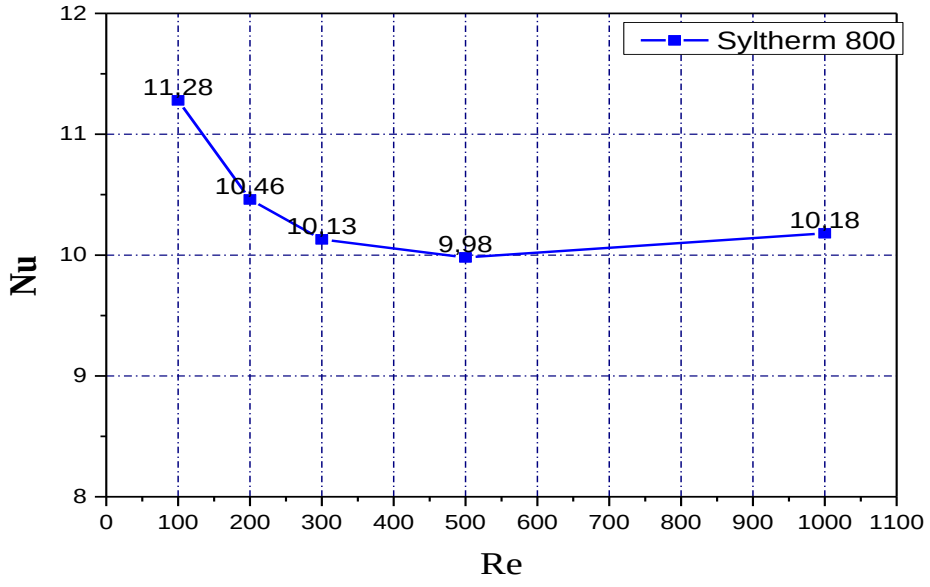

Figure V.4. Variation of Nusselt number as a function of Re

V.3.1.1.4.Variation du coefficient de convection h as a function of the Reynolds number

Figure V.5 illustrates the relationship between average heat transfer coefficient (h) and Reynolds number (Re) . The numerical results suggest that the average heat transfer coefficient (h) decreases first with Reynolds number and then increases after it reaches the minimum value (14.77W/m^2.K) for Re = 300.

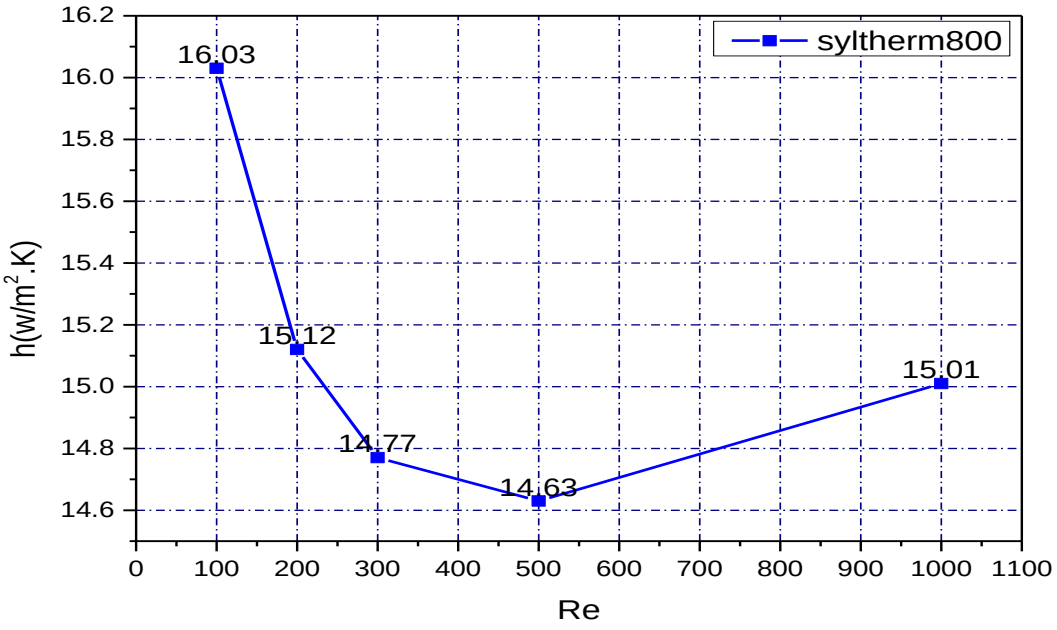

Figure V.5. Variation of convection heat coefficient as a function of Re

V.3.1.1.5. Velocity contours

To obtain important details about the flow structure, velocity contours are presented in Figures (V.6) & (V.7) on seven different cross-sections with z =0.2, 1, 1.5, 2, 2.5, 3 ,3.8 m for Reynolds numbers Re=200 , Re=500.

The velocity contours start with a uniform velocity profile at the entrance of the absorber, while they become zero at the tube wall due to the no-slip condition applied on the inner surface of the absorber and increase as they move away from the wall to reach maximum values. We also observe that the flow velocity increases from the inlet to the outlet of the absorber due to the increase in fluid temperature. We can also note that the flow velocity increases with the increase in Reynolds number.

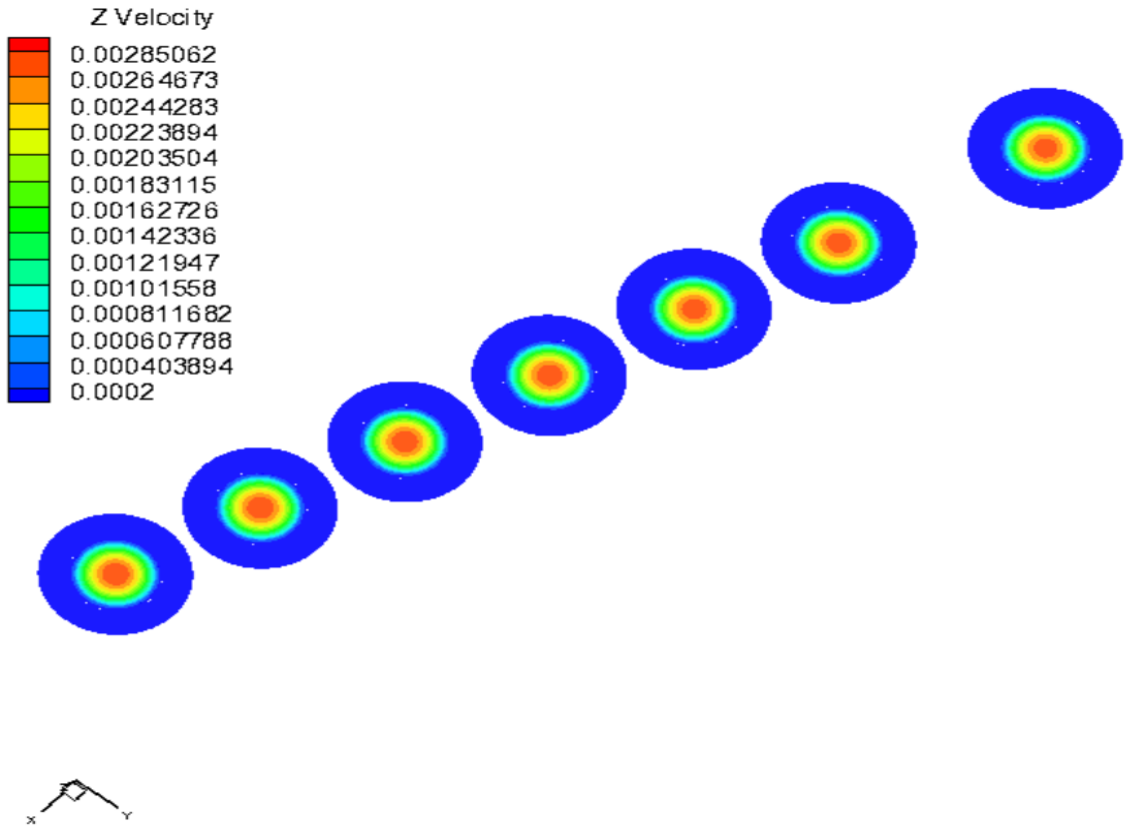

Figure V.6.Velocity contour for Re = 200

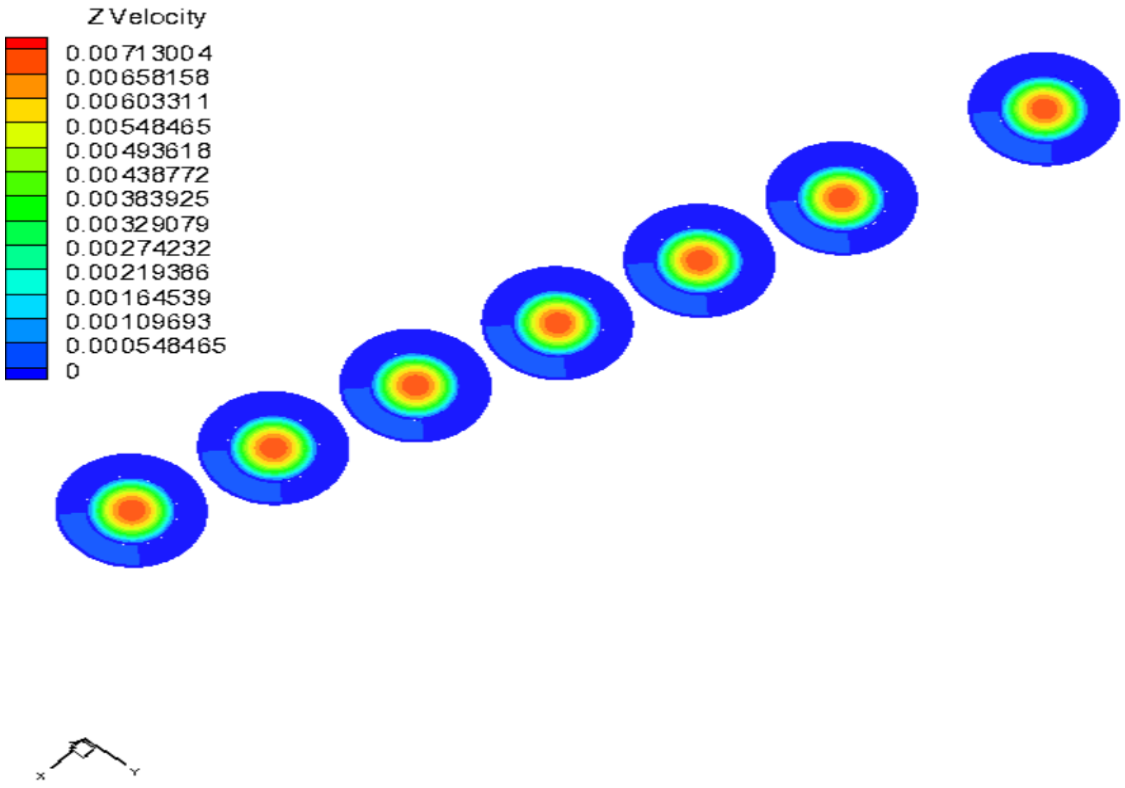

Figure V.7.Velocity contour for Re = 500

V.3.1.1.6. Streamlines and Velocity vectors:

To obtain important details about the flow structure, streamlines are presented in Figures (V.8) & (V.9) on seven different cross-sections with z =0.2, 1, 1.5, 2, 2.5, 3 ,3.8 m for Reynolds numbers Re=200, Re=500. We see that the flow is in the form of parallel lines (fluid threads) because the flow is laminar. We can also notice that the streamlines depend on the flow velocity, the increase in the Reynolds number causes an increase in the flow velocity and consequently an increase in the values of the streamlines.

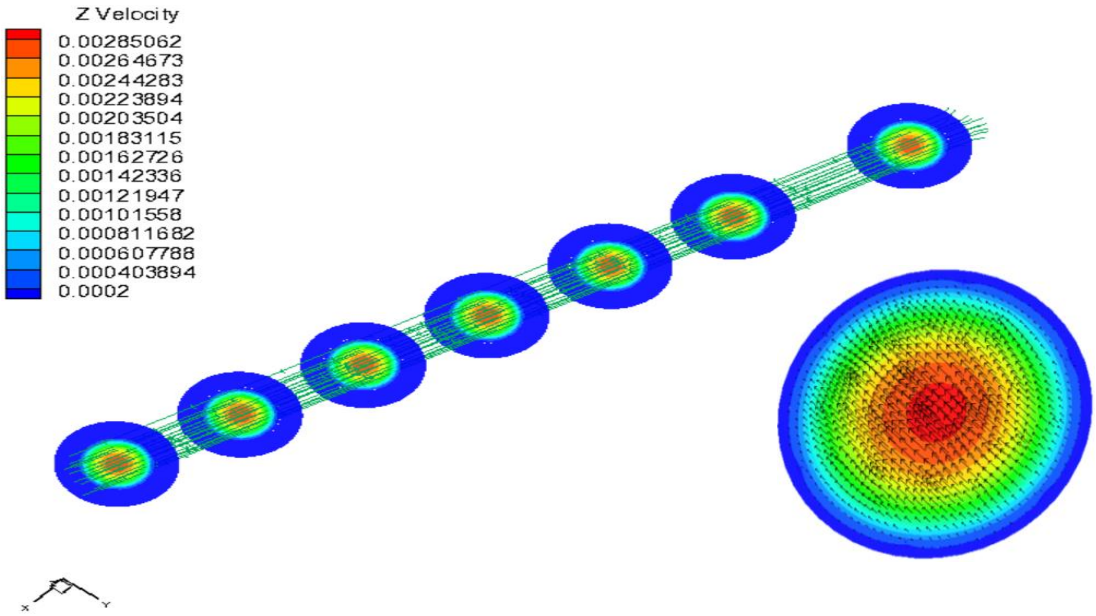

Figure V.8. Streamlines for Re = 200

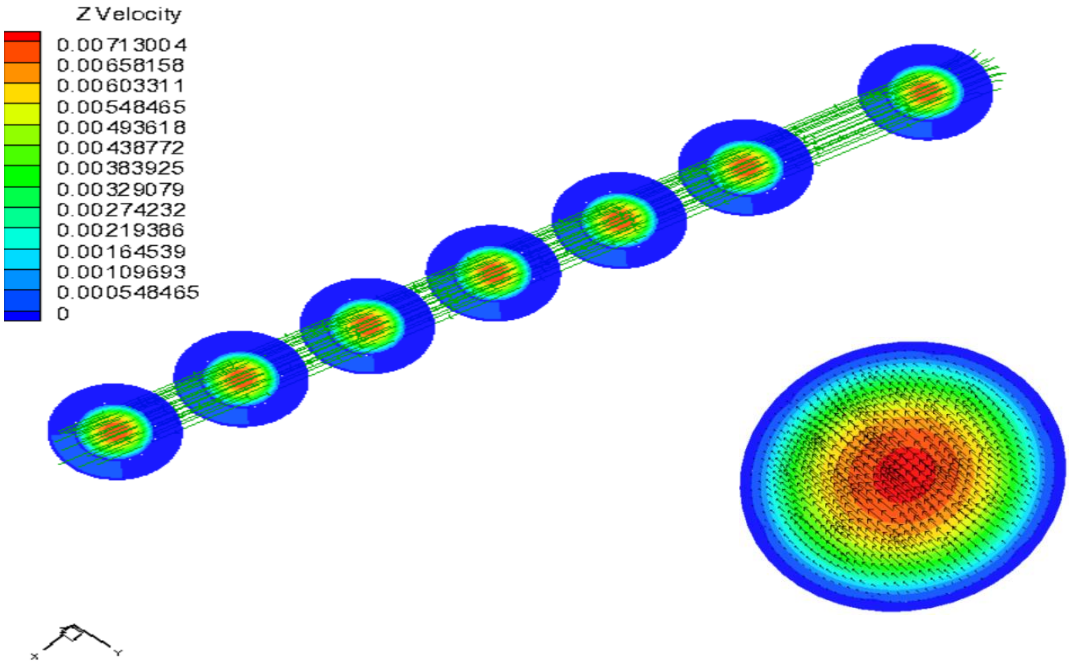

Figure V.9.Streamlines for Re = 500

V.3.1.2. Case of nanofluid (Syltherm800+Cu)

V.3.1.2.1.Temperature contours

The Figures (V.10) & (V.11) show the temperature contours for the nanofluid (Syltherm 800+Cu) for concentrations φ= 1%, 3% on seven different cross-sections with z =0.2, 1, 1.5, 2, 2.5, 3 ,3.8 m for Reynolds numbers Re=200.

This figures show that the use of nanofluid (syltherm800+cu) as a HTF instead of Syltherm improves the heat transfer process by increasing the outlet temperature at the absorber.

It has been noticed that the nanofluid (syltherm800+cu) temperature is better than that of Syltherm 800. The addition of nanoparticles (Cu) to Syltherm 800 significantly enhances convective heat transfer process and improves the nanofluid temperature at the outlet absorber .

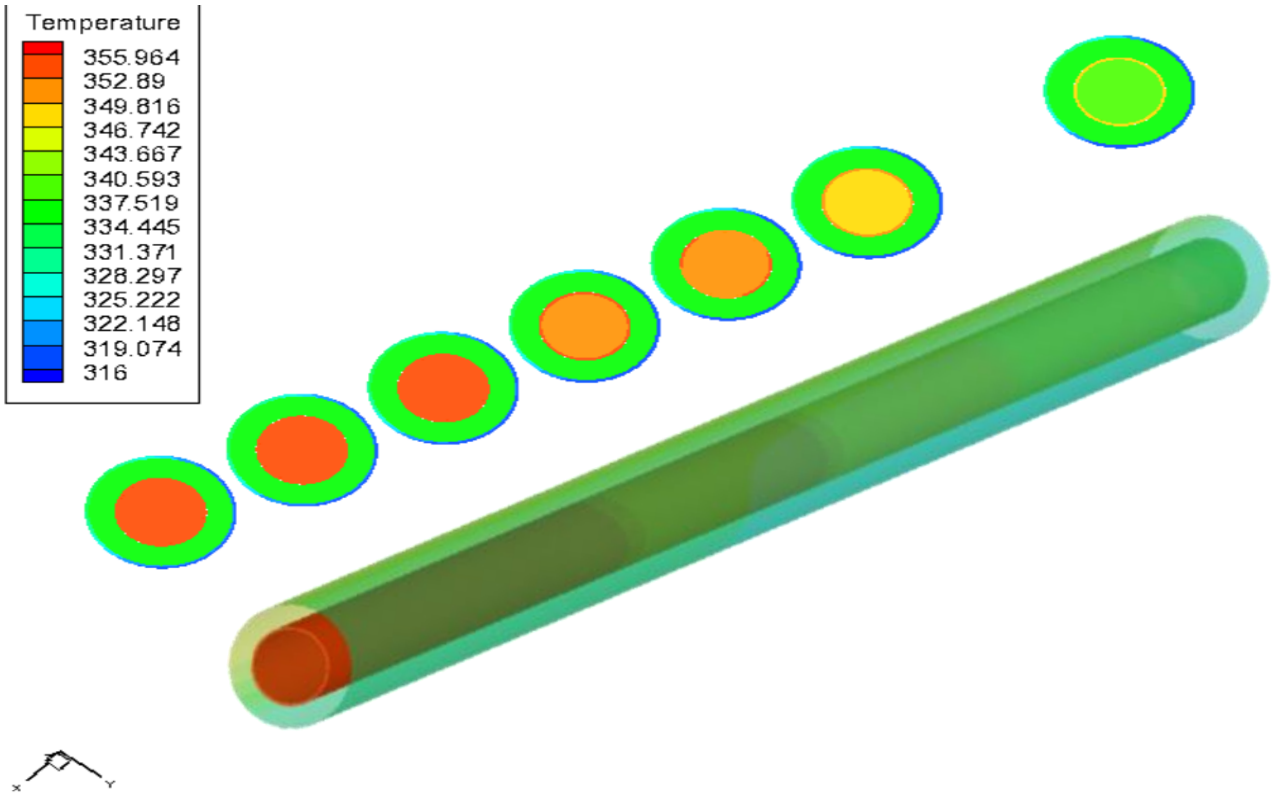

Figure V.10. temperature contours for Re = 200 , φ= 1%,

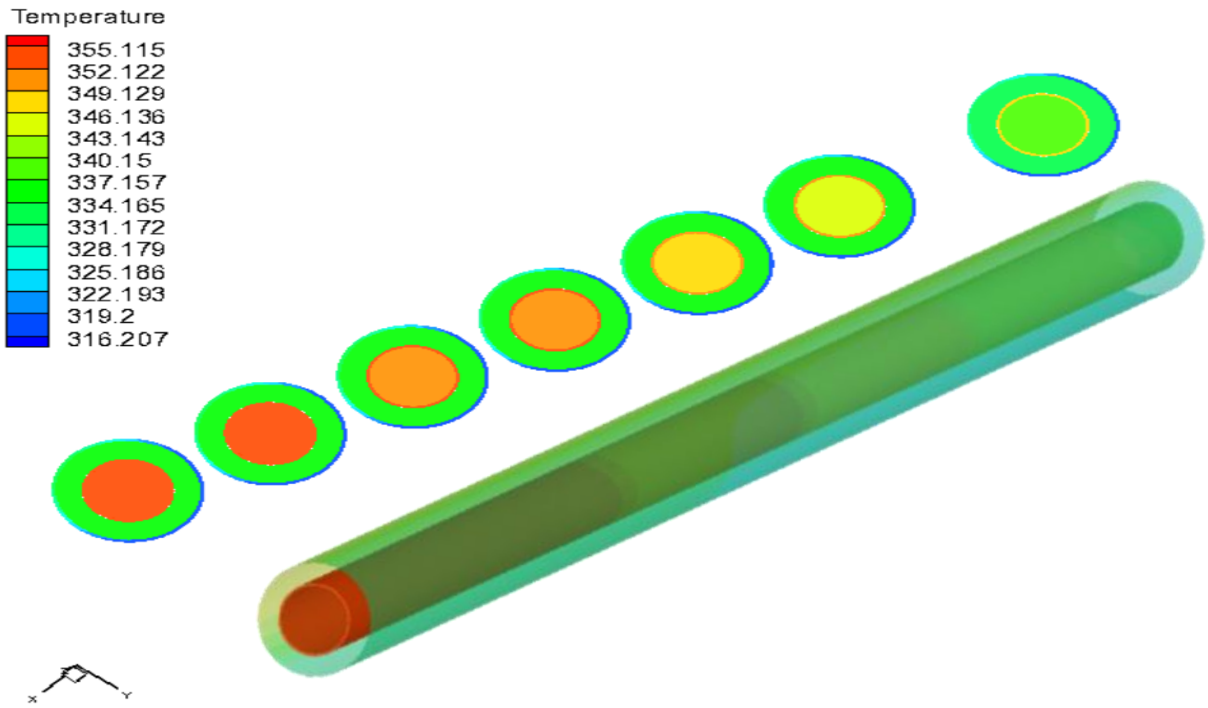

Figure V.11. Temperature contours for Re = 200 , φ= 3%

Figure V.12 shows the variation of T_{out} as a function of the Reynolds number for the Syltherm 800 and syltherm800+Cu. The results are presented for nanoparticle volume fractions φ= 1%, 2%, 3%, 4%. We can note that the temperature T_{out} decreases with the increase in the Reynolds number. This figure also shows that all nanoparticle volume fractions used offer a more interesting heat transfer than in the case of the base fluid. This implies that whatever the value of used as a heat transfer fluid, it contributes to improving heat transfer.

This result is due to the thermophysical properties of copper. Copper nanoparticles allow for better heat exchange. This exchange is favorated by a higher conductivity to absorb heat.

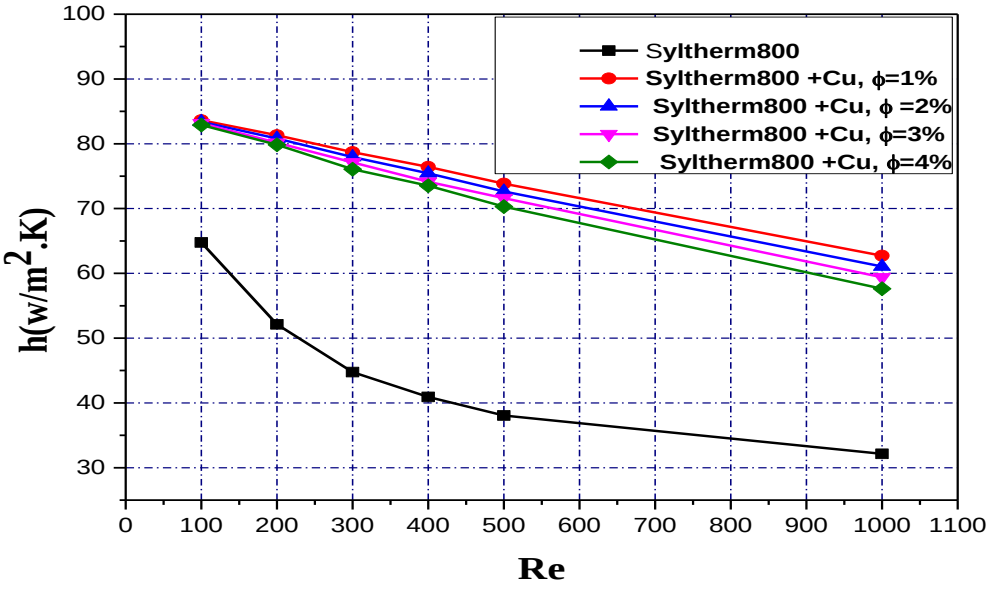

Figure V.12. The temperature difference in both cases as a function of Re

V.3.1.2.2. Velocity contours

The Figures (V.13) &(V.14) show the velocity contours in the nanofluid on seven different cross-sections with z =0.2, 1, 1.5, 2, 2.5, 3 ,3.8 m for a Reynolds number Re=200 and for different concentrations φ=1%, 3%. It is noted that the flow velocity of the nanofluid is better than that of syltherm 800. The addition of nanoparticles to syltherm 800 results in an improvement in temperature and consequently an acceleration of the flow.

It can also be noted that the velocity of nanofluide with φ=1% is better than of φ=3% , because when the concentration of nanoparticles in the fluid increases, the fluid becomes more viscous, thereby reducing the flow velocity of the fluid in the absorber .

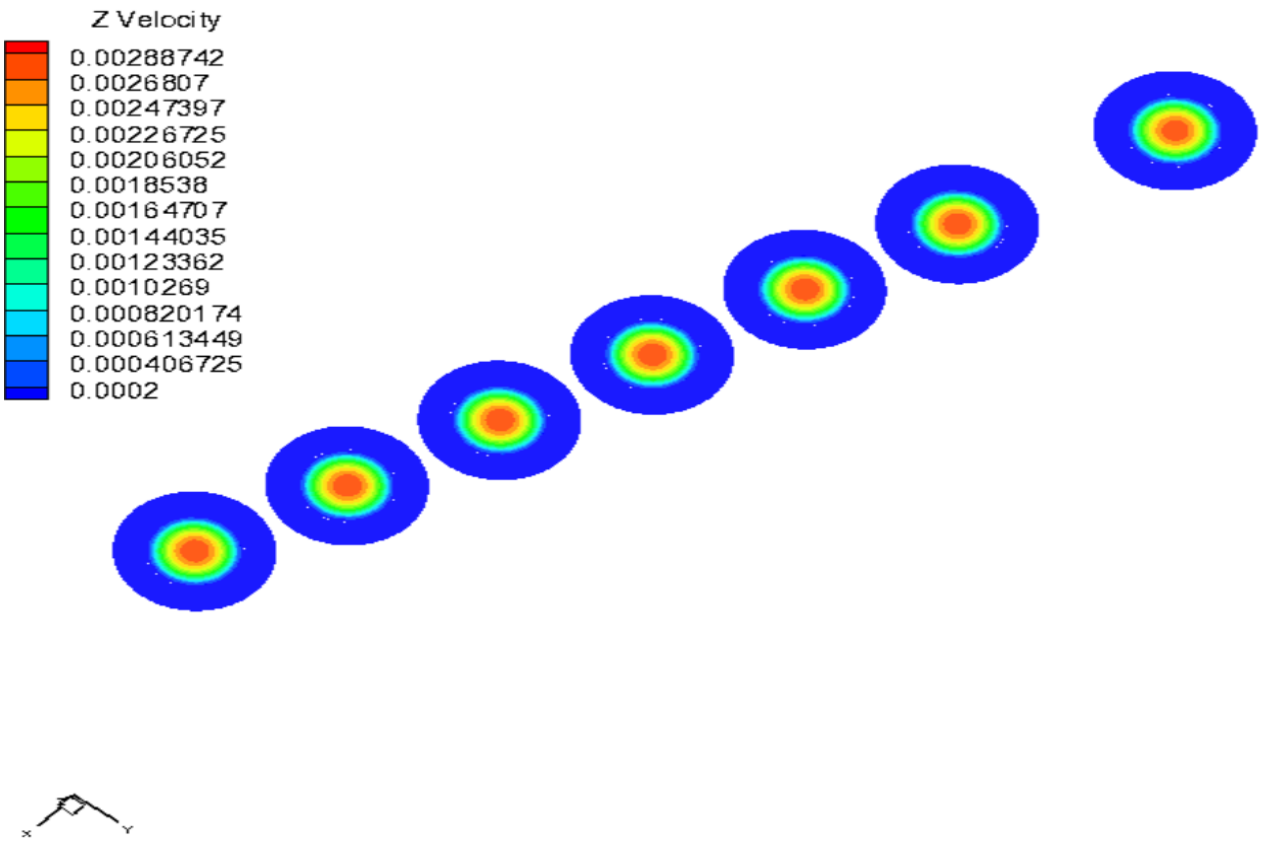

Figure V.13. Velocity contours for Re=200 , φ=1%.

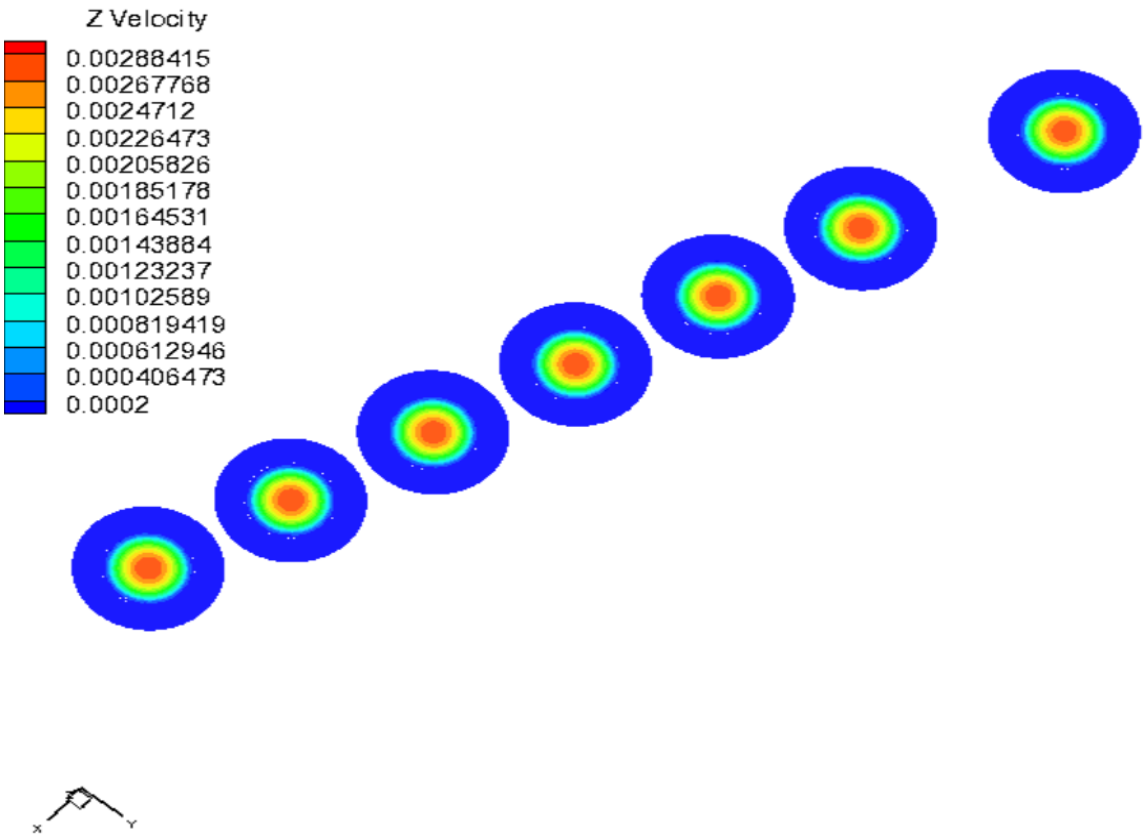

Figure V.14. Velocity contours for Re=200 , φ=3%.

V.3.1.2.3. Streamlines and Velocity vectors

The Figures (V.15) & (V.16) show the variation of streamlines and velocity vectors on seven different cross-sections with z =0.2, 1, 1.5, 2, 2.5, 3 ,3.8 m in the absorber tube for a Reynolds number Re = 200 and for different concentrations φ = 1%, 3%

We can also notice that the streamlines depend on the concentration. An increase in nanoparticles leads to a decrease in flow velocity and consequently a decrease in the values of the streamlines.

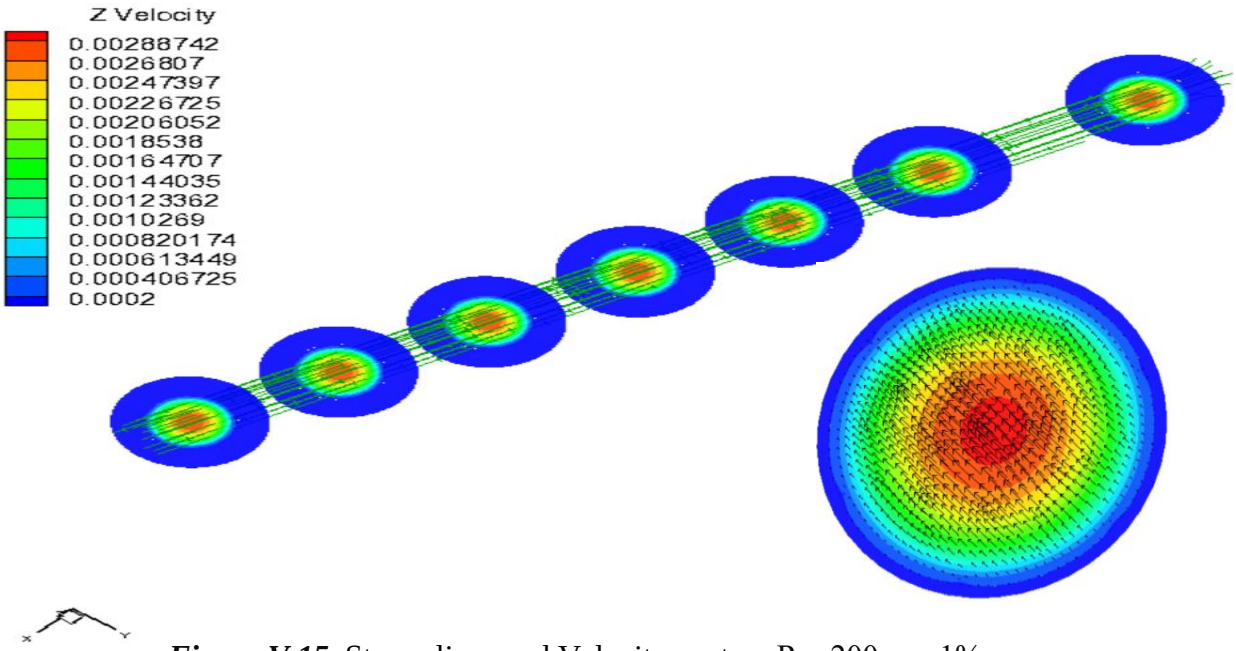

Figure V.15. Streamlines and Velocity vectors Re=200 , φ=1%.

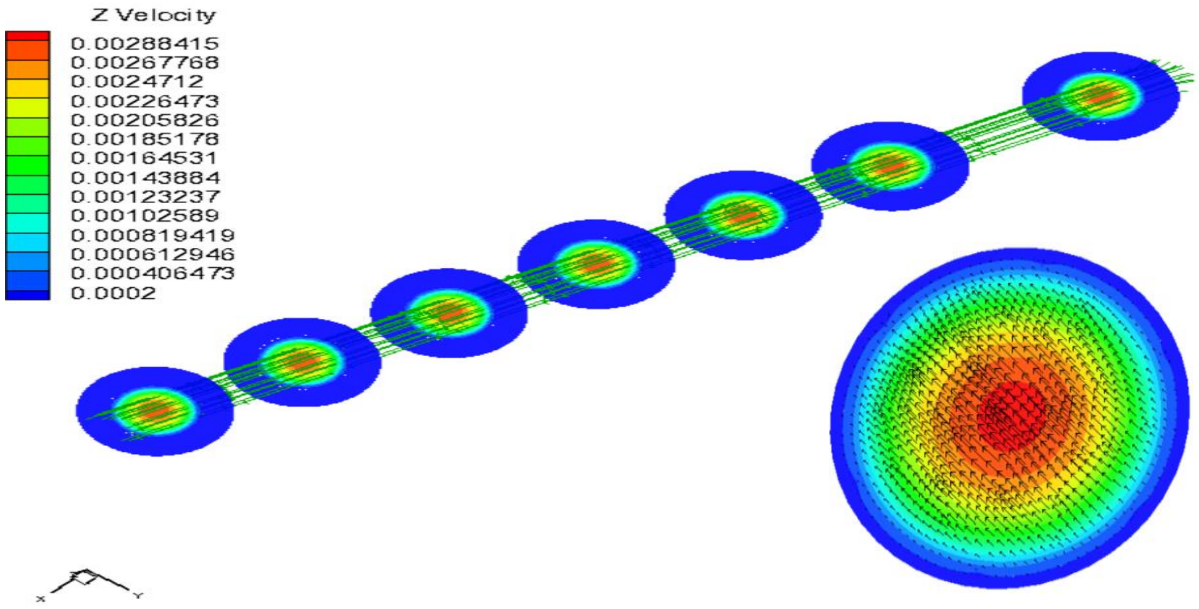

Figure V.16. Streamlines and Velocity vectors Re=200 , φ=3%.

V.3.2. Case of twisted tape with nanofluid (syltherm 800 + Cu)

V.3.2.1. Temperature contours

The Figures (V.17) and (V.18) show the temperature contours in the twisted tape tube on seven different cross-sections with z =0.2, 1, 1.5, 2, 2.5, 3 ,3.8 m for different Reynolds dnumber Re=200,Re=500 for concentration φ=1%.

We notice that the fluid enters the tube cold and exits hot, with the temperature being at its lowest upon entry and gradually increasing as it progresses from the inlet to the outlet.

Also, we observe that the temperature of the fluid decreases with an increase in the Reynolds number.

The radial distribution of temperature shows that it reaches its maximum value on the inner wall of the tube and gradually decreases towards the center.

We also notice an increase in the fluid temperature with the addition of the twisted tape, as the introducing of the twisted tape the area exposed to thermal convection increased and the interaction between walls and fluid was better, which increases the convective heat transfer.

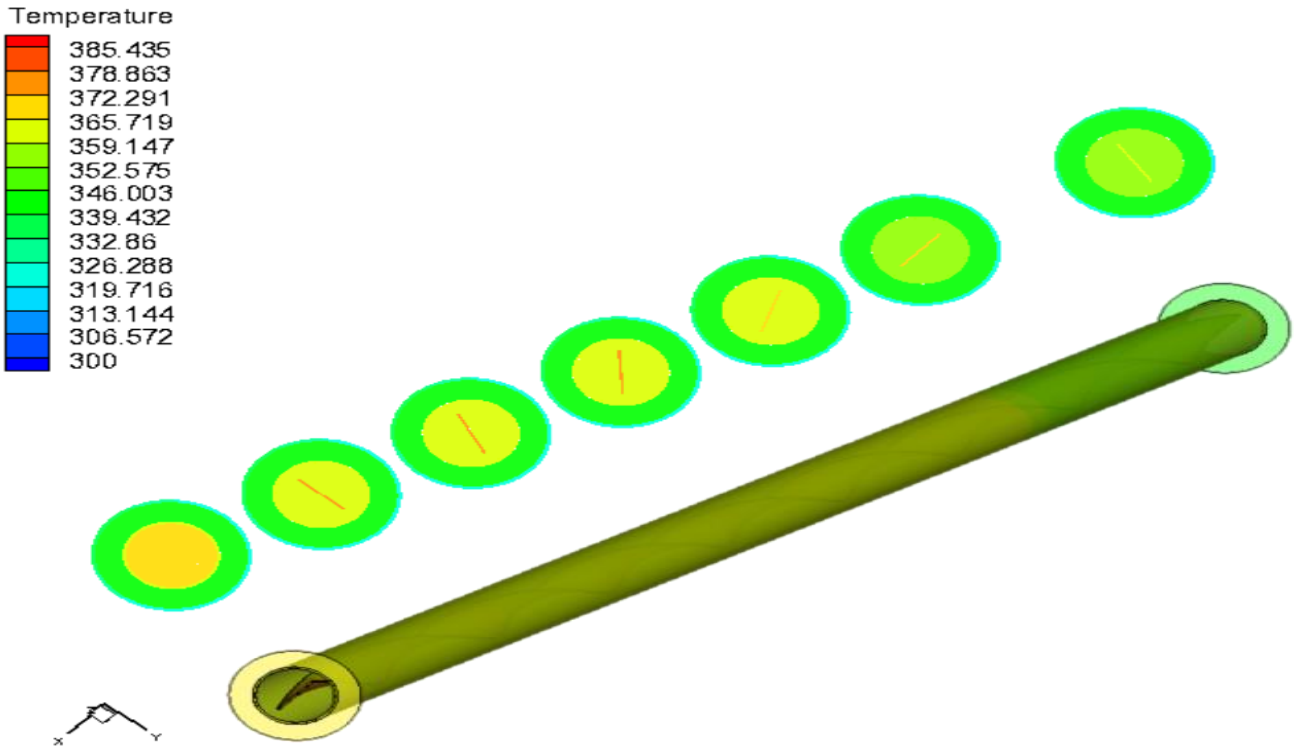

Figure V.17. Temperature contours for Re = 200 , φ= 1%

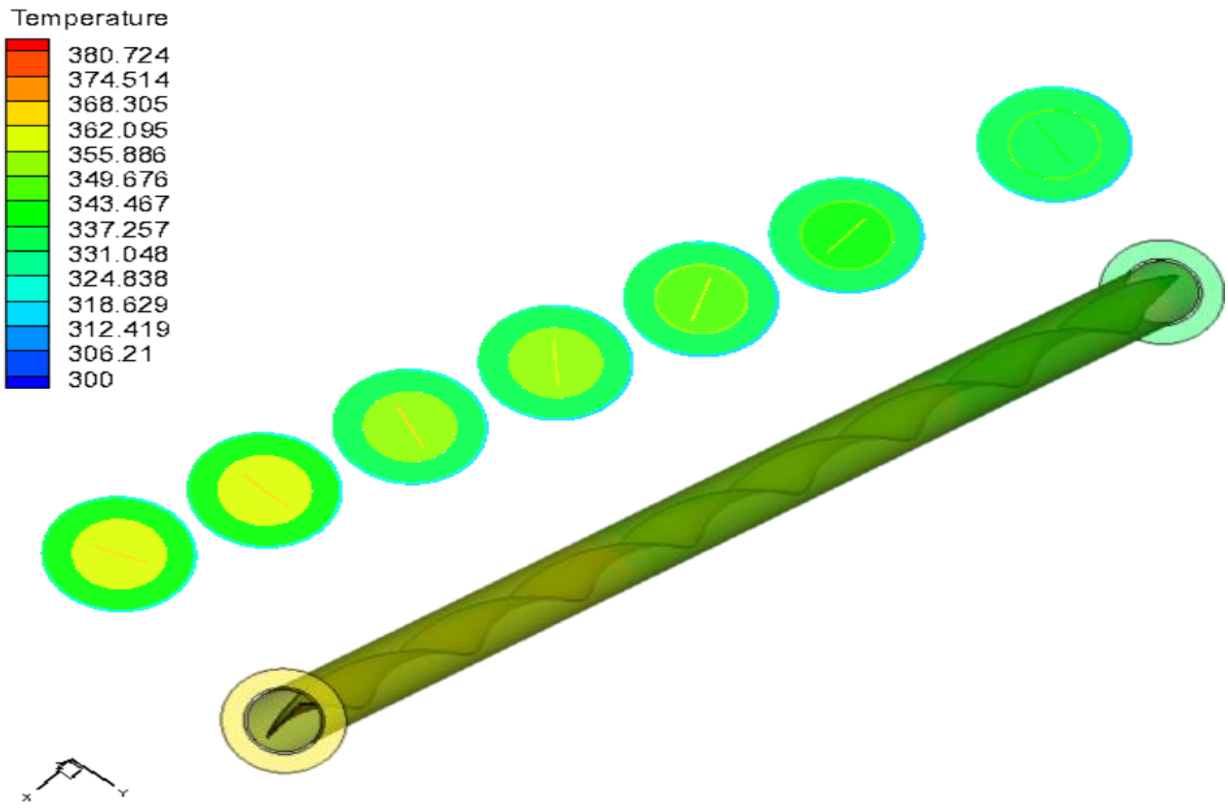

Figure V.18. temperature contours for Re = 500, φ= 1%

V.3.2.2. Velocity contours

The Figures (V.19) and (V.20) show the velocity contours in the twisted tape tube on seven different cross-sections with z =0.2, 1, 1.5, 2, 2.5, 3 ,3.8 m for different Renold number Re=200,Re=500 for concentration φ=1%.

We observe that the flow velocity increases with the increase in Reynolds number.

Also, we notice that the velocity decreases when adding the twisted tape into the absorber , causing disruption in the flow and increased fluid mixing, resulting in a decrease in flow velocity.

We can also see that the velocity profile around the twisted tape has the same tendency for different fractions. The flow velocity within in the space between wall absorber and twisted tape reaches maximum values due to the reduction of the space, the acceleration of the hot nanofluid promotes thermal transfer by convection.

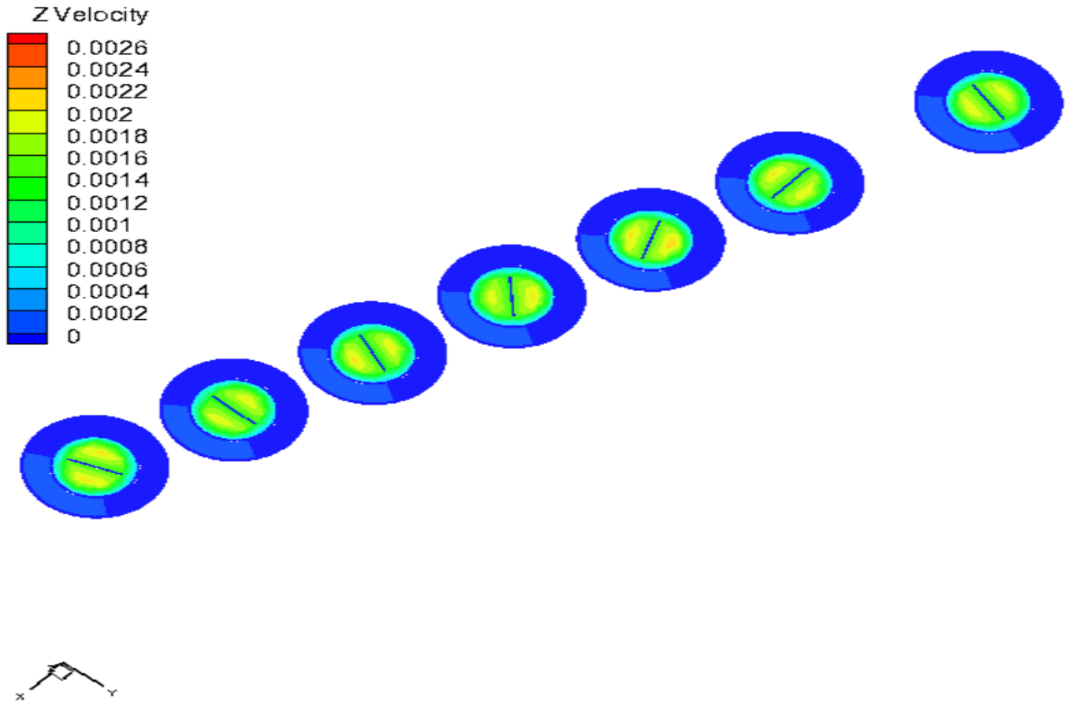

Figure V.19. Velocity contours for Re=200 , φ=1%.

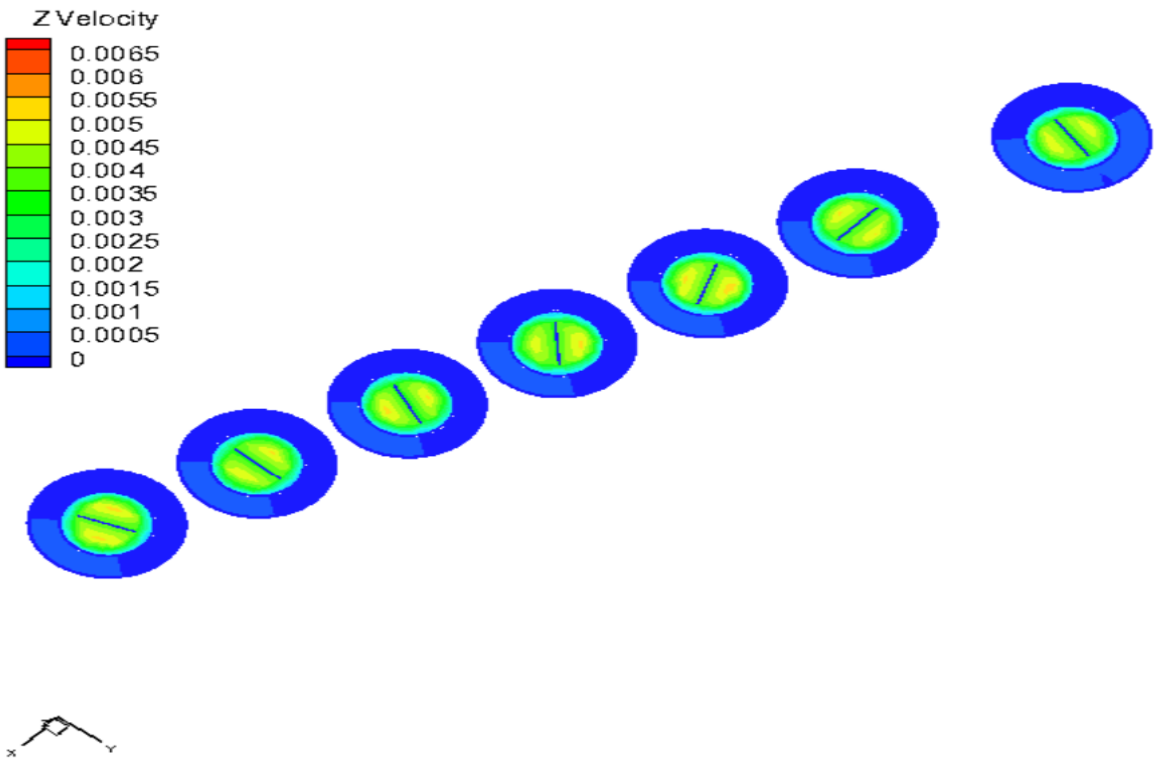

Figure V.20. Velocity contours for Re=500 , φ=1%.

V.3.2.3. Streamlines and Velocity vectors

The Figures (V.21) and (V.22) show the Streamlines and Velocity vectors in the twisted tape tube on seven different cross-sections with z =0.2, 1, 1.5, 2, 2.5, 3 ,3.8 m for different Renold number Re=200,Re=500 for concentration φ=1%.

This figures clearly show that the dynamic fields undergo a uniform velocity profile at the input of the absorber. The direction of the velocity vector changes as the nanofluid particles approach the twisted tapeand move above it. After passing through the body at a short distance, the velocity vectors return to their original direction, showing that the flow is laminar.

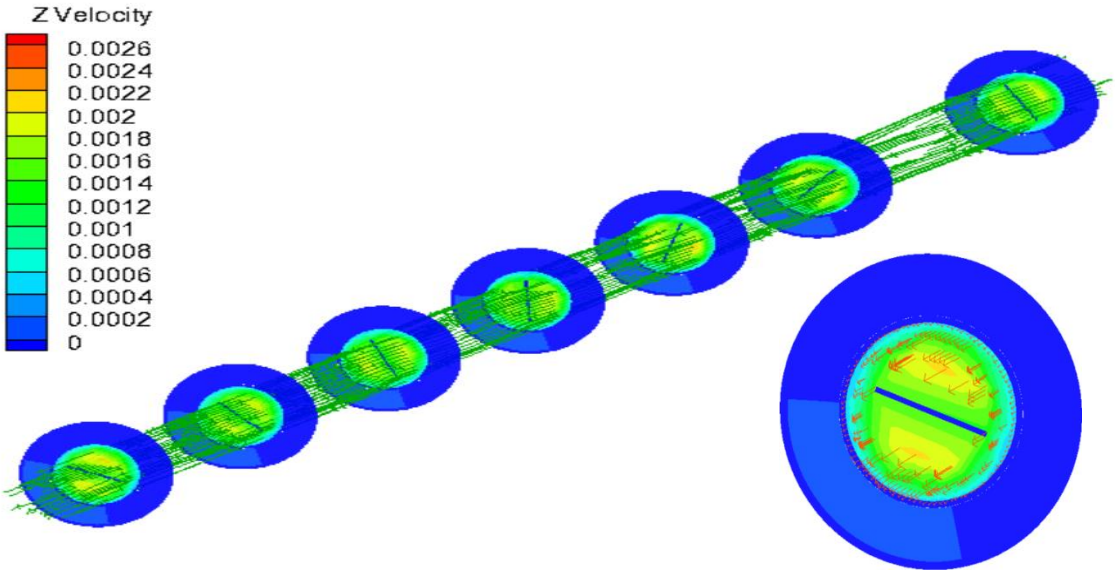

Figure V.21. Streamlines and Velocity vectors for Re=200, φ=1%.

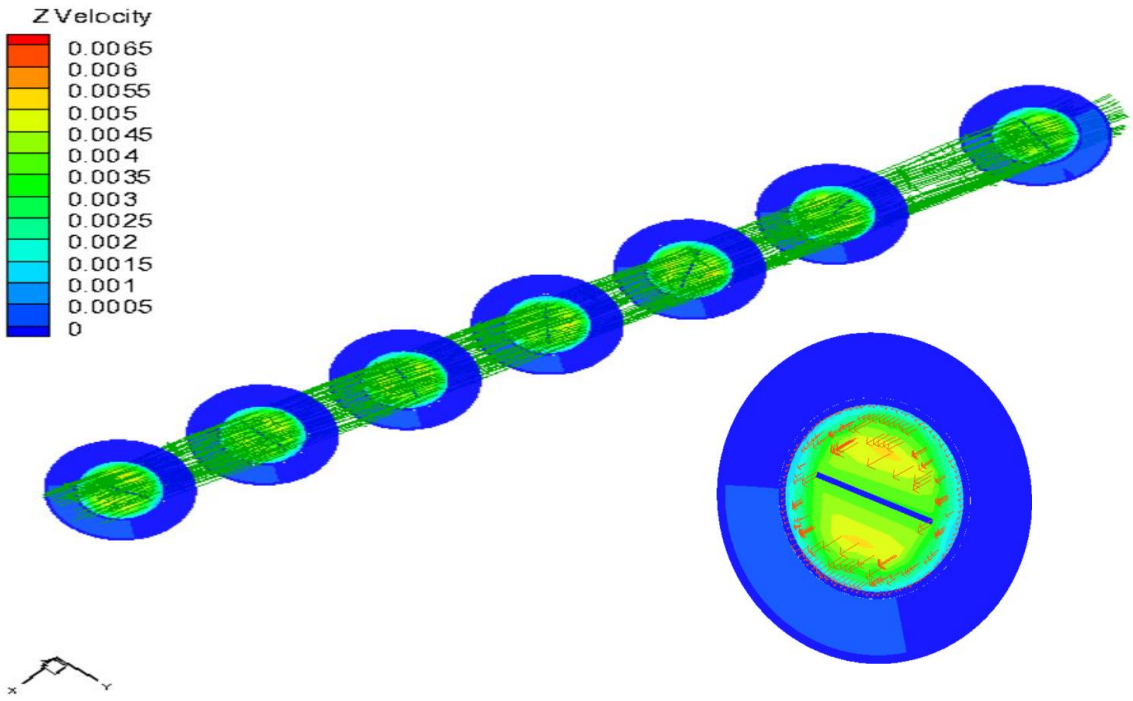

Figure V.22. Streamlines and Velocity vectors for Re=500, φ=1%.

V.3.3. Variation of the Nusselt number as a function of the Reynolds number

A comparison of the variation of the average Nusselt number against Reynolds number (based on the hydraulic diameter) for Syltherm 800 and Syltherm800+Cu with twisted tape are shown in Figure V.23.

From this figure, we observe that for the two cases the Nusselt number decreases with increasing Reynolds number. The decrease is rapid at lower Reynolds numbers and becomes lower at higher Reynolds numbers.

The Syltherm 800 maintains a constant Nusselt number Nu around 10, indicating stable heat transfer characteristics regardless of the Reynolds number.

Syltherm800+Cu with twisted tape yield the highest Nusselt number and Syltherm 800 the lowest values at all Reynolds numbers in the considered range. The twisted tape have a higher Nusselt number because, with introducing the twisted tape the area exposed to thermal convection increased and the interaction between fin and fluid was better, which increases the convective heat transfer.

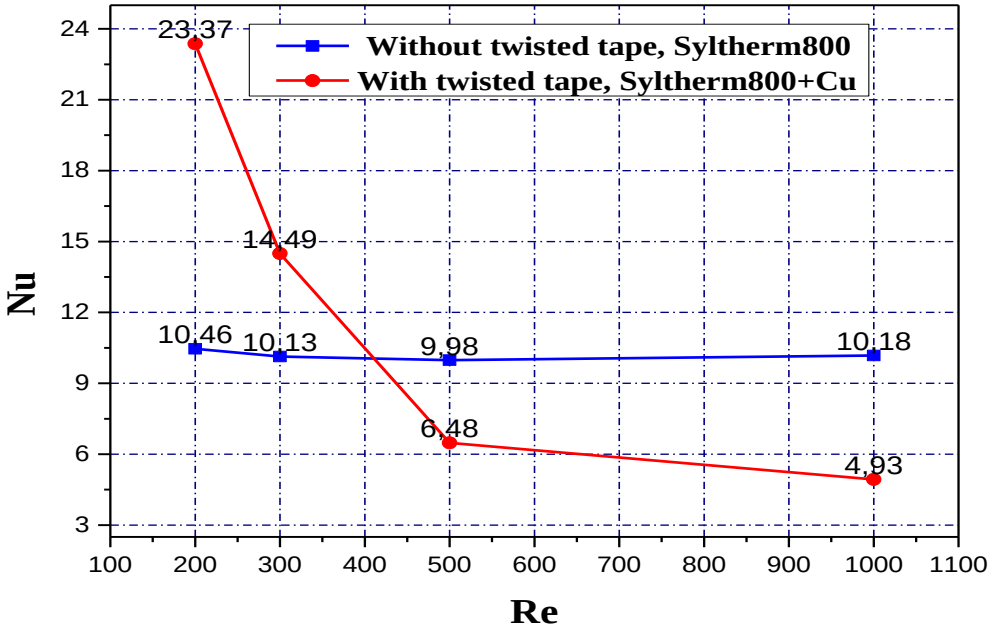

FigureV.23. Variation of Nusselt number (Nu) as a function of Re

V.3.4.Variation du coefficient de convection h as a function of the Reynolds number

Figure V.24 illustrates the relationship between average heat transfer coefficient (h) and Reynolds number (Re) of the Syltherm800 and Syltherm800+Cu with twisted tape. For both cases, the numerical results suggest that the average heat transfer coefficient (h) decreases with Reynolds number. Also, it can be seen that the twisted tape plays an important role in increases of the heat transfer by increasing the heat transfer area and creating the mixing in flow; for this reason, the absorber with twisted tape have a higher heat transfer coefficient than without twisted tape one for a low Reynolds number.

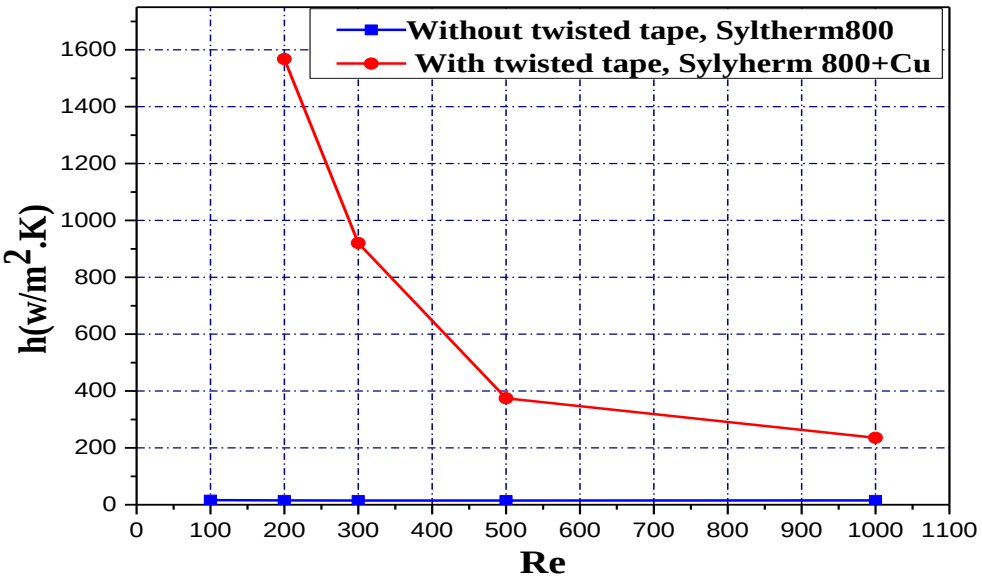

Figure V.24. variation of convection coefficient h as a function of Re

V.3.5.Variation of Temperature Out as a function of Reynolds number

The Figure V.25 shows the variation of the outlet temperature $Tout$ as a function of the Reynolds number Re for two cases: “twisted tape + nanofluid” and “Syltherm 800”.

The outlet temperature Tou decreases as the Reynolds number Re increases. The decrease is gradual across the entire range of Reynolds numbers. At low Reynolds numbers (200), the outlet temperature T_{out} is high at (91.53°C). As Re increases to 1000, T_{out} decreases to approximately 71.34°C .

For both cases, the outlet temperature To decreases with increasing Reynolds number, indicating improved heat transfer at higher flow rates.

The twisted tape + nanofluid consistently has a higher outlet temperature T_{out} compared to Syltherm 800 at the same Reynolds numbers.The difference in outlet temperature between the two cases decreases as the Reynolds number increase.

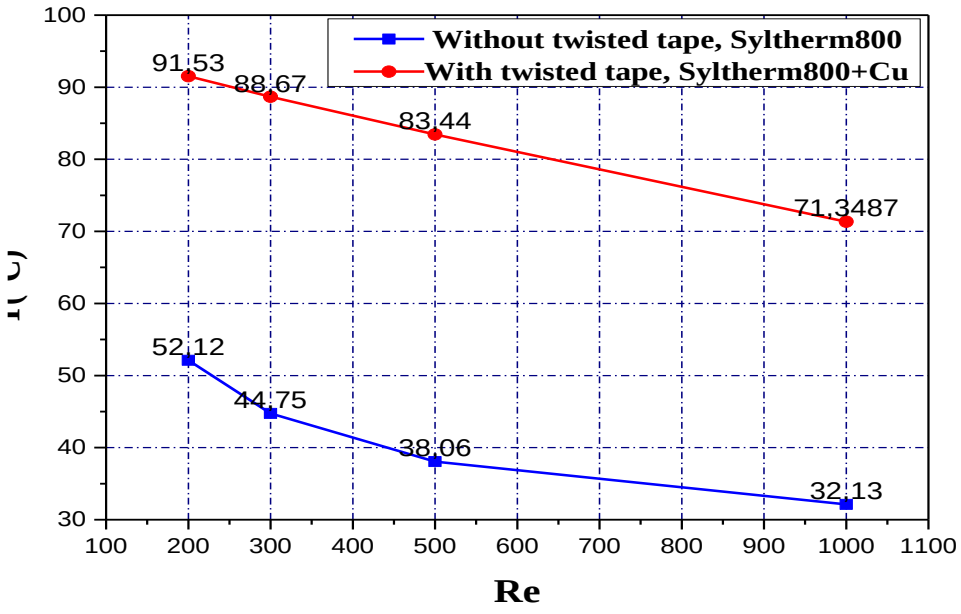

Figure V.25. Variation of Temperature as a function of Re

V.4.Conclution

In this chapter, we have presented the numerical results of a flow with heat transfer in a cylindro-parabolic collector for Syltherm 800 and the nanofluid (Syltherm 800+Cu) with and without twisted tape. Our simulations were conducted for a variation of independent parameters, such as the Reynolds number Re=100-1000 and concentrations φ=1%, 2%, 3%, 4%.

The results show an increase in temperature and the Nusselt number of the nanofluid compared to Syltherm 800. The use of nanofluids as a heat transfer fluid, and nanofluid with a twisted tape, has improved the thermal performance of the cylindro-parabolic collector.

General Conclusion

General Conclusion

In this work, we numerically simulated the thermal performance of flow in the collector of a cylindrical-parabolic solar collector filled with Syltherm 800 and nanofluid (Syltherm 800 + Cu) with different concentrations and for various Reynolds numbers.

The equations governing our physical problem are the continuity equations, momentum equations, coupled with the energy equation. The method chosen for solving these equations is the finite volume method adopted by The Fluent software .

After designing and meshing the geometry using Gambit software, the configuration is exported to Fluent software for simulation.

Numerical simulations were conducted for Reynolds numbers ranging from 200 to 1000 for Syltherm 800 and for the nanofluid (Syltherm 800+Cu) at various concentrations φ = 1%, 2%, 3%, and 4%.

The numerical results obtained show that the outlet temperature in the collector with the nanofluid is better than that of Syltherm 800, and this temperature decreases with increasing Reynolds number.

When adding a twisted tape, it causes an increase in the heat exchange surface area and enhances convective heat transfer (increasing the Nusselt number and the convective coefficient).

At the end of our study, we can conclude that the thermophysical properties of the heat transfer fluid and a twisted tape have a significant influence on the thermal performance of the cylindro-parabolic collector.

Bibliographic References

Bibliographic References

[1]science.nasa.gov/sun/facts/

[2]sciencing.com/five-characteristics-sun-8720219.html

[3]science.nasa.gov/sun/facts/

[4]science.nasa.gov/sun/facts/

[5]Earth and Moon ViewerNational Geographic Science: Planet Earth, earthNASA: Earth Fact Sheet

[6]extrait de la fiche connaissance n°19 Mouvement apparent du Soleil - Documents d'application des programmes cycles 2 et 3, Scéren CNDP, 2002

[7]extrait de la fiche connaissance n°19 Mouvement apparent du Soleil - Documents d'application des programmes cycles 2 et 3, Scéren CNDP, 2002

[8]https://www.energy.gov/eere/solar/solar-radiation-basics

[9]Shannon Brescher Shea (shannon.shea@science.doe.gov) is the social media manager and senior writer/editor in the Office of Science's Office of Communications and Public Affairs.

[10]Britannica, The Editors of Encyclopaedia. "celestial sphere". Encyclopedia Britannica, 24 Nov. 2023,

[11]P. I. Cooper, "The absorption of radiation in solar stills", Solar Energy, vol. 12, pp. 333 - 346, 1969. 2.M. Blanco-Muriel, Alarcón-Padilla, D. C., López-Moratalla, T., and Lara-Coira, M. Í., "Computing the solar vector", Solar Energy, vol. 70, no. 5, pp. 431 - 441, 2001.

[12]Britannica, The Editors of Encyclopaedia. "latitude and longitude". Encyclopedia Britannica, 25 Mar. 2024,

[13]Britannica, The Editors of Encyclopaedia. "azimuth". Encyclopedia Britannica, 3 Nov. 2023,

[14]https://www.pveducation.org/pvcdrom/properties-of-sunlight/azimuth-angle

[15]J, Bernard. Energie solaire calculs et optimisation, Ellipse Edition Marketing. (2004).

[16]Y. Jannot. Thermique solaire, Mars 2011.

[17]Ashok, S.. "solar energy". Encyclopedia Britannica, 23 Mar. 2024,

[18]https://www.trade.gov/country-commercial-guides/algeria-renewable-energy

[19]S.Brigand. « Installations solaires photovoltaïques ». Édition Moniteur. 2011.

[20]lenergie-solaire.net ,Auteur: Oriol Planas - Ingénieur Technique IndustrielDate de Publication: 30 mai 2018

Dernière Révision: 25 août 2020

[21]Philip Kosky, ... George Wise, in Exploring Engineering (Fifth Edition), 2021

[22]Thermal performance of a parabolic trough collector under different climatic zones in Morocco

[23]Apmann K, Fulmer R, Soto A, Vafaei S. Thermal Conductivity and Viscosity: Review and Optimization of Effects of Nanoparticles. Materials (Basel). 2021 Mar 8;14(5):1291. doi: 10.3390/ma14051291. PMID: 33800374; PMCID: PMC7962854.

[24]Nanofluids for Heat and Mass Transfer , Fundamentals, Sustainable Manufacturing and Applications , Book • 2021 Bharat Bhanvase and Divya Barai

[25]Nanofluids for Heat and Mass Transfer , Fundamentals, Sustainable Manufacturing and Applications , Book • 2021 Bharat Bhanvase and Divya Barai

[26]Nanofluids for Heat and Mass Transfer , Fundamentals, Sustainable Manufacturing and Applications , Book • 2021 Bharat Bhanvase and Divya Barai

[27]Nanofluids for Heat and Mass Transfer , Fundamentals, Sustainable Manufacturing and Applications , Book • 2021 Bharat Bhanvase and Divya Barai

[28]Chamsa-Ard W, Brundavanam S, Fung CC, Fawcett D, Poinern G. Nanofluid Types, Their Synthesis, Properties and Incorporation in Direct Solar Thermal Collectors: A Review. Nanomaterials (Basel). 2017 May 31;7(6):131. doi: 10.3390/nano7060131. PMID: 28561802; PMCID: PMC5485778.

[29]Mahmoud Salem, A. 2019. Nanofluid: New Fluids by Nanotechnology. In S. Aamir (Ed.), Thermophysical Properties of Complex Materials: Ch. 4. Rijeka: IntechOpen.

[30]Sheremet MA. Applications of Nanofluids. Nanomaterials (Basel). 2021 Jun 29;11(7):1716. doi: 10.3390/nano11071716. PMID: 34209726; PMCID: PMC8308184.

[31]RIKI Saad Saoud et MEKEFES Abdelbasset Etude numerique de l'eEfee des nanoparticules sur le transfert de chaleur dans une cavlterempl le de nanofluidE

[31]Apmann K, Fulmer R, Soto A, Vafaei S. Thermal Conductivity and Viscosity: Review and Optimization of Effects of Nanoparticles. Materials (Basel). 2021 Mar 8;14(5):1291. doi: 10.3390/ma14051291. PMID: 33800374; PMCID: PMC7962854

[32]RIKI Saad Saoud et MEKEFES Abdelbasset Etude numerique de l'eEfee des nanoparticules sur le transfert de chaleur dans une cavlterempl le de nanofluidE

[33]http://www.dow.com.heattrans

Abstract

In this memoir, we numerically studied enhancing heat transfer in an equivalent cylindrical-parabolic collector. collector in three cases Syltherm 800, nanofluids (Syltherm 800 + Cu), and with a twisted tape. The equations governing continuity, momentum, and energy were solved using the finite volume method implemented in the Fluent software. The studied configuration was created using Gambit, and meshing and simulation were performed using both Fluent and Gambit software. Numerical simulations were conducted for various Reynolds numbers ranging from 200 to 1000 and for concentrations of 1%, 2%, 3%, and 4%. The numerical results showed that the outlet temperature in the collector with the nanofluid and twisted tape was better than that with just the nanofluid, and that the outlet temperature in the collector with the nanofluid was better than that with Syltherm 800. This temperature decreases with increasing Reynolds number. The Nusselt number in the nanofluid with the twisted tape is higher than in Syltherm 800 and decreases with increasing Reynolds number.

Résumé

Dans ce memoire, nous avons étudié numériquement l'amélioration du transfert de chaleur dans un collecteur cylindro-parabolique dans trois cas Syltherm 800, des nanofluides (Syltherm 800 + Cu) et avec un ruban torsadé. Les équations régissant l'ecoulement sont : equation de continuité, de quantité de mouvement et l'énergie ont été résolues en utilisant la méthode des volumes finis implémentée dans le logiciel Fluent. La configuration étudiée a été créée à l'aide de Gambit, le maillage et la simulation ont été réalisés à l'aide des logiciels Fluent et Gambit. Des simulations numériques ont été effectuées pour différents nombres de Reynolds allant de 200 à 1000 et pour des concentrations de 1 %, 2 %, 3 % et 4 %. Les résultats numériques ont montré que la température de sortie dans le collecteur avec le nanofluide et le ruban torsadé était meilleure que celle avec seulement le nanofluide, et que la température de sortie dans le collecteur avec le nanofluide était meilleure que celle avec Syltherm 800. Cette température diminue avec l'augmentation du nombre de Reynolds. Le nombre de Nusselt dans le nanofluide avec le ruban torsadé est plus élevé que dans Syltherm 800 et diminue avec l'augmentation du nombre de Reynolds.